The Distribution and Quantities of Radioactive Trace Elements, in Particular Uranium and Thorium, within the Waterberg Coalfield

MSc (50/50) RESEARCH REPORT

Prepared by: S. Murdoch (1140999)

Submitted to:

School of Geosciences, University of the Witwatersrand, Johannesburg, South Africa

October 2018

1140999

Declaration

I declare that this research report is my own unaided work. It is being submitted in fulfilment of the degree of Master of Science to the University of the Witwatersrand, Johannesburg. It has not been submitted before for any degree or examination to any other University.

____

S. MURDOCH

Student Number: 1140999

Signed on the __2nd__ day of ______October____________ Year ___2018_____

Abstract

In an uncertain future with regards to coal utilisation due to environmental regulations, coal mining, and particularly the future of coal mining located in the Waterberg Coalfield of the Ellisras Basin in South Africa, needs to be aware of all the risks and possible pitfalls that could hamper its further development.

The radioactive elements, U and Th, which are typically associated with sedimentary environments where coal is formed, if found in elevated quantities, would be one of the risks that needs to be quantified. Based on the impact elevated U levels has had on the development of the Springbok Flats Basin, this study was instigated to evaluate if there was a similar risk to the coal resources and reserves in the Waterberg Coalfield, which lies 150 km to the northwest of the Springbok Flats Basin.

Due to limitations related to access to samples it was not possible to sample the entire Karoo Supergroup sequence within the Waterberg Coalfield. However, a database of downhole wireline geophysical logs was compiled and used as a first order study to identify the most suitable horizons for sampling for geochemical analysis. A total of 34 exploration holes and 7,451 blast holes were used to compile the geophysical database.

Trends related to gamma anomalies were determined where gamma values, here measured in American Petroleum Institute (API) values, are greater than 300. These were associated with the Eendragtpan (Beaufort) and Swartrant (Vryheid) Formations. The 54 anomalies (where API values greater than 300) within the Eendragtpan (Beaufort) Formation did not appear to follow any apparent trend. The 118 anomalies within the Swartrant (Vryheid) Formation conformed to two trends – the first was associated with a gradual increase in gamma values towards the base of the interburden between the coal zones 3 and 4A, Grootegeluk Bench 8. The second trend identified was that the anomalies were not associated with the coal seams, but instead with the interburden. The largest anomalies occurred in the interburden between the coal zones 2 and 3, at Grootegeluk Bench 10.

Geochemical analysis of the Bench 10 interburden yielded only two anomalous U and Th values (compared to U and Th values reported by Swaine (1994)), with the mean values for U and Th being 2.89 ppm and 2.47 ppm respectively. Various classifications and analysis were applied to the geochemical results to help ascertain if there was any correlations or trends within the results; 1) Th/U ratios indicate that Bench 10 was deposited under reducing conditions; and 2) the samples with anomalous U and Th values also report elevated values for Y, Zr, Nb and Ag, and are depleted in Na and Al.

The overall conclusion of the study was that while there was some U and Th, as would be expected in such an environment, there was not significant quantities found for exploitation purposes and it is unlikely that the radioactive elements will pose a health risk within the region. As such there is little cause for concern regarding the mining of coal within the Waterberg Coalfield, in particular pertaining to U or Th.

Acknowledgements

The author wishes to thank Exxaro and the management of Grootegeluk Mine for granting access to the geological database and to samples.

Personal thanks go to:

- Gavin Wepenar - for his support and advice throughout the research project. Without Gavin this completed project wouldn't have been a reality today.
- Dr John Hancox – for his time, advice, comments, and corrections. The feedback and insights, provided by Dr Hancox, provided the author with much needed reassurance. Thank you
- The Supervisors - Prof Judith Kinnaird and Dr Nikki Wagner. Thanks go to the supervisors who proved their time, mentorship and encouragement required to perform this project.
- Exxaro Colleagues - Sifiso Mhlongo, Coert van Ryneveld, and the many others. Thanks to the colleagues at Exxaro for their assistance and advice provided throughout the project.
- Notable others – Prof Paul Nex & Tsheko Ratsheko.

Lastly and most importantly; the author wishes to thank his family, and in particular his wife Candice – she gave the author the encouragement and drive to start, continue and finish this project.

Table of Contents

Table of Figures

Table of Tables

Table of Appendixes

Table of Equations

Nomenclature

ppm	parts per million, 1 in 10^6, µ.g/g, 10^{-6}
ppb	parts per billion, 1 in 10^9, n.g/g, 10^{-9}
MKB	Main Karoo Basin
ROM	Run of Mine
Mt	Million tons
CBM	Coalbed methane
Formation	Formation
API	American Petroleum Institute
SACRM	South African Coal Roadmap
FFF	Fossil Fuel Foundation
IPP	Independent Power Producer

List of Units and Symbols

1 morgen	0.8565 hectares

Chapter 1

Introduction

1.1. Background

As South Africa forges forwards towards an uncertain future with regards to global climate change and the mitigation thereof, the South African Coal Roadmap (SACRM) was developed in 2013 to help explore the short, medium and long-term activities of, and to support, the coal industry in South Africa (Fossil Fuel Foundation (FFF), 2013). Within the SACRM there are several scenarios suggesting that the medium- and long-term growth of the South African coal industry is ultimately dependent on the opening of the Waterberg Coalfield of the Ellisras Basin (Figure 1.1). However, if such a scenario is to be implemented, the environmental effects of mining must be considered.

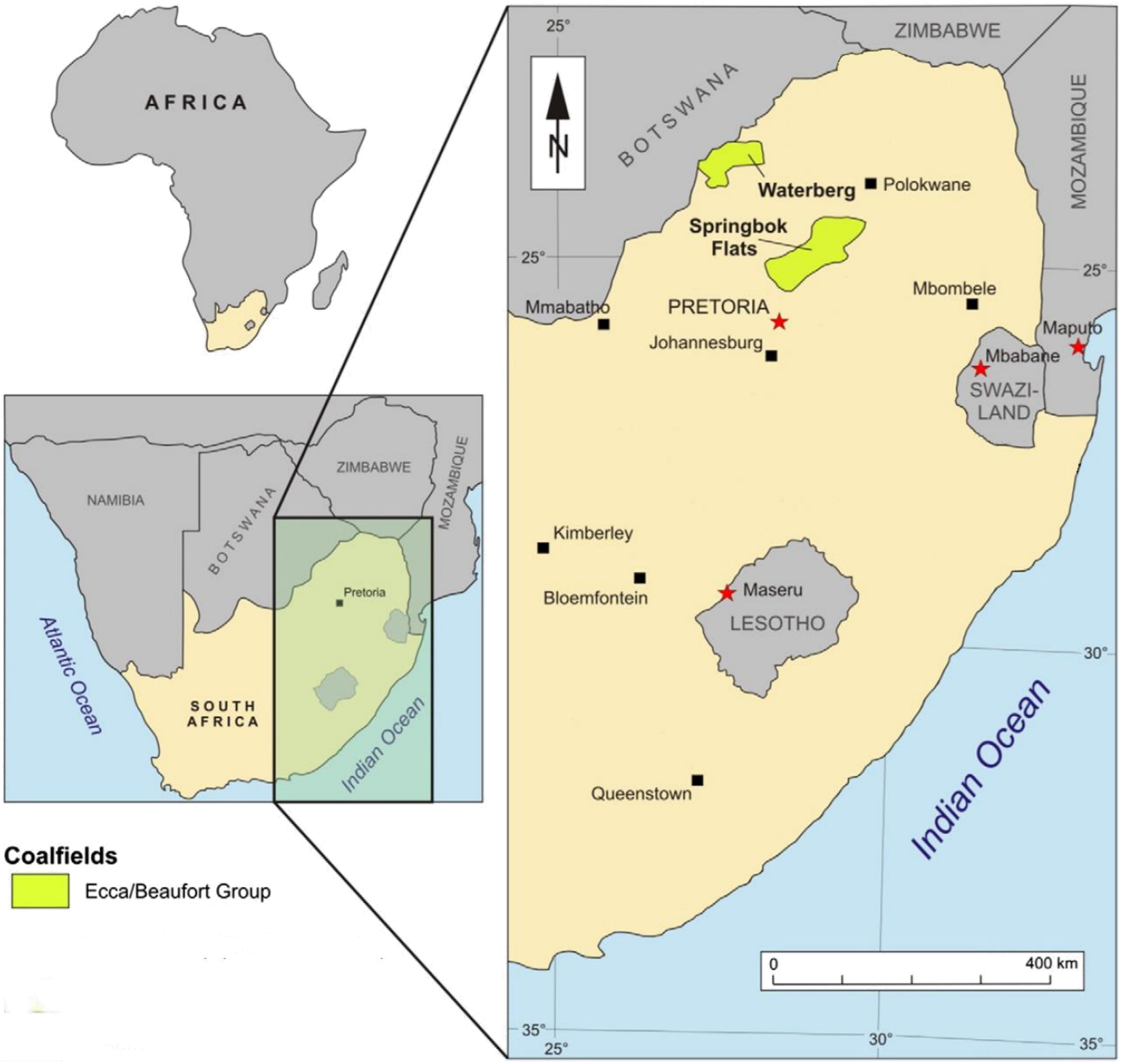

Figure 1.1: Location of the Waterberg and Springbok Flat Coalfields (Adapted from Hancox and Götz, 2014)

While some workers (Wagner and Tlotleng, 2012; Aphane and Vermeulen, 2015) undertook studies to determine some of the more hazardous trace elements in the coals, namely As, Cd, Cr, Hg, Pb and Se, (Swaine, 1990, 1994, 1998, 2000; Kolker and Finkelman, 1998), there has been little to no work that focuses on the radioactive trace elements such as Th and U, and their distribution within the Waterberg Coalfield.

It is worth noting that the nomenclature used for describing the study area is confusing; (for examples see Mtimkulu, 2009; Wagner and Tlotleng, 2012; Fossil Fuel Foundation (FFF), 2013; and Fourie et al., 2014). In summary there are several terms that create confusion i.e. “Waterberg Coalfield”, “Ellisras Basin”, and “Waterberg sediments”. The challenge arises from the usage of the word “Waterberg” in that 1) geographically the region is known as the Waterberg; 2) there is the Waterberg Supergroup (~2000 to 1900 Ma) stratigraphy that was deposited in the Waterberg Basin, located on the southern border of the study area; and 3) a Karoo Basin in Namibia referred to as “Waterberg Karoo Basin”. An alternative term of “Waterberg Coalfield” can be used, noting that that the Waterberg Coalfield is contained within the “Ellisras Basin”. For the purposes of this study the term Waterberg Coalfield will be used in this context.

1.2. Aims and Objectives

The aim of this research report is to determine the distribution and quantities of trace elements, in particular U and Th, within the Waterberg Coalfield.

1.3. Hypotheses

The following information is noted:

- The Waterberg Coalfield contains commercial quantities of coal (Faure et al., 1996b; a; Hancox and Götz, 2014; Hancox, 2016);
- The Waterberg Coalfield formed in a similar environment as the Springbok Flats (Johnson et al., 2006);
- U and Th are commonly associated with coal (Swaine, 1990, 2000; IAEA, 2009);
- The Springbok Flats Basin and associated coal is uraniferous (Jeffrey, 2005a; Cole, 2008; Ndhlalose, 2015; Ndhlalose et al., 2015);
- Cole (1998) states that the U in the Springbok Flats originates from the sediments derived from the Bushveld Complex;
- Falcon (1986) and Fourie et al. (2014) state that the sediments within the Waterberg Coalfield derived are from the Limpopo Belt and Bushveld Complex rocks;
- There are two types of U-hosted deposits within South Africa Karoo Supergroup – coal and sandstone (Cole, 2008; IAEA, 2009);
- Both the Waterberg and Springbok Flats coalfields occur within Karoo aged basins (Cadle et al., 1993; Cairncross, 2001; Catuneanu et al., 2005; Johnson et al., 2006; Cole, 2008);
- U, associated with coal, is typically held in organo-metallic compounds (Hambleton-Jones, 1980; Cole, 2008);
- The global average for U in coal is 0.5 – 10 ppm and for Th 0.5 – 10 ppm (Swaine, 1994).

Based on the above, the following hypotheses were derived:

- There is elevated U (and Th) within the Waterberg Coalfield, greater than the global average (0.5 - 10 ppm U; 0.5 - 10 ppm Th) (Swaine, 1994);
    - The U is associated within the coal or sandstones due to a reducing environment in which the coal formed;
    - The likely source of the U, is the Bushveld Complex rocks.

1.4. Importance of the research

The Waterberg Coalfield contains a significant proportion of South Africa's future coal resources, and while U and Th are not considered to be as toxic as As or Hg, they still pose a threat to the environment and human health if not managed correctly. The first step in the management of these elements is the quantification and identification of the forms they occupy within the coalfield.

1.4.1. Possible challenges

- Conflicting provenance of sediments and U (Falcon, 1986; Faure et al., 1996a; Cole, 2008; Fourie et al., 2014).
- Previous work on trace elements within Waterberg Coalfield has not determined elevated levels of U (Faure et al., 1996b; Wagner and Tlotleng, 2012).
- An alternative global average for U in coal is 3.1 ppm and for Th 2.0 ppm (Zhang et al., 2004).
- Access to samples and data.

1.5. Study area

The study area (Figure 1.2) consists of two Exxaro mines (Grootegeluk and Thabametsi) and a project (Zonderwater). The project and mines consist of several farms located within the Waterberg Coalfield.

The primary focus covers the Grootegeluk mine and the Zonderwater Project area, as the majority of the information supplied originates from boreholes on these localities.

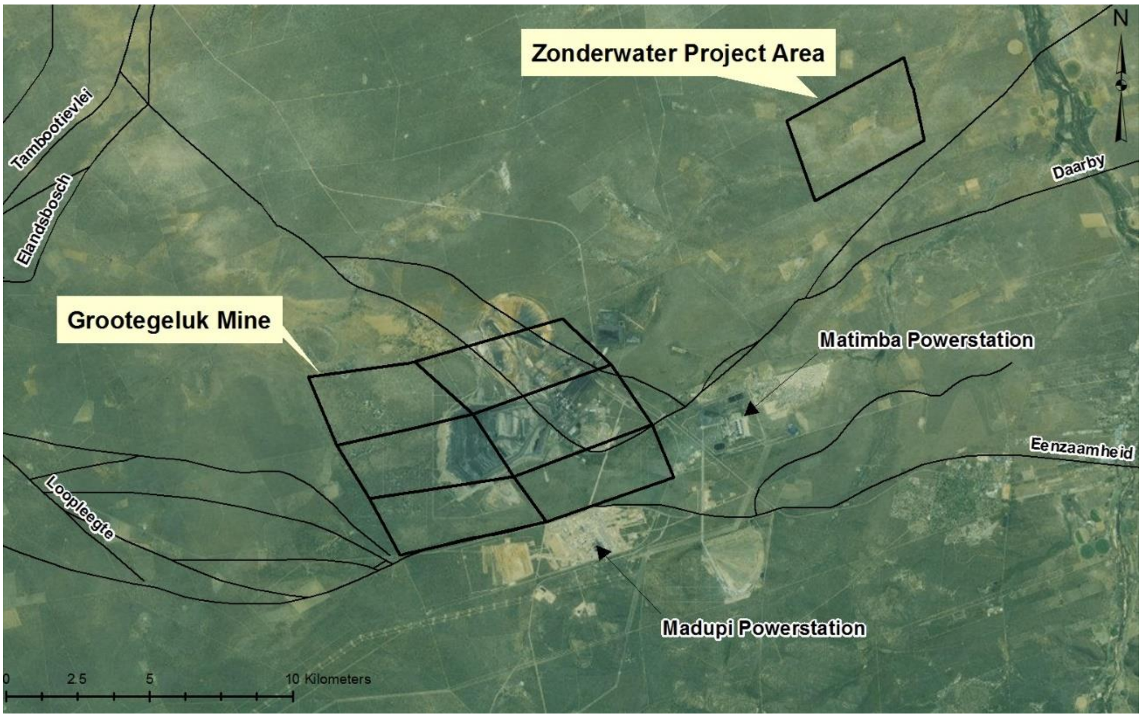

Figure 1.2 Study Area

1.6. Scope

This study was conducted in three phases namely:

1. Phase 1 – Literature review and identification of high level targets based on information contained within the literature

2. Phase 2 – Downhole Geophysics – As the author had access to several Exxaro projects and the associated geophysics, the geophysics was used to further narrow the search for U and Th.
3. Phase 3 – Sample and Analysis – After identification of targets from Phase 1 and 2, sampling was conducted on the targets and analysis conducted.

Phase 2 of the project included the compilation of geophysical data from 34 exploration boreholes and 7,451 blast holes into a geological database for analysis using 3D geological modelling software.

Phase 3 included the taking and analysis of eighteen (18) samples – The samples originated from five boreholes, two of which originated from Zonderwater and three from Grootegeluk; as well as three bulk samples which were taken from Grootegeluk.

Chapter 2

Literature Review/Survey

The purpose of this chapter is to provide information on 1) the geological setting in which the Waterberg Coal is found (Section 2.1); 2) the impact that development has had on research within the Waterberg Coalfield (Section 2.2.1); 3) the previous research conducted within the Waterberg Coalfield (Section 2.2.2); and 4) the previous research within the Waterberg Coalfield where U and Th were reported.(Section 2.3)

2.1. Geological setting of the Ellisras Basin

The Carboniferous to Jurassic-aged Ellisras Basin is situated near the town of Lephalale (formally Ellisras) in the Limpopo Province. The basin is approximately 35 km wide by 80 km long, with the Limpopo Mobile Belt to the north defined by the Zoetfontein Fault Zone and the Waterberg Basin to the south defined by the Eenzaamheid Fault Zone (see Figure 2.1). The eastern edge of the basin is characterised by an unconformable contact with the Bushveld Complex and the Limpopo Mobile Belt, while it extends westwards into Botswana (Figure 2.1) (Faure et al., 1996b; a; Cairncross, 2001; Johnson et al., 2006). The Ellisras Basin is underlain by rocks of the Mokolian Waterberg Supergroup which itself is underlain by the Bushveld Complex. These Waterberg Supergroup and the Bushveld Complex are believed to be the source of the Karoo sediments of the Ellisras Basin (Fourie et al., 2014).

2.1.1. Structural and tectonic framework

The Ellisras Basin has been controlled to a considerable extent by the crustal evolution and development of the original ancient crustal nuclei. This process began more than 3000 Ma ago and up to 550 Ma these nuclei increased by accretion into larger stable units or cratons, namely the Kaapvaal and the Zimbabwe cratons, whilst the zones or regions affected by orogenesis and/or intercratonic instability associated with these developing nuclei were very active sites of tectonic and sedimentary activity. Despite the stability of the major part of the African continent, the presence of large deposits of coal-bearing and other sediments on the continent during Permian through to Tertiary times indicates that the continental topography lent itself to some sedimentation, specifically in areas of negative relief relative on the ancient cratons (Falcon, 1986). Falcon (1986) draws the following conclusions in reference to the deposits of Karoo strata in that the following features appear to have exerted a major influence:

1. The ancient nuclei, as originally defined 3 000 Ma ago, appear to have represented the major areas of positive relief or mountainous regions, thus providing the source for Karoo sedimentation (Falcon, 1986);
2. The areas between the ancient cratons became the sites for Karoo deposition. These large areas include: (a) large cratonic paralic basins, often with stable cratonic shelves, i.e. the Karoo basins; (b) intercratonic lineament zones or mobile belts along which the Karoo strata occur in narrow, elongated fault-bounded grabens or valleys, e.g. the Limpopo belt; and (c) localised cratonic grabens or fault blocks, e.g. Springbok Flats and Ellisras Basin (Falcon, 1986).

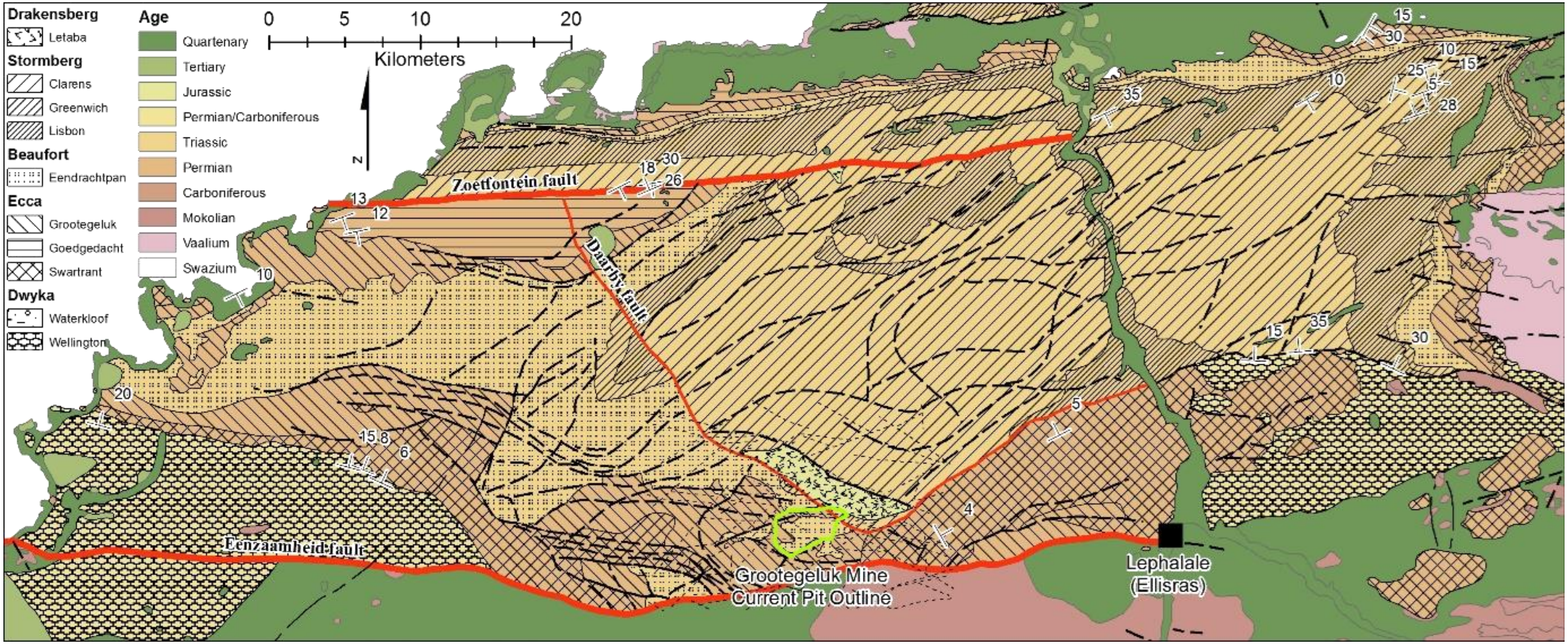

Figure 2.1: Simplified geological map of the Ellisras Basin (Based on the 1:250 000 Geological Sheet, 2326 Ellisras (Brandl, 1996)

The Karoo Supergroup ranges in age from Late Carboniferous to Early Jurassic, and reflects a progressive climatic shift from glacial to cool, moist conditions to progressively warm, semi-arid and finally to a hot environment. The arid conditions are attributed to the latitudinal drift from cold/glacial to desert climatic belts.

The development of the Main Karoo Basin (MKB) within a defined tectonic setting proposed by Lock (1978); Hälbich (1983); Winter (1984); Wit et al. (1988); and Johnson (1991), and built upon by Catuneanu et al. (1998), has led to the interpretation that the MKB formed within a retroarc foreland environment, with the smaller basins to the north interpreted either as rift basins or intracratonic thermal sag basins (Groenewald et al., 1991; Bordy and Catuneanu, 2002). Catuneanu et al. (2005) concludes that for the south-central Africa Karoo basins' formation: 1) tectonism was the primary control for accommodation, in which the authors provide support for the retroarc foreland model; and 2) note that sedimentation patterns observed within the Karoo basins' were influenced by shifting climate regimes. Turner and Thomson (1998) and Turner (1999) propose an alternative model to the foreland basin for the Upper Karoo Basin, based on evidence from sequence stratigraphy and crustal doming related to mantle plume activity, and early continental rifting prior to lava eruption. The concerns and arguments raised by Turner and Thomson (1998) and Turner (1999) are disputed by Bordy et al.(2005) and to-date there has been no counter arguments. Tankard et al. (2009), building on the work by Pysklywec and Mitrovica (1999), reject the foreland basin model or a flexural foreland basin, and instead argue that large-scale episodes of subsidence were the result of lithospheric deflection due to mantle flow coupled to distant subduction-driven mantle flow.

The Ellisras Basin is located on the southern border of the Limpopo Belt, which during the Early Triassic underwent tensional faulting, the effect of which created some tectonic instability that in turn contributed towards the structural development of the basin. The effects of sediment loading within the basin may have also contributed towards the re-activation of the surrounding faults. The stratigraphic column (Table 2.1) of the basin reflects the changes in energy levels of deposition and reflects several changes in depositional environment including glacial lacustrine at the base of the sequence, braided and meandering rivers, deltaic plains (coal- bearing), alluvial fans, and desert settings towards the top (Faure et al., 1996b; Cairncross, 2001; Johnson et al., 2006).

As there are few surface outcrops within the Waterberg Coalfield, much of the geological mapping and interpretation has been done using the drill hole data. Most work recognised the fault-bounded nature of the coalfield, but its subsurface structure was not clarified (De Jager, 1986; Siepker, 1986; Brandl, 1996). Fourie (2009) and Fourie et al. (2009, 2014) from the results of a 2008 high-resolution airborne geophysical survey across the Waterberg Coalfield were able to: 1) reinterpret the structures of the Ellisras sub-basin; 2) show that the Karoo Supergroup fill to be twice the thickness originally believed; and 3) classify the sub-basin as a half-graben. Several cross-sections (Figure 2.2) of the gravity and magnetics surveys flown over the Waterberg region have provided evidence of the basin geometry, and how it is bounded and influenced by faults and tectonic forces over time. The predominant scientific opinion is that the sub-basin formed within a graben (Jeffrey, 2005a; Mtimkulu, 2009; Bester and Vermeulen, 2010; Roux, 2011; Wagner and Tlotleng, 2012; Sullivan et al., 2013). In addition to the geological mapping, several palynological and palynostratigraphic correlation studies have been undertaken within the Waterberg Coalfield, and these assisted with the biostratigraphic correlation, the correlation of lithological units from different basins, and the determination of lithological boundaries within the basin (MacRae, 1987, 1991; Barbolini, 2010; Bordy et al., 2010).

Fourie et al. (2011) proposed that the basin evolution is similar to that of the Tuli Basin, whereby a period of extensional tectonics, which probably coincided with subsidence and deposition of the Karoo aged rocks, has resulted in a series of east-west trending faults. A final period when tectonic resetting occurred about 180-200 Ma may have caused reactivation along pre-existing normal faults.

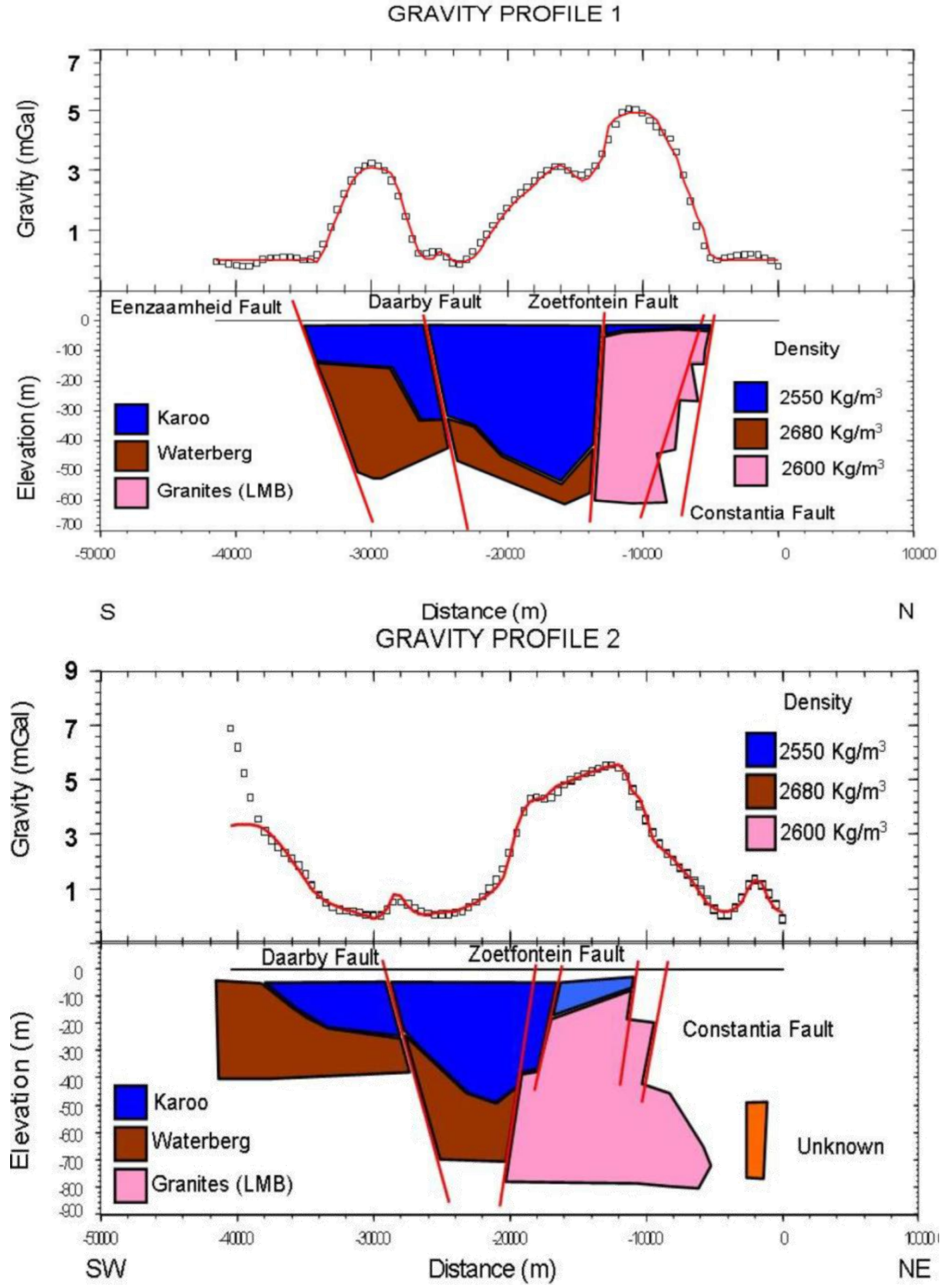

Figure 2.2 Gravity profiles of the Waterberg area showing the half-graben nature of the basin (Fourie and Stettler, 2011)

Table 2.1: Stratigraphy of Waterberg Coalfield

Group	Formation (South African Committee for Stratigraphy, 1980)	Formation Johnson et al., 1996	Lithological Description (Siepker, 1986; Mtimkulu, 2009)	Average thickness (m) (Siepker, 1986)	Paleoclimate (Mtimkulu, 2009)
Drakensberg	Letaba	Letaba Formation	Basaltic Lava	>125	
Stormberg	Clarens	Clarens Sandstone	Massive, cream to off-white, well sorted, fine- grained sandstone; with locally occurring coarser-grained units and pebbly sandstones	130	Desert dominated by dunes with minor wadis feeding sabkhas and playas
	Elliot	Lisbon Formation	Succession of largely red massive mudrocks and minor (lenticular) fine to coarse sandstones with pebble washes. Calcareous concretions are common in the mudrocks, and also present are 5-10 m thick cycles of thin basal sandstone passing up into siltstone or mudstone	100-110	Meandering rivers and floodplains under warm and dry conditions
	Molteno	Greenwich Formation	Medium- to coarse-grained purple-red-green-white sandstone (slightly feldspathic; fine sandstones are micaceous). Commonly cross-bedded, with grit, and local thin conglomerate lenses and thin laminated mudstones. Upward-fining units are common, mostly capped by thin mudstones Low level of radioactivity associated with the mudstone directly under the sandstone	7-33	Braided stream deposits
Beaufort	Beaufort	Eendragtpan Formation	Variegated mudstones, becoming silty in the lower third of the succession. The colour varies from grey to blueish grey with purple and red towards the top, with common reduction spots. There are thin beds of yellow-grey mudstone locally with a low level of radioactivity. Sharp boundaries exist between differently coloured beds	40-110	Floodplain or flood basin deposit – with total absence of plant or coaly material
Ecca	Volksrust	Grootegeluk Formation	Mudstone, carbonaceous shale and coal, all repeated cyclically – cycles have basal coal layer with sharp basal contact, grading up into mudstone. Lenses, concretions and nodules of siderite are common throughout the succession, along with fracture-fillings of calcite and pyrite. Mudrocks vary from a dark very carbon-rich and laminated type, to a light coloured slightly carbonaceous and massive type (thicker beds which overlie the former type gradationally). Coals and highly carbonaceous shales are prominent in the lower half of the succession	10-110	Tectonically stable area with delta abandonment and fluctuating water table – muddy material was probably derived from an alluvial fan to the N
	Vryheid	Goedgedacht Formation	Mudstones with graded bedding as well as with angular quartz grains (sand to pebble sizes) in their basal parts, which may be capped by thin impure vitrinite-rich coal. Also present is soft sediment deformation, and intra-formational clay pellets and coaly material are common. Upward-coarsening units (coaly mudstone-mudstone-siltstone- medium- to course- grained sandstone) only occur locally; upward-fining cycles are rare. The contacts between units are generally sharp but not erosive. A few outcrops are comprised of alternating gritty sandstone and mudstone, or of gritty feldspathic sandstone (all in basal part of formation). Mudstones are massive and are thought to reflect mudflows, with localized sandstones probably reflecting braided streams on a fan surface	0-80	Alluvial fan in a proglacial setting with stagnant or retreating glaciers to the N, and progradation of the fan to the S. Scattered grains of quartz (not of feldspar) in mudstones decrease from N to S, with southern-most mudstones having none
	Pietermarizburg	Swartrant Formation	**Lower zone**: Sandstones, some finer material, No. 1 coal seam (dull coal) – with flaser structures, ripple cross-laminations and cross-bedding; plant root imprints are also quite common. **Middle zone**: various sandstones and mudstones, also coaly shales and sandstones, and No. 2 coal seam, with plant root imprints. **Upper zone**: N facies: sandstones, mudstones and coal seams, erosionally overlain coarse, cross-bedded feldspathic sandstone. S facies: immature coarse cross-bedded sandstone erosionally overlying No. 2 coal seam, and grading up into flaser bedded and wavy laminated mudstone with a thin, impure coal seam.	2-130	**Lower zone**: delta-front which, in time, became a delta plain for the deposited coal **Middle zone**: glaciolacustrine with a delta front approaching from the east – with deep water formation for the coals. **Upper Zone**: Braided or meandering streams migrating onto a delta or flood plain
Dwyka	Not named	Wellington Formation	Basal mudrocks with sandy lenses and small dropstones, coarsening upward to silty or even sandy rocks. In some boreholes the Wellington Formation starts with extensive fine- to coarse-grained sandstones. In outcrops, limestones are up to c. 30 cm thick and are associated with sandy shales and feldspathic sandstones.	20-160	Formed in a large standing body of water, which was brackish or salty
	Not named	Waterkloof Formations	Diamictite, mudstone and conglomerate. In the SW, in place of diamictite, there is mudstone and rhythmite with common dropstones	26	Outwash formed from reworked tills from glaciers retreating in the N and NE areas

2.2. Waterberg Coalfield

Fourie et al. (2014) and Hancox and Götz (2014) provide a comprehensive summary of the previous work reported for the Waterberg Coalfield. These were used as a basis for the following section with additional information.

2.2.1. History of Mining within the Coalfield, especially at Grootegeluk Mine

A brief history of coal mining in the area is summarized in Table 2.2, with a focus on Grootegeluk.

The possible future of the Waterberg Coalfield is uncertain, as will be discussed later, as is the future of coal mining in South Africa. However, as indicated in Figure 2.3 there are several prospecting, mining, exploration and production rights and permits over the basin. It is worth pointing out the difference in the different legal terms used in South Africa mineral tenure – Prospecting and Mining Rights relate to minerals, in this case coal and strangely underground coal gasification ('UCG'), while Exploration Permits and Production rights relate to petroleum and gas. Prospecting Rights and Exploration Permits are the required precursors to the exploitation phase of an operation. There are many other differences, but for the purposes of this research report, the above will suffice.

As indicated in Figure 2.3 the majority of the Waterberg Coalfield has approved mineral rights granted for either coal or shale gas. The companies that retain the majority of the rights within the region are Exxaro and Anglo Gas. However only Exxaro's Grootegeluk Mine is operational. There are several companies that are attempting to open coal mines within the coalfield (Kruger, 2013; Mc Kenna and Myburg, 2013; Joubert et al., 2016) but to-date these companies have accrued little success. This puts forward the question as to why there hasn't been more development within the coalfield. Jeffrey (2005b) considers the question and identifies several challenges to further development as follows: 1) a lack of market for low-grade coal; 2) challenges associated with extraction i.e. faults, underground vs opencast vs alternative technology (UCG); 3) beneficiation – low yields vs large tonnage mined; 4) lack of water; 5) mitigation of environmental impacts i.e. impact on groundwater, air pollution and spontaneous combustion; 6) Not enough rail infrastructure; and 7) socio-economic impacts – the majority of the population in the region is unskilled and unemployed. While there is an option for the development of a Secunda-type petrochemicals complex in the region, the establishment of such a complex would have a profound impact on the region.

Table 2.2: Brief summary of the history of Grootegeluk Coal Mine and Waterberg Coalfield.

From	To	Comment	Ref
1920		Discovery of coal within the area occurred in 1920 during water drilling operations on the farm Grootegeluk 459LQ	(Snyman, 1998)
1920	1922	Reconnaissance study of the area was undertaken by A.L. Du Toit and H.F. Frommurze. A few other boreholes were drilled in the vicinity and the coals samples were sent for analysis	(Trevor and Du Toit, 1922; Alberts, 1982; Roux, 2011; Hancox and Götz, 2014)
1922		The results of 1920-1922 drilling were published in 1922 in the South African Journal of Industries	
1941	1952	The Geological Survey Division of the Department of Mines determined the extent of the Waterberg Coalfield and the qualities of the coal by means of geological mapping, 143 boreholes, and two prospecting shafts. The results indicated vast reserves of metallurgical and non-metallurgical coal.	(Cillié and Visser, 1945; Cillié, 1951, 1957)
1955		Minister of Mines reserved coal on 29 farms in the coalfield for ISCOR and SASOL.	(Alberts, 1982; SRK Consulting, 2006;

From	To	Comment	Ref
1955		The first extensive drilling subsequent to the Geological Survey work was exploration drilling undertaken in 1955 in a joint programme by ISCOR and SASOL.	Roux, 2011; Hancox and Götz, 2014)
1957		ISCOR acquired the property rights over six farms in the area that formed part of the 29 farms on which coal was reserved for ISCOR and SASOL.	
1959	1960	Samples of coal for coking tests were obtained from 22 large diameter boreholes (254 mm core), drilled along a line between the prospecting shafts on Grootegeluk 459LQ and Hieromtrent 460LQ	
1960	2010	Preliminary mining occurring on the farm Grootehoek 504LQ during the 1960s until the mid-20th century with several studies conducted to determine the extent and the resource and the feasibility of a proposed larger scale operation	(Kruger, 2013)
1961		Minister of Mines reserved coal on 2 farms in the coalfield for ISCOR and SASOL	(Alberts, 1982; SRK Consulting, 2006; Roux, 2011; Hancox and Götz, 2014)
1964		Minister of Mines reserved coal on 5 farms in the coalfield for ISCOR and SASOL	
1965	1966	SASOL undertook an additional 120 borehole programme, this is the first extensive drilling subsequent to the original 143 holes done during 1941-1952	
1965		Minister of Mines reserved coal on 86 farms in the coalfield for ISCOR and SASOL. As a result of the reservations, ISCOR and SASOL were the only two parties qualifying to apply for prospecting or mining leases in respect of coal over a total of 125 farms in the Waterberg Coalfield.	
1973		ISCOR starts an intensive exploration programme on the six farms originally purchased in 1957 for a final assessment of the resource and quality of coal on these properties	
1974	1980	Following on a positive feasibility study the Iscor board approved the opening of the Grootegeluk mine in February, with the commissioning date set for the 1st of July, 1978. Difficult economic conditions in South Africa in the early 1970s, coupled to ISCOR's commitment to other capital projects saw the postponement of the commissioning to the middle of 1980. The coal mine and beneficiation plant at Grootegeluk were commissioned on the revised schedule, with the first train of metallurgical coal loaded and dispatched to the Vanderbijlpark works on the 23rd of July, 1980	
1975		ISCOR established a trial box-cut on Enkelbult 462 LQ to obtain a bulk sample for beneficiation tests.	
1979		ISCOR and ESKOM reach an agreement to provide coal to a power station still to be erected at the time. Although the initial tender was for a 2 400 MW station, it was later increased to 3600 MW. The projected life of this power station (Matimba) was 40 years and therefore a pit layout containing 40 years saleable thermal coal was designed.	
1980		Grootegeluk Mine is commissioned, originally designed to supply semi-soft coking coal to be used as a reduction agent for ISCOR's steel production	
1980	1990	Bulk samples were excavated from the farm Grootehoek 504LQ in the 1980's from a small vertical shaft sunk to a depth of 70-80m	(Kruger, 2013)
1980	1981	Eight drillholes were drilled on four of the five Thabametsi farms	(Exxaro (Pty) Ltd, 2015)
1988		Two drillholes were drilled on the remaining Thabametsi farm, van der Waltspan	
1989		ISCOR privatised	(SRK Consulting, 2006; Roux, 2011; Hancox and Götz, 2014)
1990		The potential for CBM production in the deeper eastern portion of the Waterberg Coalfield was identified by Anglo Coal	
2001		ISCOR unbundled as Kumba Resources and ISCOR	

From	To	Comment	Ref
2006		Kumba Resources separated into Kumba Iron Ore and Exxaro Resources	
2006		Grootegeluk reports that it has reserves of 2986 Mt from a total resource base of 4887 Mt.	(Dreyer, 2006)
2008		DMR grants approval for Medupi Expansion at Grootegeluk. The expansion project will result in an increased rate of mining, but the total volumes mined will be the same as originally approved, however, life of mine will be reduced from 70 years to 40 years.	(SRK Consulting, 2006; Roux, 2011; Hancox and Götz, 2014)
2008		Exploration activities began in earnest on the Thabametsi project area with 61 holes planned at the time	(Exxaro (Pty) Ltd, 2015)
2016		Grootegeluk reports that it has reserves (measured) of 3298 Mt from a total resource base of 4528 Mt. Using approx. 611 drillholes Thabametsi Project has 112 drillholes	

Jeffrey (2005b) also provided suggestions for the future development in the region, i.e. from 2005 onwards. It is interesting reflecting on these suggestions with the 20/20 vision of hindsight. A new power station accepting low-grade coal within the Waterberg Coalfield was suggested by Jeffrey (2005b). Madupi is currently nearing finalization; and the Independent Power Producer (IPP) programme process announced in 2016 that there will be an IPP power station built within the Waterberg. To address the water supply issues, the Mokolo and Crocodile Water Augmentation Project (MCWAP2) was drafted and is in the process of being implemented. Unfortunately the process has stalled as the project requires financial backing from the mines requiring access to the water, but the mines requiring the water to operate do not have the financial resources upfront to back the project. The National Development Plan (National Planning Commission, 2011) put forward the framework to address the infrastructure challenges. Here again a scenario has developed where the government has committed to build the necessary infrastructure if there is a need, and this need will only materialise once the additional mines start, but the mines require the assurance that the infrastructure will be in place before they start operations. Steyn (2009) as part of a MSc thesis reviewed the marketing aspects of coal within South Africa, and as a recommendation echoed similar sentiments as put forward by Jeffrey (2005b).

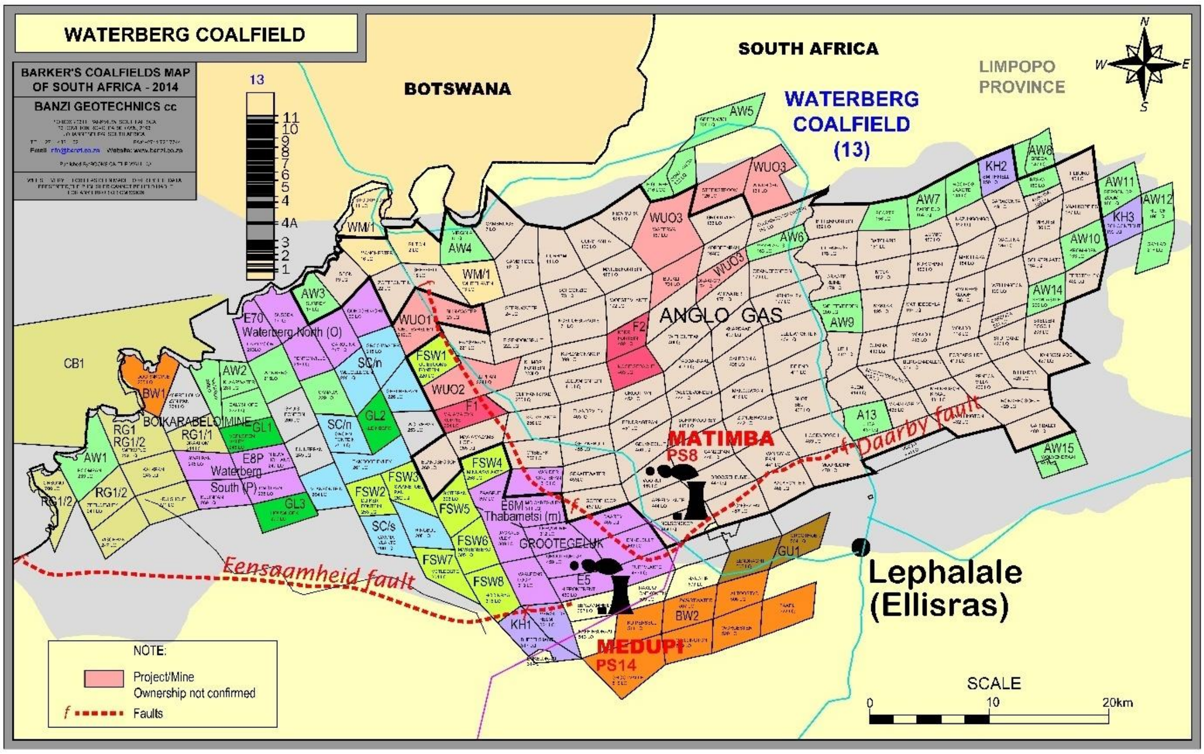

Figure 2.3: Plan showing the farms contained within the Waterberg Coalfield with the various colours indicating the ownership of mineral rights to various entities. The mineral rights indicated are associated with coal or shale gas prospects. (Banzi Geotechnics, 2014).

2.2.2. Previous Research within the Waterberg Coalfield

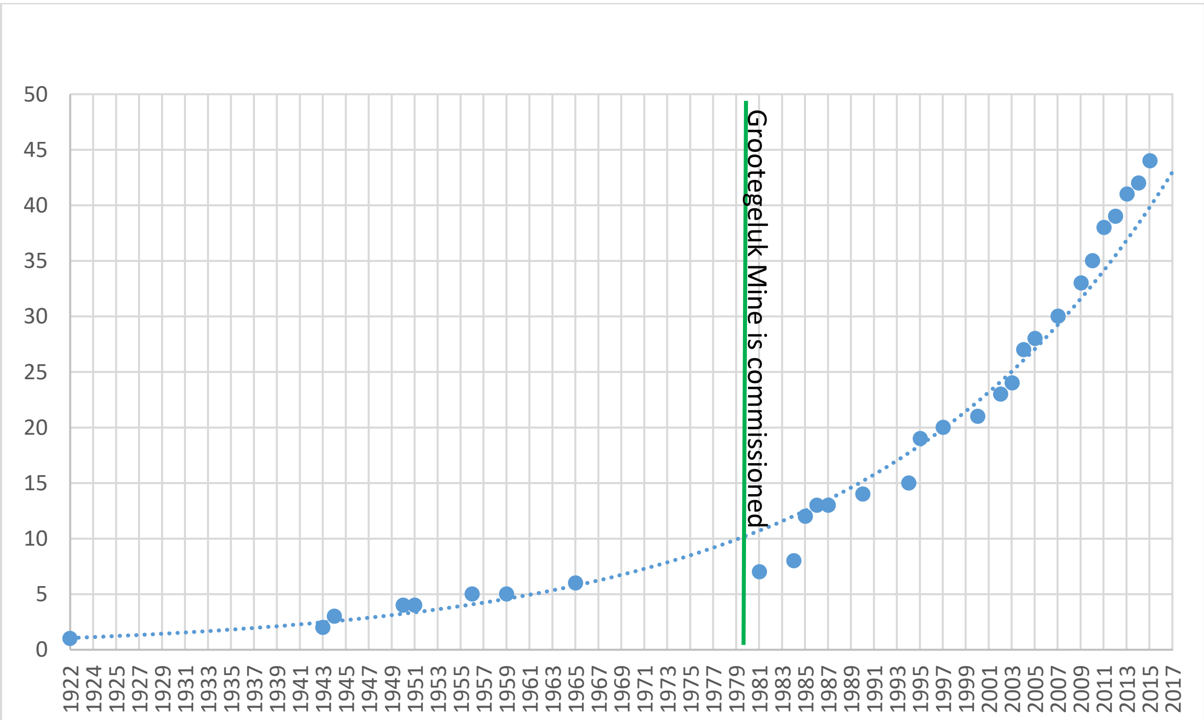

Figure 2.4 The approximate cumulative number of publications related to the Waterberg Coalfield over time and the effect of the opening of the Grootegeluk mine has had on research

Initial work within the Waterberg Coalfield was slow, but based on Figure 2.4 and Appendix A, there is a clear, near exponential, growth in the number of publications following the commissioning of the Grootegeluk in 1980.

Several overview or review papers over the years have discussed the coal resources of southern Africa: Falcon (1986) provided one of the earliest, most comprehensive, reviews on the origin, formation and distribution of the coal within southern Africa. Smith and Whittaker (1986) provided a summary of the southern African coalfields, while De Jager (1986) provided a more detailed look into the then Transvaal (now Limpopo) coalfields. It is worth noting at this point that while there was information pertaining to the Waterberg Coalfield there was very little available when Anhaeusser and Maske (1986) complied the "Mineral Deposits of Southern Africa". Snyman (1998) provided a detailed overview of coal within South Africa while Barker (1999) gave a review of the coal industry. Cairncross (2001) reviewed the Permian coal deposits within southern Africa. Jeffrey (2005a) gave a characterisation of the coal resources of South Africa, while Johnson et al. (2006) discussed the Karoo Supergroup. Hancox and Götz (2014) provided a detailed review of South Africa's coalfields and Hancox (2016) published a review of the coalfields of South-Central Africa.

Pre-1980s work focused on the results of the exploratory holes across the basin (Venter, 1944; Cillié and Visser, 1945; Cillié, 1951, 1957). The unpublished sedimentological study by Ryan (1966) based on the few outcrops of Karoo, focused mainly on the carboniferous clastic matter from the exploratory holes' logs.

The Journal of the South African Institute of Mining and Metallurgy vol. 82, no. 12. Dec. 1982 provides several papers that focus on the establishment of the Grootegeluk Coal Mine (Alberts, 1982; Buermann, 1982; Ferreira and Coreejes, 1982; Gilliland, 1982; Kotze, 1982). Alberts (1982) provides a history of the establishment of the Grootegeluk Coal Mine, noting that the reserves of the mine to be 2300 Mt and that the first train left the mine on 23rd July 1980. Snyman and Botha (1993) placed the Waterberg Coalfield reserves at 55 Gt, with a potential resource of 121 Gt. Due to improvements in estimation and mining methods, some 35 years later after the first train leaving the Grootegeluk Mine the *Exxaro CMRR* (2015) states that there is still 3200 Mt run-of-mine (ROM) remaining from the current 4500 Mt resource, with 46 Mt mined during the 2014/2015 period. Van Heerden (2016) in an MSc thesis considers the phosphorous content of the coal within the Grootegeluk Mine, and provides recommendations on how to utilise the resource more effectively by blending and via selective mining.

Building on the previous work done by Beukes (1985), Siepker (1986) provided a complete overview of the stratigraphy, sedimentology and depositional environments of the Waterberg Coalfield. Hancox and Götz (2014) considered this work as the most comprehensive academic coverage of the coalfield to date. Building on Siepker's (1986) seven genetic increments of sedimentation (GIS 1–7), Beukes et al. (1991) established a genetic stratigraphy for the Waterberg Coalfield. Brandl (1993, 1996) based much of the information for the Waterberg Coalfield on the work done by Siepker (1986). Mtimkulu (2009), using 830 borehole logs and the work done by Siepker (1986), put forward a provisional basinal analysis of the Waterberg Coalfield, the aim of which was to create a theory relating to the formation of the Ellisras Basin and its sedimentary fill.

Faure published several papers (Faure, 1993; Faure et al., 1995, 1996b; a) which focused on the geochemistry of the mudstones within the Waterberg Coalfield. Further trace element studies were conducted by Wagner and Tlotleng (2012) on four Run of Mine (RoM) coals and density fractioned samples. Here the results showed that the concentrations of most trace elements, except Se and Cd;

and As in the Vryheid sample, exceed the global averages or Coal Clarks values.(Ketris and Yudovich, 2009)

The provenance of the sediments within the Waterberg Coalfield has been a topic of discussion since 1967 when Ryan (1967) proposed that the sediments had originated from the north-west and east of the present Kwa-Zulu coast. Falcon (1986) on the other hand considered the Kaapvaal and the Zimbabwe cratons to be the source(s) of the Karoo strata. Siepker (1986) proposed the following: 1) the Swartrant Formation palaeocurrents and sandstone-channels were orientated east-west; 2) the Grootegeluk and Eendragtpan Formations had a provenance from the north. Faure et al. (1996b) supported Siepker (1986) and put forward the Damaran orogenic belt to the northwest as a possible source for the Grootegeluk and Eendragtpan Formations. They go further to state that the Grootegeluk and Eendragtpan Formations do not have the same provenance as the stratigraphic equivalent sediments in the northern Main Karoo basin, but that the Swartrant Formation had a common average provenance. Fourie et al. (2014) state that the Bushveld Complex and Limpopo Mobile Belt rocks are the source of the sediments within the Ellisras Basin.

Bester and Vermeulen (2010) studied and modelled the aquifers within the Waterberg Coalfield with regards to their geohydrological parameters in particular the quantity and quality of the existing water resource. Additionally these workers studied the acid-generating potential and buffering capacity of the sediments within the Waterberg Coalfield. Aphane and Vermeulen (2015) conducted acid-base accounting for the Waterberg Coalfield to determine the acid mine drainage potential of the sediments exposed during proposed mining, the authors found that the interburden from the Vryheid and Volksrust Formations held the largest potential for acid generation. Additionally, that both the oxidation of the coal and the carbonaceous shale/mudstones results in acid generation, which in turn contributes towards the leaching of sulphates and iron into the environment.

2.2.3. Coal Seams in the Waterberg Coalfield

The South African guide to the systematic evaluation of coal resources and coal reserves (Standards South Africa, 2004) provides two coal deposit types i.e. “multiple seam deposit type” and “thick interbedded seam deposit type”. The majority of authors divide the Waterberg Coalfield into both types of deposits, with the Volksrust Formation classified as a ‘Thick Interbedded Seam Deposit Type’ and the Vryheid Formation classified as a ‘Multiple Seam Deposit Type’ (Jeffrey, 2005a; Mtimkulu, 2009; Roux, 2011; Mc Kenna and Myburg, 2013; Hancox and Götz, 2014; Exxaro (Pty) Ltd, 2015; Hancox, 2016; Van Heerden, 2016)

The Volksrust Formation, or upper coal, is represented by inter-bedded carbonaceous shales and coal. At the Grootegeluk Mine this Formation is divided into seven zones and mined in benches named from top to bottom as benches 1 to 5 (see Figure 2.5). The upper portion of the Volksrust Formation yields semi-soft coking coal, while the rest of the Formation yields varying grades of thermal coal (Dreyer, 1994).

The Vryheid Formation, or lower coal, is locally made up of five distinct coal seams composed of predominantly dull coal interbedded with carbonaceous mudstone and shale. These coal seams are named from the bottom upwards from Zone 1 through Zone 4 with Zone 4 being further subdivided into Zone 4 seam at the top and Zone 4A which is inter-bedded coal and shale towards the base. Grootegeluk extracts these coal zones in four distinct benches with the exception of Zone 1 of which is considered uneconomical. Both Zone 3 and Zone 2 coal seams are known to yielding small quantities of semi-soft coking coal (Dreyer, 1994).

2.3. U and Th within the Waterberg Coalfield

The purpose of discussing the role of U and Th within the literature is that the literature itself provides evidence in support of the hypothesis that the Waterberg Coalfield contains U and Th. In addition, as per Phase 1 of the scope of the study, the literature provides target horizons/zones that were further investigated in subsequent phases.

2.3.1. U and Th within the literature

Siepker (1986), while discussing the Eendragtpan Formation indicated that there was a khaki-yellow mudstone which displays radioactivity. In addition, the author notes that the mudstone associated with the basal contact between the Greenwich Formation and Eendragtpan Formation also displays radioactivity.

Faure (1993) and Faure et al. (1996a; b) reported values for U and Th within mudstones and shales in the Beaufort Formation, Grootegeluk Formation and Vryheid Formation. The values are contained in Table 2.3 fall above the global average range proposed by Swaine (1990) (5-10 ppm).

Table 2.3 U and Th values from Faure (1993) and Faure et al. (1996a; b)

	Beaufort / Eendragtpan		Grootegeluk		Vryheid / Swartrant	
	(mean)	**1 standard deviation**	**(mean)**	**1 standard deviation**	**(mean)**	**1 standard deviation**
U (ppm)	25	14	8	2	12	2
Th (ppm)	28	4	38	10	51	10
Number of samples	6		209		6	

Oboirien et al. (2016), used a coal sample from the Waterberg Coalfield to determine if there is enrichment of trace elements in bottom ash. While the author does not explicitly state from which lithology the sample originated, it is possible to make an estimate based on the proximate, ultimate and ash chemistry provided. Based on these values it appears to have originated from the Vryheid Formation. The U value for the coal sample is given as 2.17 ppm.

Airborne geophysical studies conducted and reported by Fourie et al. (2008, 2009, 2014), Fourie (2009), and Fourie and Stettler (2011) provides airborne radiometric surveys of the Waterberg. A study of the radiometric results in respect to the exposed open cast and dump areas of the Grootegeluk Mine, Figure 2.6, indicates values of more than 17 counts per second for U.

While the airborne radiometric survey results need to be approached with caution, as the depth of penetration is limited to approximately 0.3 m and much of the Waterberg Coalfield has more than 2 meters of soil cover, the airborne geophysical studies indicate that the exposed Vryheid; Grootegeluk; and Eendragtpan Formations have elevated values for U.

Wagner and Tlotleng (2012) sampled four run of mine (ROM) samples from the Grootegeluk Mine coal benches, namely Benches 3, 4, 5 and 11 (See Table 3.2 for reference to general location of the samples with reference to the benches). The coal samples were then density fractionated and the individual fractions analysed. Table 2.4 indicates that the majority of the samples fall below the global average range proposed by Swaine (1990) (5-10 ppm for both Th and U).

Formation	COAL ZONES & SAMPLES	Average Thickness	% Coal (in situ)	Lithology	Bench Heights
VOLKSRUST FORMATION	Overburden	16.5m		Sand and topsoil (±1m) with scattered ferricrete and calcrete nodules, yellow-brown mudstone, massive and weathered in top half, light gray mudstone and bright coal bands in bottom half.	15.8m
	ZONE 11 Sample 1a-d	7.56m	38.33	Bright coal interbedded with gray mudstone, carbonate lenses, no siderite present.	13.5m
	ZONE 10 Sample 2-6	9.37m	53.86	Bright coal interbedded with carbonaceous shale/mudstone, carbonate lenses, small amount of siderite present, thick mudstone plies present in bottom half.	
	ZONE 9 Sample 7-9	6.53m	48.34	Bright coal with prominent siderite present at base, interbedded with carbonaceous shale/mudstone. Thick basal coal seam.	16.1m
	ZONE 8 Samp. 10-14	9.04m	42.82	Bright coal with prominent siderite present at base, interbedded with carbonaceous shale/mudstone. Thick coal seam at base.	
	ZONE 7 Samp. 15-18	10.15m	39.94	Bright coal, sideritic, interlayered and interlaminated with carbonaceous shale/mudstone.	16.9m
	ZONE 6 Samp. 19-21	6.54m	32.17	Bright coal, very sideritic at bottom, interlaminated with carbonaceous shale/mudstone.	
	ZONE 5 Samp. 22A-22E	13.54m	21.97	Carbonaceous shale/mudstone, thin coal bands present in bottom two-thirds, less prominent siderite content, 2.5m coal-rich shale at base.	16.7m
VRYHEID FORMATION	ZONE 4 Samp. 23a-c	4.02m	99.13	Dull coal, interlaminated with bright coal in bottom portion, few thin shale bands present.	4.1m
	Interburden	4.28m		Mudstone, dark-grey, with fossil bearing siltstone at base.	5.7m
	ZONE 4A	1.52m	96.37	Dull coal, few thin bright coal laminae and few thin shale bands.	1.4m
	Interburden	4.28m		Mudstone, dark-gray	3.7m
	ZONE 3 Samp. 25-29	7.82m	96.41	Dull coal, with bright coal laminae present in bottom 1.6m portion, low ash content, few thin shale bands.	8.2m
	Interburden			Sandstone, medium to coarse grained, few thin shale bands present, few thin coal laminae at top.	4.1m
	ZONE 2 Samp. 30-31	3.73m	98.22	Dull coal, bright coal laminae present in the bottom 2m portion, low ash content, show coking characteristics.	4.3m
	Interburden	13.85m		Sandstone, medium to coarse grained, few thin shale bands present, thin coal laminae at top.	
	ZONE 1	1.53m	98.34	Dull coal, few coal laminae and thin shale bands.	

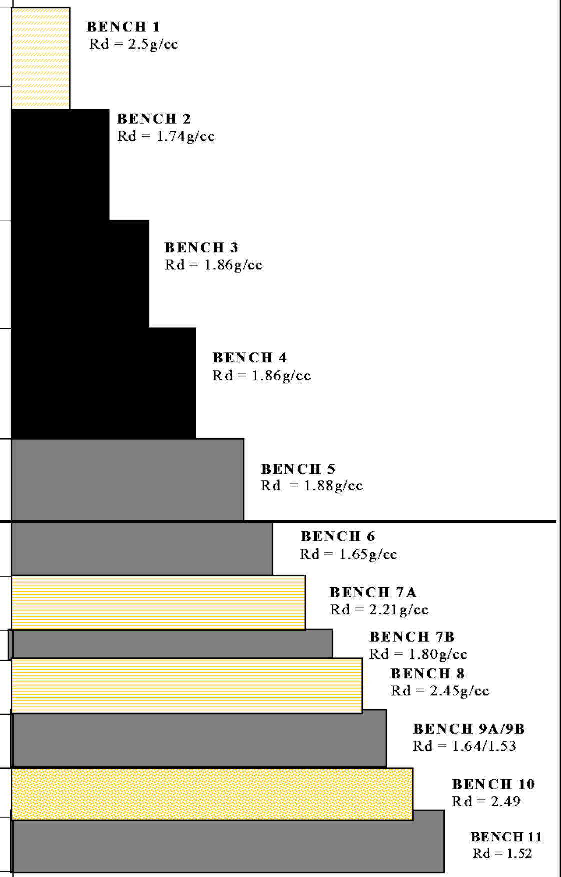

Figure 2.5 Exxaro Grootegeluk Mine Zone (seam) nomenclature by mining bench showing thickness & lithology (Kumba Coal (Pty) Ltd, 2005; Roux, 2011)

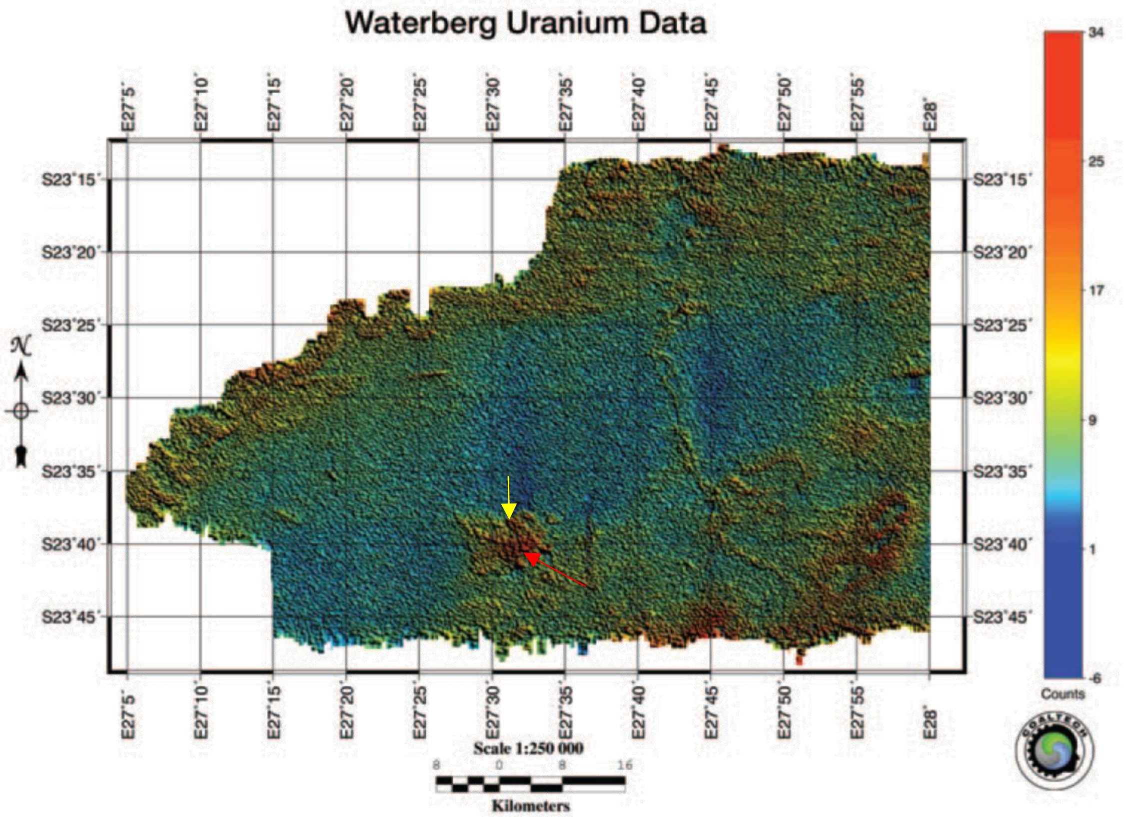

Figure 2.6 "New U Radiometric Data collected across the Ellisras Basin in which the Waterberg Coalfield is situated" (Fourie et al., 2014, fig. 4 (c)). The red arrow shows the location of the Grootegeluk Mine open cast pit, while the yellow arrow indicates the location of the dump.

Table 2.4 Excerpt of the analysis with regards to U and Th from Wagner and Tlotleng (2012). The bold values indicates when the value is in exceedance of the global average range as per Swaine (1990).

Formation	Sample	Th	U
Grootegeluk	Wagner B3 Coal (unfractionated)	**7.51**	3.07
	Wagner B3 float RD 1.5 Coal	2.15	2.24
	Wagner B3 float RD 1.9 Coal	2.33	1.95
	Wagner B3 float RD 2.4 Coal	**6.86**	3.26
	Wagner B3 sink RD 2.4 Coal	2.59	3.77
	Wagner B4 Coal (unfractionated)	1.23	3.51
	Wagner B4 float RD 1.5 Coal	3.06	3.49
	Wagner B4 float RD 1.9 Coal	**11.7**	3.33
	Wagner B4 float RD 2.4 Coal	0.95	3.1
	Wagner B4 sink RD 2.4 Coal	1.48	4.15
	Wagner B5 Coal (unfractionated)	**9.48**	**5.37**
	Wagner B5 float RD 1.5 Coal	**5.66**	**5.27**
	Wagner B5 float RD 1.9 Coal	3.31	4.82
	Wagner B5 float RD 2.4 Coal	3.82	**5.53**
	Wagner B5 sink RD 2.4 Coal	**5.82**	1.96
Vryheid	Wagner B11 Coal (unfractionated)	2.19	1.88
	Wagner B11 float RD 1.5 Coal	1.63	1.23
	Wagner B11 float RD 1.9 Coal	2.12	2.37
	Wagner B11 sink RD 1.9 Coal	**12.3**	2.47

2.4. Chapter Summary

The primary purpose of this chapter was to provide the reader with the pre-requisite knowledge and background that will be needed for following chapters. Ancillary to this was the initial identification of possible areas of further study in line with Phase 1 of the aim of the project. In this regard both the Grootegeluk Formation's Bench 5 coal, and the Eendragtpan Formation khaki-yellow mudstones were identified as the best possible targets for further study.

Chapter 3

Methodology

3.1. Introduction

The purpose of this chapter is to address the methodology used throughout this study (Figure 3.1).

Figure 3.1 Schematic of methodology and limits used within the study

The project essentially can be grouped into three phases:

Phase 1: Literature compilation and review to address the primary hypothesis. Here a review was conducted on all available literature to 1) identify if there is above the average Th or U contained with the Waterberg Coalfield; and 2) identify lithologies, horizons or geological formations for future study. These results have been provided in Chapter 2.

Phase 2: The generation of a downhole geophysical database with a specific focus on the gamma and density results. The downhole geophysical data originated from either from 1) Exxaro blastholes within the Grootegeluk Mine; 2a) exploration holes from forward drilling at Grootegeluk and Thabamesti Mines; or 2b) prospecting holes drilled at the Zonderwater

Project. The database was analysed for lithologies, horizons or geological formations that displayed gamma values greater than 300 API. These "anomalies" were marked for future study, in addition correlations were attempted across the study areas (blastholes, exploration and prospecting holes) where an anomaly trend was persistent across boreholes.

Phase 3: Samples and analysis. Based on the results of Phases 1 and 2, several targets were identified. These targets would be sampled and an analysis conducted.

3.2. Downhole geophysical surveys (wireline logging) (Phase 2)

The downhole geophysical surveys performed a fundamental aspect of this study. All the subsequent investigations were determined by the results and discoveries found during this phase and therefore the majority of the time spent on this study was focused on the study of the geophysical logs.

For the purposes of this study a total of 7495 boreholes were studied. This consisted of 18 prospecting boreholes from the Zonderwater Project; 26 forward exploration boreholes from the Grootegeluk and Thabamesti Mines; and 7451 blastholes drilled at Grootegeluk (Figure 3.2). The wireline data from these holes were standardised, consolidated and centralised into a single database for the purposes of analysis and correlation.

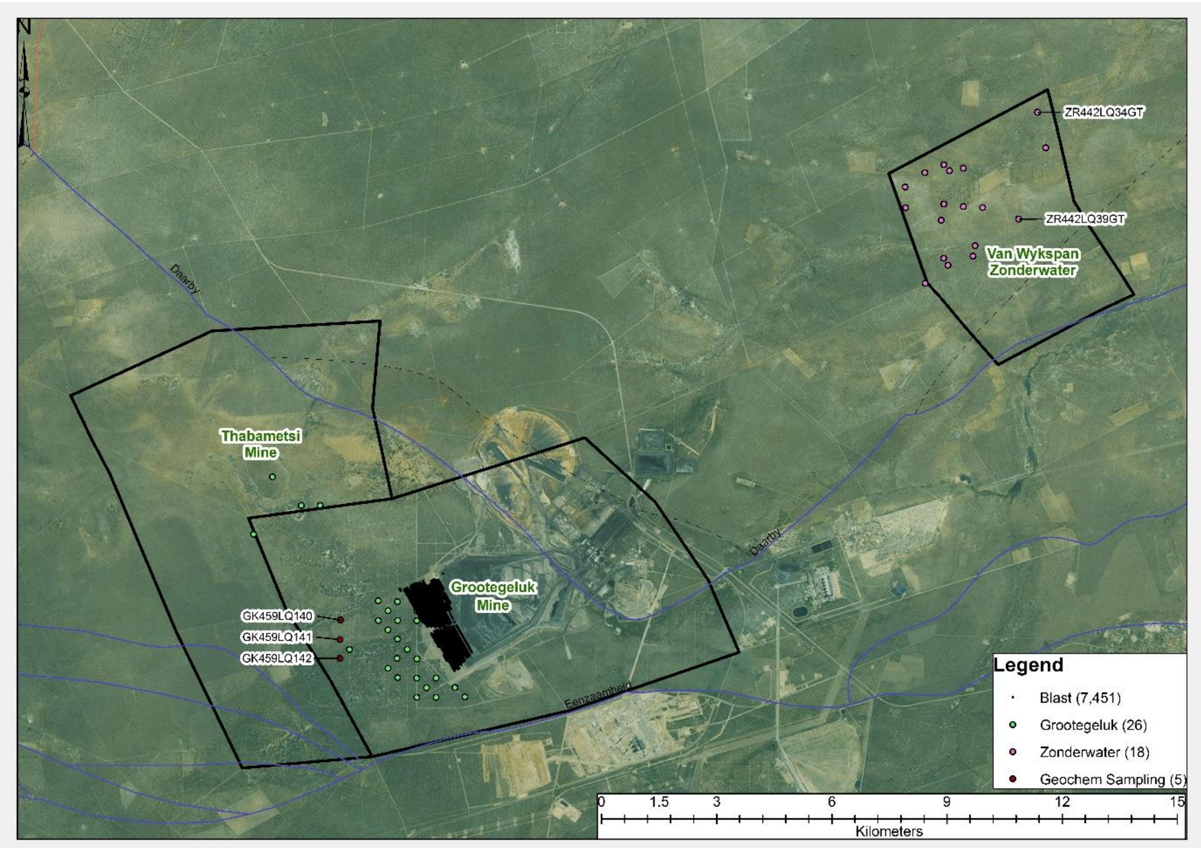

Figure 3.2 Location of boreholes used for geophysical survey within the study area

Wireline logging of completed boreholes was conducted by the utilisation of downhole free-hanging geophysical equipment. Wireline logging was conducted in tandem with traditional geological logging and supplements the geological logging in that the wireline surveys assist in the identification descriptions and boundaries; the accurate determination of lithological thicknesses, identification of facies changes, and borehole correlations. The geophysical tests carried out for each borehole are briefly explained in Table 3.1, and how each test was used for this study.

Table 3.1 Downhole Geophysical tests conducted and the application the test provided to the current study

Geophysical Tests	Information derived	Application to this study
Density	Measures the electron density in the ground which is then translated to the rock density from the atomic number of the compounds present.	1) Aids in the accurate determination of lithology depths. 2) Aids in lithology identification in un-cored boreholes.
Caliper	Measures the borehole diameter along the length of the hole.	None
Gamma	Measures the naturally occurring gamma radiation in the surrounding rock mass.	1) Identify lithologies/zones with high radiation 2) Aids in lithology identification in un-cored boreholes 3) Aids in the accurate determination of lithology depths.
Neutron	Measures a 'hydrogen index' where the number of neutrons detected relates to porosity.	None
Sonic	Measures the rock's capacity to transmit seismic waves giving indication of porosity and strength.	None
Verticality	Measures the dip and azimuth of the borehole trajectory.	None
Resistivity	Measures the electrical conductivity of the rocks which is translated into resistivity.	None
Acoustic Scan	Measures sound wave velocity to generate high resolution formation images.	None

3.2.1. Gamma ray surveys

The logging device responds to the natural gamma radiation in the formation. Potassium, thorium, and uranium are the predominant sources of the natural gamma radiation within formations, with potassium being the largest source of formation radioactivity. Gamma ray (GR) logs are recorded in API units, the definition of the API unit of radioactivity comes from an artificially radioactive formation hosted in University of Houston. This artificially radioactive formation, containing approximately 4% K, 24 ppm Th and 12 ppm U, was defined to be 200 API units. The relationship between compositions and equivalent API contributions to a GR log is given approximately by the multipliers of: 8 for Th (ppm), 16 for U (ppm), and 4 for the K (%) estimates. (Ellis and Singer, 2007; Thomas, 2012)

Equation 1 Prediction formula for the API unit using elemental compositions.

$$Predicted\ API\ Value = \left(8 * Th_{(ppm)}\right) + \left(16 * U_{(ppm)}\right) + \left(4 * K_{(\%)}\right)$$

This relationship provides a useful method to predict GR logging values of shale samples from outcrop and core, based on laboratory geochemical measurements. Thus, applying the 4-8-16 multipliers on several reference shales e.g. North American Shale Composite (NASC) and the Marine Sciences Group Black Shale Composite (BSC) yields API values of 121.7 and 215.84 API units respectively, and based on the ranges generated a value of 300 API units was selected as the upper limit of a normal formation for the generation of targets for further study.

To account for single value anomalies in the data, a thickness constraint of a minimum of 10 cm was applied to the targets. Thus, a target needed to meet the following requirements: 1) Average API value of greater than 300; and 2) a minimum composite thickness of 10 cm.

3.2.2. Density surveys

The density surveys were used to confirm changes in lithology and to help identify lithologies based on the density ranges of each lithology.

3.3. Samples (Phase 3)

Sample selection was determined on two primary factors, namely: 1) identification of zones/formations from Phase 1 and Phase 2; and 2) availability of samples - this study relied on cored samples provided by Exxaro, which were drilled as part of prospecting activities and resource exploration.

Due to Exxaro's drilling methods and sampling systems (Table 3.2), the sampling for this study was limited to 1) formations and benches not previously sampled by Exxaro; and 2) where the core had not been destroyed.

Table 3.2 Sampling nomenclature system used at Grootegeluk Mine to be read in conjunction with Figure 2.5

Formation	Grootegeluk Bench	Coal Zones	Sample Numbers
Volksrust	2	Zone 11	1A - 1D
		Zone 10	2 - 6
	3	Zone 9	7 - 9
		Zone 8	10 - 14
	4	Zone 7	15A - 18
		Zone 6	19 - 21
	5	Zone 5	22A - 22E
	Not mined	**Interburden**	22F**S**
Vryheid	6	Zone 4	23A - 23C
	7A	**Shale**	23A**S** - 23B**S**
	7B	Zone 4A	24
	8	**Shales**	24**S**
	9A/9B	Zone 3	26 – 29
	10	**Interburden**	**Not Sampled by Exxaro**
	11	Zone 2	30A, 30B, 31
	Not mined	**Interburden**	**Not Sampled by Exxaro**
	Not mined	Zone 1	32

3.3.1. Sampling

The 18 samples (Table 3.3 and Figure 3.3) were sourced from two sites, namely the Grootegeluk mine and Zonderwater Project, and taken from five (5) boreholes and 3 bulk samples.

The sandstone to carbonaceous mudstone that forms the interburden of the Zone 2 and Zone 3 coal seams (Bench 10) in the Swartrant Formation was targeted. While the shale interburden between Zone 3 and Zone 4A (Bench 8) was a target for sampling, there was no core available for sampling as Exxaro had previously sampled.

Three (3) bulk samples were obtained from the Grootegeluk mine: two from Bench 10, and one from Bench 8. The location and depth of where these samples originate from are uncertain as they were supplied by Exxaro.

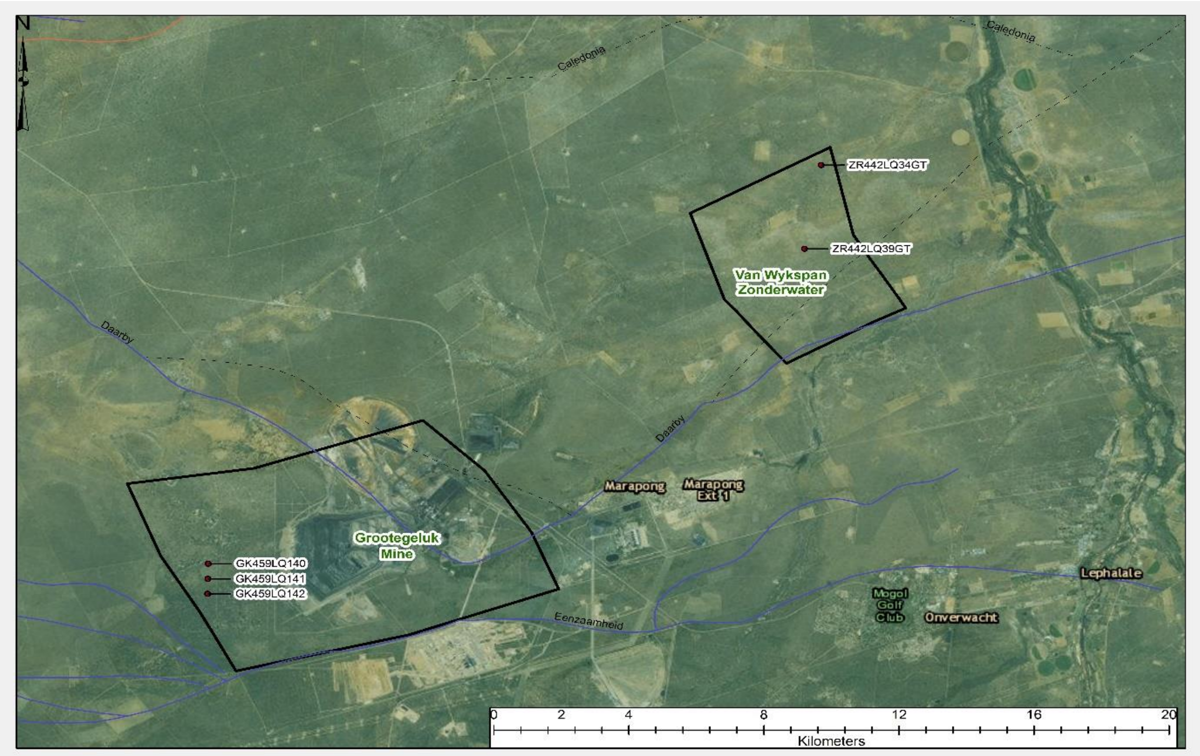

Figure 3.3 Location of boreholes used for samples within the study area

3.3.2. Sample Analysis

All of the analyses were outsourced to UIS (Unique Innovative Scientific) Analytical Services, Centurion. Table 3.4 gives a high-level summary and purpose of each of the preparations and analysis used in this study.

Table 3.3 Summary of samples taken, their respective locations, depths, and analyses conducted

Sample site	Source Type	Borehole / Trench ID	# Samples	Sample ID	Depth	Oxide [1]	Trace [2]	Trace + [3]
Zonderwater	Borehole	ZR442LQ34GT	2	S13	327.55	Y	Y	
				S14	329.16	Y	Y	
		ZR442LQ39GT	1	S15	343.6	Y	Y	
Grootegeluk	Borehole	GK459LQ140	4	S1	91.73	Y	Y	
				S4	92.79	Y	Y	
				S2	93.77	Y	Y	
				S3	94.86	Y	Y	
		GK459LQ141	4	S8	105.75	Y	Y	
				S7	106.64	Y	Y	
				S6	108.45	Y	Y	
				S5	109.39	Y	Y	
		GK459LQ142	4	S12	96.41	Y	Y	
				S9	97.27	Y	Y	
				S10	97.88	Y	Y	
				S11	98.25	Y	Y	
	Bulk	GG – Bench10	2	10A	Representative	Y		Y
				10B		Y		Y
		GG – Bench8A	1	8A		Y		Y

[1] – SiO_2, Al_2O_3, BaO, CaO, Cr_2O_3, Fe_2O_3, K_2O, MgO, Mn_3O_4, Na_2O, P_2O_5, SO_3, TiO_2, V_2O_5 and Loss on Ignition (LOI)
[2] – Ni, Cu, Zn, Ge, As, Se, Br, Rb, Sr, Y, Zr, Nb, Mo, Ag, Cs, Pb, Th and U.
[3] – Ag, As, Au, B, Ba, Be, Bi, Cd, Ce, Co, Cr, Cs, Cu, Ga, Ge, Hf, Hg, Ho, Ir, La, Li, Lu, Mn, Mo, Nb, Nd, Ni, Pb, Pt, Rb, Sb, Sc, Se, Sm, Sn, Sr, Ta, Te, Th, Tl, U, V, W, Y, Yb, Zn and Zr + Suphur Speciation + Acid/Base Accounting

Table 3.4 Analysis conducted in this study[1]

Preparation / Analysis	Purpose
Pulverisation of samples	Preparation of the samples for further analysis
XRF	Whole-rock chemical composition (Major and minor element concentrations)
Microwave digestion	Preparation of the samples for further analysis (ICP-MS)
ICP-MS	The concentrations of selected trace elements
Bulk Ashing	Preparation of the samples for further analysis (Ash composition (XRF))
Ash composition (XRF)	Whole-rock chemical composition (Major and minor element concentrations) of the ash

3.3.2.1. Microwave digestion

The major task of sample digestion is to convert the form of sample into one suitable for chemical analysis. Generally, after the sample is digested, the component of interest is in the solution as a soluble salt. The major advantage of the solution is its excellent homogeneity. During microwave digestion, a mixture of nitric acid; hydrochloric acid and hydrofluoric acid is used. The samples are heated to approximately 210°C at 20 atm pressure for several hours. After a first stage of digestion a

[1] The techniques, analysis and procedures used in this study are only briefly touched upon herein, if the reader requires additional information on the said processes the author recommends the following papers: Sampling (Demetriades, 2014); Sample digestion (Hu and Qi, 2014); XRF (Nakayama and Nakamura, 2014); and ICP-MS (Olesik, 2014).

second stage digestion is performed to ensure that all the material is dissolved and homogeneity is achieved. (Hu and Qi, 2014)

3.3.2.2. Mineral composition

The mineral composition was determined via x-Ray fluorescence (XRF) and Inductively Coupled Plasma Mass Spectroscopy (ICP-MS). XRF spectroscopy is commonly used to produce accurate and precise compositional data for the ten major oxides (Na_2O, MgO, Al_2O_3, SiO_2, P_2O_5, K_2O, CaO, TiO_2, MnO, and total Fe_2O_3) and some minor elements. While analysis can be conducted on a raw, unprepared rock; sample preparation typically involves the creation of powdered pellets to ensure homogeneity. The sample is then exposed to x-rays, the emitted x-rays reflected from the sample are spectroscopically dispersed according to the x-ray diffraction law and an element is detected on the basis of its x-ray wavelength. (Nakayama and Nakamura, 2014).

Trace element analysis consisted of microwave digestion followed by Inductively Coupled Plasma Mass Spectroscopy (ICP-MS) to give the elemental analysis of the elements typically in the ppm to ppb ranges. (Olesik, 2014)

Chapter 4

Results and Analysis

4.1. Phase 1: Literature compilation and review

As discussed in the Chapter 2, there has been some, albeit limited, reference to radioactivity within the Waterberg Coalfield. What is more apparent is the lack of study or focus on the radioactivity itself.[2]

Based on previous information discussed in the Chapter 2 the target lithologies within the Waterberg Coalfield were limited to the Grootegeluk Formation’s Bench 5 coal, and the Eendragtpan Formation khaki-yellow mudstones were identified as the best possible targets for further study.

4.2. Phase 2: Downhole geophysical surveys

The gamma anomalies, where the API value was recorded as greater than 300 API units, are grouped and discussed below by stratigraphy and locality for ease of reference. As the stratigraphy of the study area is of sedimentary origin, the expectation is that an anomaly should persist across the basin, would be strata bound, bedding hosted or related to faulting. To account for elevation and geological variation that occurs the anomalies depths were recalculated to the top of the respective formations.

Table 4.1 Summary of the number of gamma anomalies, where the API value was recorded as greater than 300 API units by locality and stratigraphy

Stratigraphy	Zonderwater	Grootegeluk
Clarens	None	Stratigraphy not encountered
Lisbon (Elliot)	1	Stratigraphy not encountered
Greenwich (Molteno)	None	Stratigraphy not encountered
Eendragtpan (Beaufort)	54	12
Grootegeluk (Volksrust)	None	None
Swartrant (Vryheid)	51	67

4.2.1. Geophysical Trends found within the Zonderwater locality

The Clarens, Greenwich (Molteno), and Grootegeluk (Volksrust) Formations did not exhibit any gamma anomalies. From the holes studied, the Lisbon (Elliot) Formation exhibited a single anomaly, the Eendragtpan (Beaufort) and Swartrant (Vryheid) Formations had 54 and 51 anomalies respectively (Table 4.1). Each formation where an anomaly was found is discussed further below.

Appendix B contains plots of the gamma versus density plot for each stratigraphic unit, while Appendix C shows the overall statistics through the stratigraphy for gamma, density and depth for the Zonderwater study area.

---

[2] While this does not detract from, nor is it a criticism of the work that the previous workers have conducted, it does raise the following question – “was radioactivity considered by the previous workers, and if it was, why wasn’t it reported?” The possible responses to the question raise the uncomfortable answers of: “There was nothing there to report on” or “Siepker was wrong or incorrect to report radioactivity”. Both these possibilities have plagued the mind of the author throughout the study.

4.2.1.1. Eendragtpan Formation (Beaufort)

The anomalies in the Eendragtpan Formation are distributed spatially throughout the strata (Figure 4.1). There are no observable trends within the distribution.

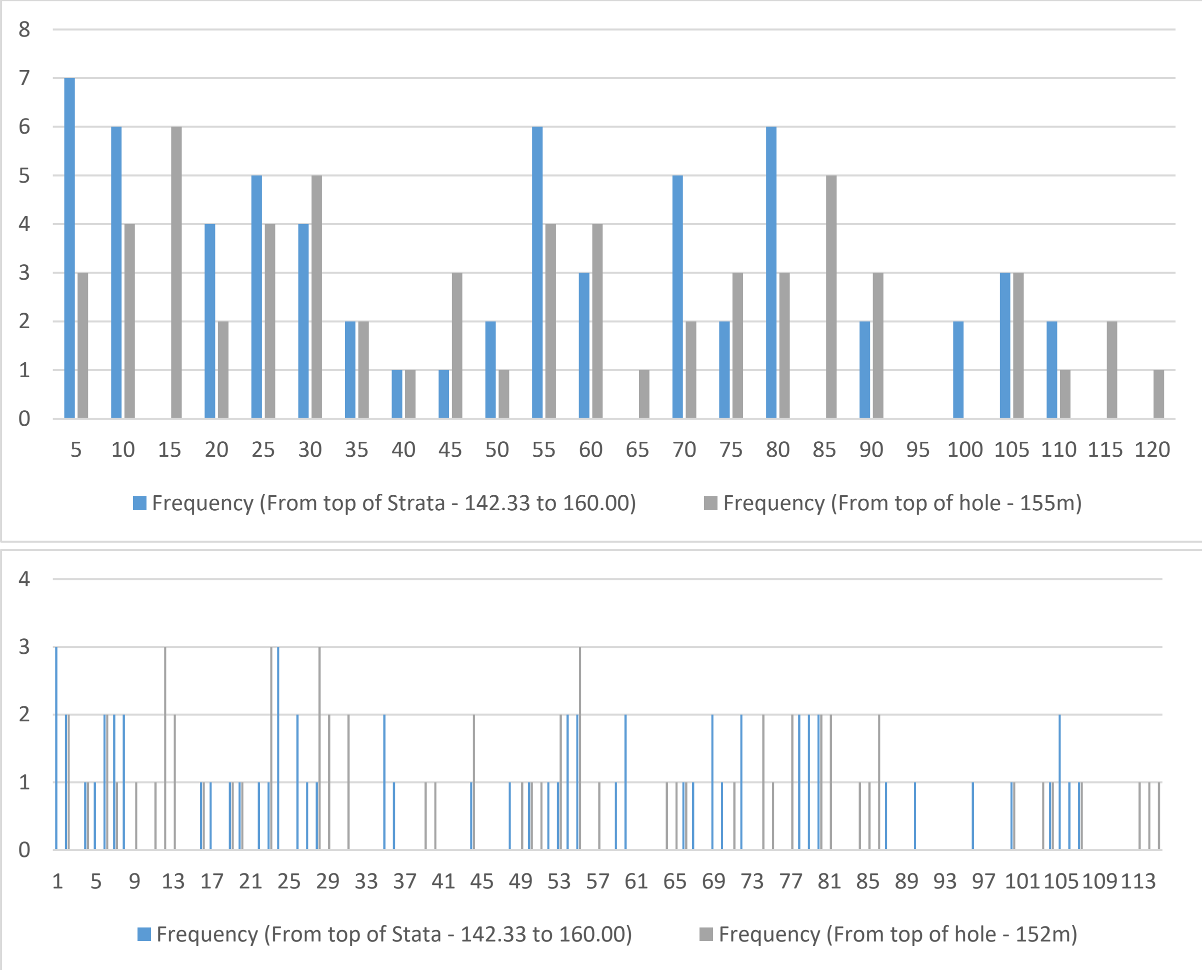

Figure 4.1: Histogram showing the spatial distribution of gamma anomalies (>300 API) within the Eendragtpan Formation from the Zonderwater boreholes. The y-axis indicates the frequency, while the x-axis indicates the depth.

4.2.1.2. Swartrant Formation (Vryheid)

The anomalies in the Swartrant Formation are distributed throughout the strata and show a cluster into two groupings. This is evident in Figure 4.3. The first group is concentrated around 13-17m from the top of the strata, and the second between 23-27m.

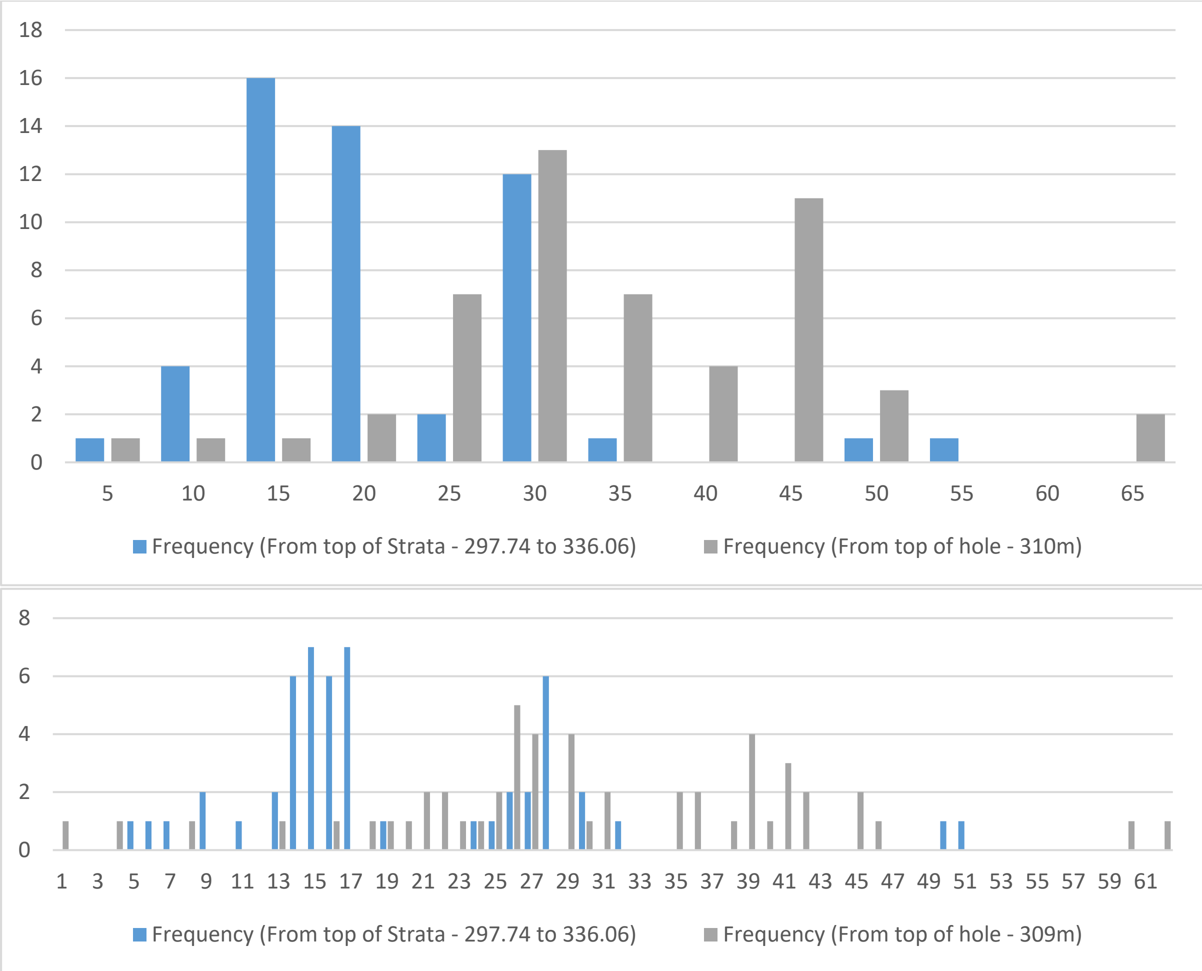

Figure 4.2: Histogram showing the spatial distribution of gamma anomalies (>300 API) within the Swartrant Formation from the Zonderwater boreholes. The y-axis indicates the frequency, while the x-axis indicates the depth.

4.2.1.3. Lisbon Formation (Elliot)

The single Lisbon Formation anomaly occurred just above the Greenwich Formation at a depth of 139.48m from the top of hole within the ZR422LQ38 hole. The anomaly had an average API count of 532.53 and was approximately 37cm thick.

4.2.2. Geophysical Trends found within the Grootegeluk locality

Within the Grootegeluk boreholes the Clarens, Greenwich (Molteno), and Lisbon (Elliot) Formations were not encountered as these formations do not occur at the Grootegeluk Mine. The Grootegeluk (Volksrust) Formation did not exhibit any gamma anomalies. The Eendragtpan (Beaufort) and Swartrant (Vryheid) Formations exhibited 12 and 67 anomalies respectively (Table 4.1). Each formation where an anomaly was found is discussed further below.

4.2.2.1. Eendragtpan Formation (Beaufort)

The anomalies in the Eendragtpan Formation are distributed throughout the strata. This is evident in Figure 4.3. There are no observable trends within the distribution.

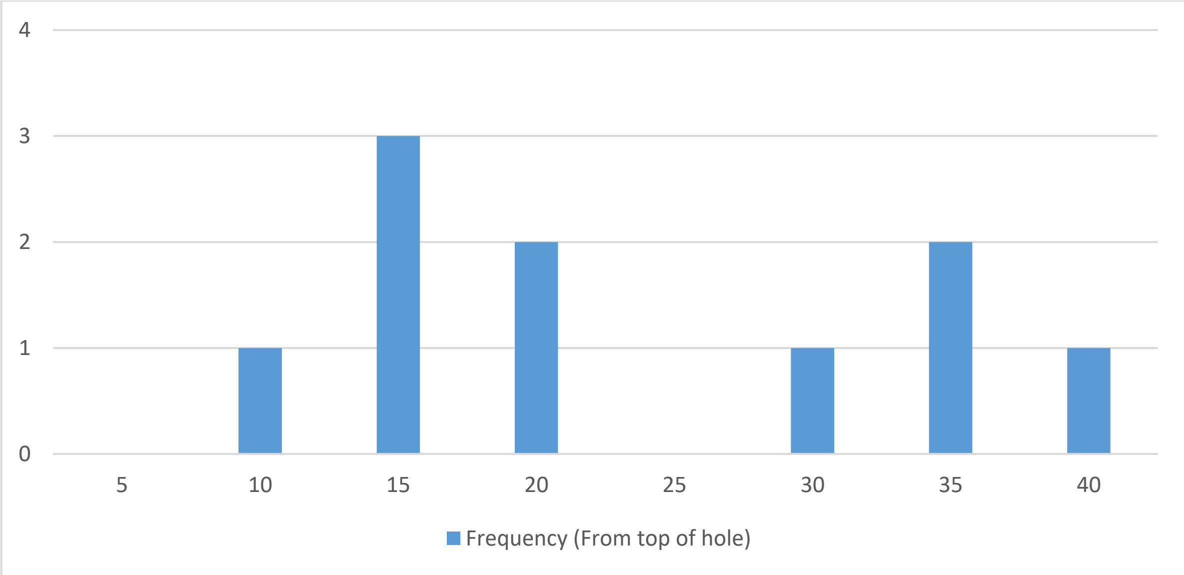

Figure 4.3: Histogram showing the spatial distribution of gamma anomalies (>300 API) within the Eendragtpan Formation from the Grootegeluk boreholes. The y-axis indicates the frequency, while the x-axis indicates the depth.

4.2.2.2. Swartrant Formation (Vryheid)

The anomalies in the Swartrant Formation are distributed throughout the strata and show a cluster into two groups. This is evident in Figure 4.4 with the clusters concentrated around the 11-15m and 35-39m from the top of the strata.

4.2.3. Correlation between Zonderwater and Grootegeluk of the gamma anomalies

The two trends within the Swartrant Formation as determined across the two study sites are reflected in Figure 4.5. The trends coincided with the mining benches at Grootegeluk, namely the lower half of Bench 8 and Bench 10. Based on these trends, these benches where proposed for sampling and analysis.

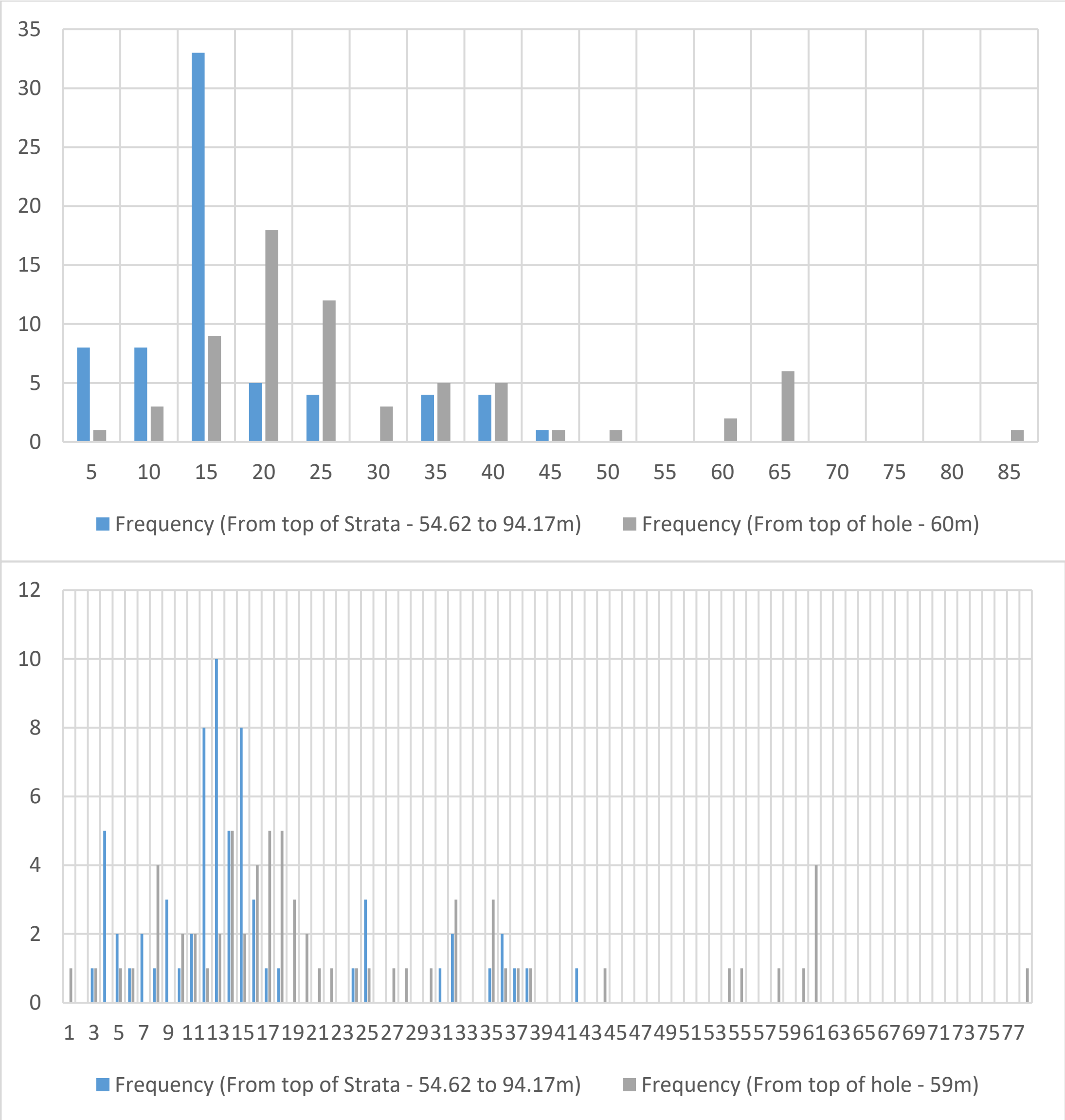

Figure 4.4: Histogram showing the spatial distribution of gamma anomalies (>300 API) within the Swartrant Formation from the Grootegeluk boreholes. The y-axis indicates the frequency, while the x-axis indicates the depth.

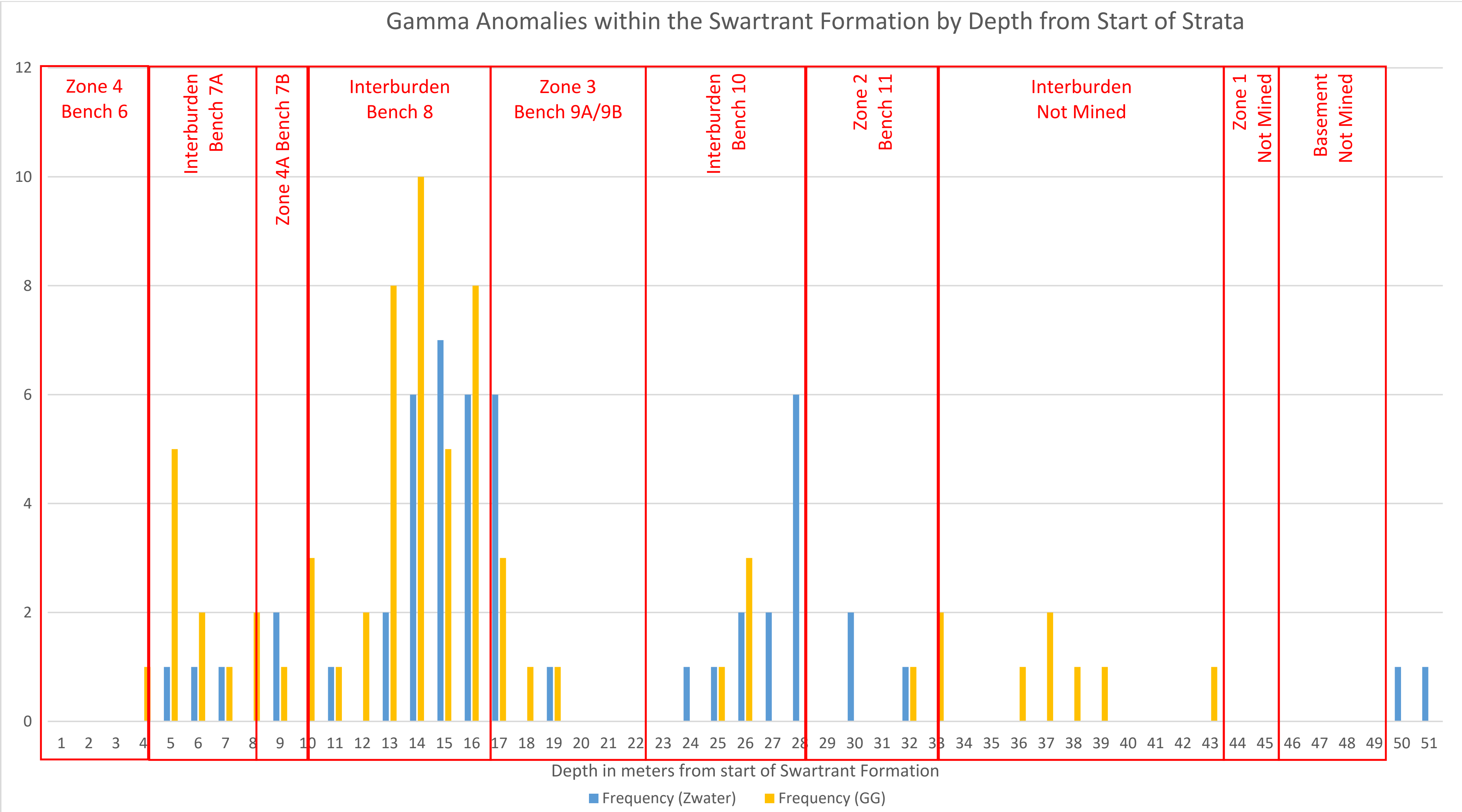

Figure 4.5 Histogram showing the spatial distribution of gamma anomalies (>300 API) within the Swartrant Formation from both Grootegeluk and Zonderwater boreholes with the Grootegeluk mining benches and coal zones included. The y-axis indicates the frequency, while the x-axis indicates the depth.

4.3. Phase 3: Sample Analysis

The sample analysis was conducted on 15 Bench 10 samples (Table 4.2). The samples varied from fine-grained shales to medium-grained sandstones

Table 4.2 Summary of borehole samples

Sample ID	Borehole ID	Depth	Sample site	Sample Description
S13	ZR442LQ34GT	327.55	Zonderwater	Grey shale
S14		329.16		Black shale
S15	ZR442LQ39GT	343.6		Grey shale
S1	GK459LQ140	91.73	Grootegeluk	Dark grey shale
S4		92.79		Grey shale
S2		93.77		Grey shale
S3		94.86		Grey shale
S8	GK459LQ141	105.75		Cream sandstone
S7		106.64		Light black shale
S6		108.45		Grey shale
S5		109.39		Black shale
S12	GK459LQ142	96.41		Grey shale
S9		97.27		Light black shale
S10		97.88		Grey shale
S11		98.25		Grey shale

4.3.1. Whole-rock chemistry

The means and ranges of the major and trace elements are presented in Table 4.3 and the whole-rock data is included in Appendix E. Values were removed that were below detection limits and replaced with zero. Although this may have biased the results towards lower values, the rationale behind the decision hinged on the uncertainty of adding data as opposed to replacing with an arbitrary value i.e. half the detection limit or the detection limit itself. As most of the previous studies within the Waterberg Coalfield focused predominantly on the coal itself (Wagner and Tlotleng, 2012; Oboirien et al., 2016), or the shales and mudstones (Faure, 1993; Faure et al., 1995, 1996b; a), it is difficult to draw comparisons to the sandstone lithologies within the study area.

Table 4.3 Means and ranges of the major (XRF) and trace element (ICP-MS) values for the 15 Bench 10, boreholes samples. CIA, Cr/V and Th/U ratios are discussed later in the chapter.

	Minimum	Maximum	Mean	Standard Deviation	Median	Unit
Depth	91.73	343.60	146.22	97.12	98.25	m
Gamma	16.85	644.88	191.42	195.66	112.59	API
Density	1.94	2.64	2.46	0.18	2.50	g/cc
Al_2O_3	3.44	26.58	15.74	7.83	18.17	%
BaO	0.00	0.24	0.06	0.07	0.03	%
CaO	0.02	1.27	0.15	0.32	0.05	%
Cr_2O_3	0.01	0.22	0.03	0.05	0.02	%
Fe_2O_3	0.06	1.77	0.47	0.53	0.29	%
K_2O	0.03	0.47	0.24	0.14	0.29	%
MgO	0.01	0.14	0.02	0.04	0.01	%
Mn_3O_4	0.01	0.07	0.01	0.02	0.01	%
Na_2O	0.02	0.12	0.07	0.03	0.07	%
P_2O_5	0.00	0.32	0.08	0.09	0.04	%
SiO_2	49.17	91.71	71.74	11.99	71.17	%
SO_3	0.08	0.10	0.09	0.01	0.09	%
TiO_2	0.46	12.96	2.12	3.12	1.17	%
V_2O_5	0.00	0.07	0.02	0.02	0.02	%
LOI	2.60	21.64	8.63	5.02	7.61	%
Ag	0.26	3.51	0.92	0.96	0.63	ppm
As	0.72	13.36	5.63	3.41	4.36	ppm
Bi	0.03	0.44	0.19	0.12	0.17	ppm
Cs	0.09	0.65	0.33	0.20	0.31	ppm
Cu	61.67	154.18	80.65	21.31	74.85	ppm
Ge	0.46	2.24	0.79	0.43	0.70	ppm
Mo	0.33	6.65	1.84	1.63	1.51	ppm
Nb	5.37	131.39	24.48	30.93	17.15	ppm
Ni	43.61	207.39	76.71	38.13	67.35	ppm
Pb	95.15	245.73	157.82	37.56	154.20	ppm
Rb	5.08	10.75	7.66	1.86	7.64	ppm
S	323.84	412.50	370.91	22.27	367.69	ppm
Se	0.01	0.13	0.05	0.03	0.05	ppm
Sr	9.79	335.53	93.99	89.72	69.45	ppm
Th	0.13	17.49	2.61	4.32	1.25	ppm
U	0.41	13.43	2.71	3.33	1.67	ppm
Y	0.03	8.46	1.25	2.74	0.18	ppm
Zn	39.93	1674.65	258.20	400.99	141.71	ppm
Zr	83.30	1357.30	328.61	380.46	179.79	ppm
CIA	72.36	98.10	95.86	6.52	97.61	
Cr/V	0.20	26.98	3.18	6.63	1.29	
Th/U	0.21	6.16	1.12	1.53	0.59	

4.3.1.1. Grootegeluk

Thorium concentrations range from 0.12 ppm to 4.7 ppm, and U concentrations range from 0.41 ppm to 4.49 ppm. Potassium concentrations range between 0.056 and 0.58 wt. %. The downhole geophysics yielded gamma values that range between 16.84 and 206.06 API units for depths where samples were taken.

4.3.1.2. Zonderwater

Thorium concentrations range from 1.25 ppm to 17.5 ppm, and U concentrations range from 1.6 ppm to 13.43 ppm. Potassium concentrations range between 0.032 and 0.16 wt. %. Gamma values range between 106.64 and 644.88 API.

An analysis of the radioactive elements against the gamma counts (Figure 4.6) provides an insight as to the primary factors that have influenced the gamma counts. It is possible to see that both U and Th had the largest influence on the Gamma API, while K_2O appears not to have influenced the gamma count at all. Further study of Figure 4.6 reveals that the Gamma API and the U plots mirror each other, while the Th peaks in S5 and S10 had little effect on the Gamma API.

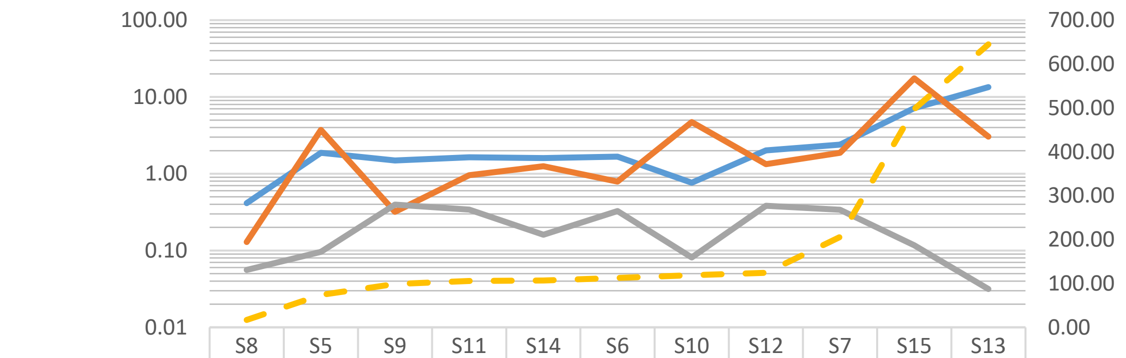

	S8	S5	S9	S11	S14	S6	S10	S12	S7	S15	S13
U (ppm)	0.41	1.87	1.49	1.64	1.60	1.67	0.76	2.01	2.39	7.15	13.43
Th (ppm)	0.13	3.72	0.32	0.96	1.25	0.79	4.71	1.33	1.87	17.49	3.04
K20 %	0.06	0.10	0.40	0.34	0.16	0.33	0.08	0.38	0.34	0.12	0.03
Gamma API	16.85	74.01	98.62	105.71	106.65	112.59	118.77	124.12	206.06	497.31	644.88

Figure 4.6 Gamma, Th, U and K_2O plot per sample. Th, U and K_2O plotted on the primary axis while Gamma values on the secondary axis

4.3.1.3. Bulk samples from Bench 8A and Bench 10

As indicated in Table 3.3 and included as Appendix F, a single bulk sample was taken from Bench 8 and two samples from Bench 10.

4.3.2. Geochemical Perspectives

Although the chemical composition of sediments may be used to constrain source-rock composition, the geochemistry of the sediments can be controlled by several factors such as the influence of tectonics, degree of weathering (chemical or mechanical), transport and sedimentation, clay-mineral adsorption, organic adsorption and bonding, and effects of diagenesis. It is not always possible to distinguish the effect that each of the factors may have had on the eventual composition of the mudstones, but fortunately some elements are affected to different extents by these processes.

McLennan et al. (1993) provides a framework for using geochemistry to determine sedimentary processes such as weathering, diagenesis, sorting and sedimentary recycling. While the framework also provides geochemical approaches that can be used to determine sedimentary provenance, the lack of isotopic analysis has restricted the ability to determine the sedimentary provenance within this study. However, the framework will be used as a guide for the following section.

4.3.2.1. Provenance

Considerable progress has been made in recent years in the use of bulk properties of fine-grained rocks for the purpose of provenance studies (Taylor and McLennan, 1985, 1995). Shales are very well suited for provenance studies of clastic sediments because of their relative homogeneity, their post-depositional impermeability, and because they dominate the sedimentary mass balance (Taylor and McLennan, 1985, 1995). The composition of shale is directly related to the composition of the parent material (Nesbitt et al., 1980; Nesbitt and Young, 1982). Secondary processes such as weathering, transport, sedimentation, diagenesis, etc. can have an effect on the composition of sediments and therefore for provenance studies it is best to use elements that have little mobility under the expected geological conditions. Taylor and McLennan (1985) point out that such elements should possess very low partition coefficients between natural waters, the upper crust, and retain short oceanic residence times. Elements that meet these criteria are Al, Ti, Th, Sc and the rare earth elements (REE). Taylor and McLennan (1985) observed that the ratios of these elements were not affected by weathering processes and that ratios can minimise the effect of mineral fractionation. Secondary processes in the mudstones were not significant enough to preclude the use of the aforementioned elements in predicting the composition of the source rock material.

Several major and trace element plots can be used to determine the composition of provenance rocks. The TiO_2 and Al_2O_3 plot of the sediments in this study suggests that most of the Grootegeluk samples had a similar origin (Figure 4.7). According to the granitic and basaltic fields defined in the TiO_2 and Al_2O_3 plot, the average composition of the provenance area of the Grootegeluk samples was greater than 50% granitic. The TiO_2 and Al_2O_3 composition of the Zonderwater samples, however, suggest that the provenance compositions of these samples were more mafic than the Grootegeluk samples.

4.3.2.2. Classification

As indicated in Figure 4.8, the majority of the samples plot as “shales” according to Herron (1988) classification. This is confirmed with the geophysics gamma ray which shows the range for the samples to be between 16.84 and 644.88, where the API values of a typical shale are between 100 to 300; organic-rich/marine shale between 100 to 800; and coal between 15 to 100 (Thomas, 2012).

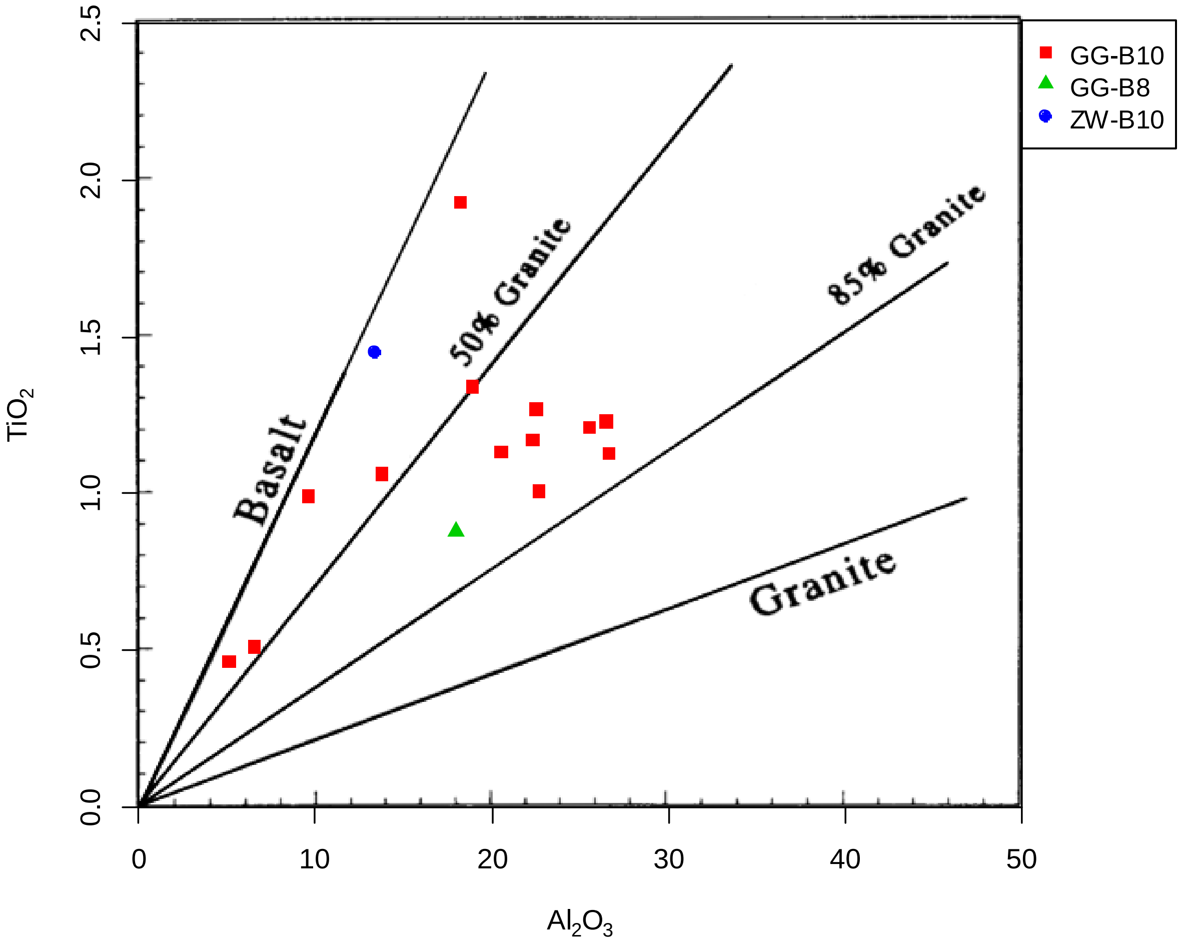

Figure 4.7 The TiO_2 and Al_2O_3 sample values with compositions for typical basalts and granites are from Cox et al. (1979). The lines of constant ratio for different proportions of granite and basalt, based on Cox et al. (1979) compositions, are also presented. GG – Grootegeluk, ZW – Zonderwater, B10 – Bench 10, B8 – Bench 8.

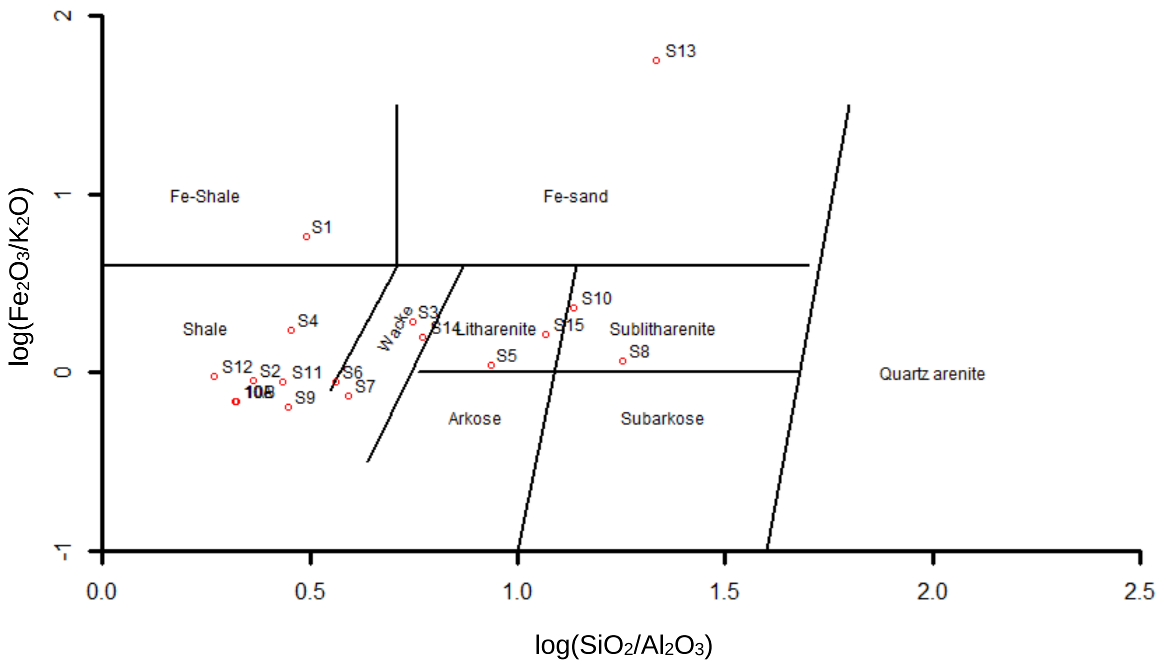

Figure 4.8 Scattergram of log (SiO_2/Al_2O_3) vs log (Fe_2O_3/K_2O) with this study samples plotted showing that most of the samples plotting as shale, wacke, and litharenite. Classification systems from Herron (1988). (Sample IDs as per Table 4.2)

4.3.2.3. Weathering and Diagenesis

A method of determining clay content is to evaluate the clay proportion by means of the abundance of Al (expressed here as the oxide Al_2O_3). The strong linear correlation (Figure 4.9) between Al and K (expressed here as the oxide K_2O) versus the negative linear correlation of Al and K against SiO_2 supports the argument that both K and Al are associated with the clay proportion.

Typically, during weathering and diagenesis there is an extensive increase in the Rb/Sr ratio of most rocks. This is due to the preferential retention of Rb compared to Sr within clay minerals. The strong correlation values for Rb (and slight negative for Sr) with K and Al indicated in Figure 4.9, indicates the Rb is most likely associated with the clay fraction. This is because Rb will substitute for K in feldspar and micas and commonly shows a positive correlation with illite, however its position within the clay proportion is unclear.

An alternative geochemical indicator of clay proportion is the Zn abundance while there is an absence of significant proportions of ferromagnesian minerals and sulphides (Svendsen and Hartley, 2002). The study data shows a very weak to weak correlation between Zn with K and Al, but instead shows a strong correlation with the ferromagnesian elements thus possibly indicating that there is little to no clay as the Zn appears to be associated with the ferromagnesian minerals.

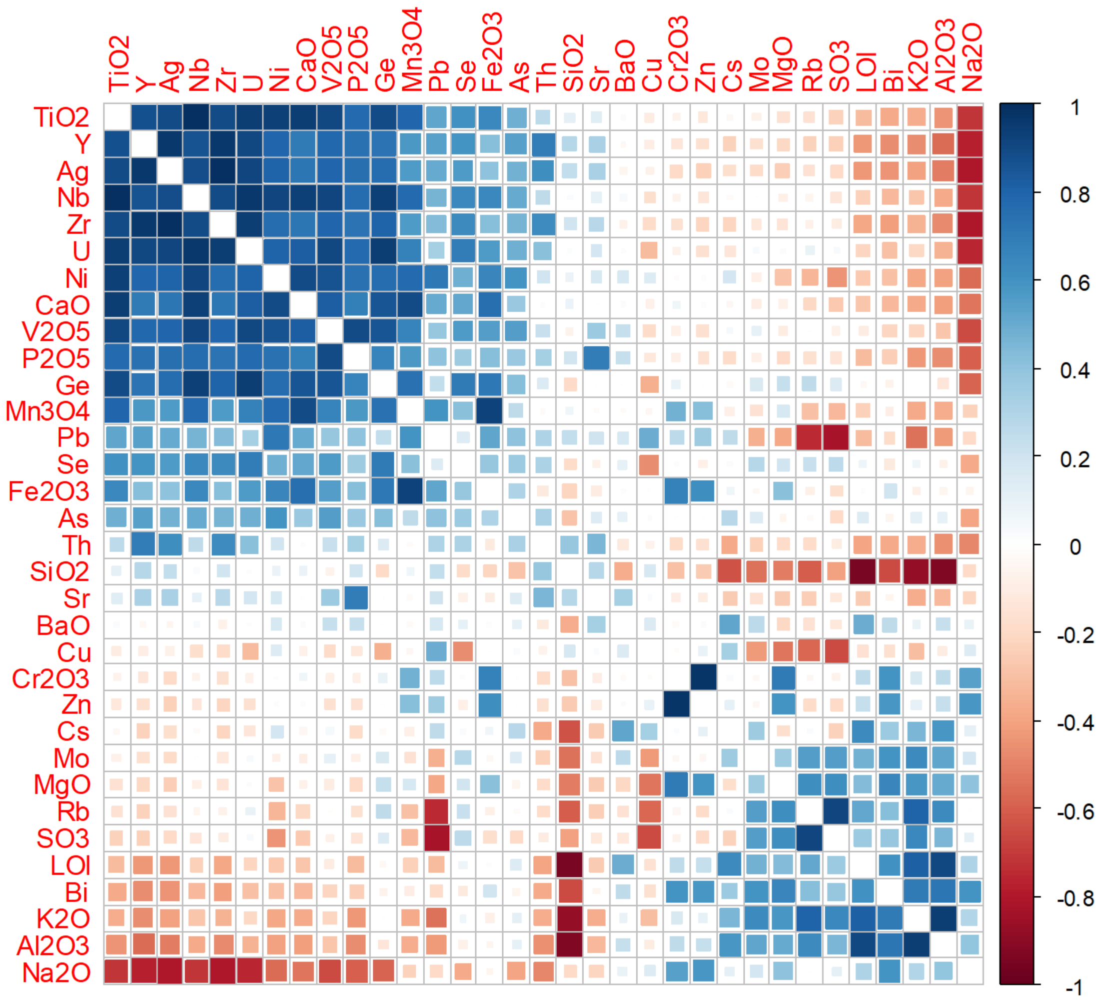

Figure 4.9 A visualisation of the correlation matrix ordered per the first principal component showing that both U and Th are strongly correlated with (positive) Y, Ti, Ag, Nb, Zr, Ni, Ca, V, P, Ge, Mn, Pb, Se, Fe, As and (negative) Na..

Th/U ratios can be used to determine redox conditions in the depositional environment and tend to be more reliable than Cr/V and Ni/Co ratios (Dypvik and Harris, 2001). High Th/U ratios would be indicative of an oxic setting, while low values reflect a dysoxic setting and therefore anoxic depositional conditions – Th/U ratios below one could result from U enrichment during deposition under reducing conditions. The Th/U ratio ranges from 0.21 to 6.16 with a mean of 1.03. For the 18 samples only 3 (S5, S10 and S15) have values greater than 1. Notwithstanding variation during deposition, and considering that bench 10 is not a single homogeneous stratum, but instead shows depositional variation akin to the greater Swartrant Formation, the overall trend is that Bench 10 was deposited under reducing conditions.

A study of the mobile elements using the index of alteration (Equation 2) illustrates that the samples have been highly to completely altered, with values between 72.36% to 98.10% with an average of 96.05%. This is further supported in Figure 4.10 where the bulk of the samples plot in the region of Kaolinite and Gibbsite.

Equation 2 Index of Alteration (CIA) is an established general guide to the degree of weathering from Nesbitt and Young (1982)

$$CIA = \frac{Al_2O_3}{(Al_2O_3 + CaO + Na_2O + K_2O)}$$

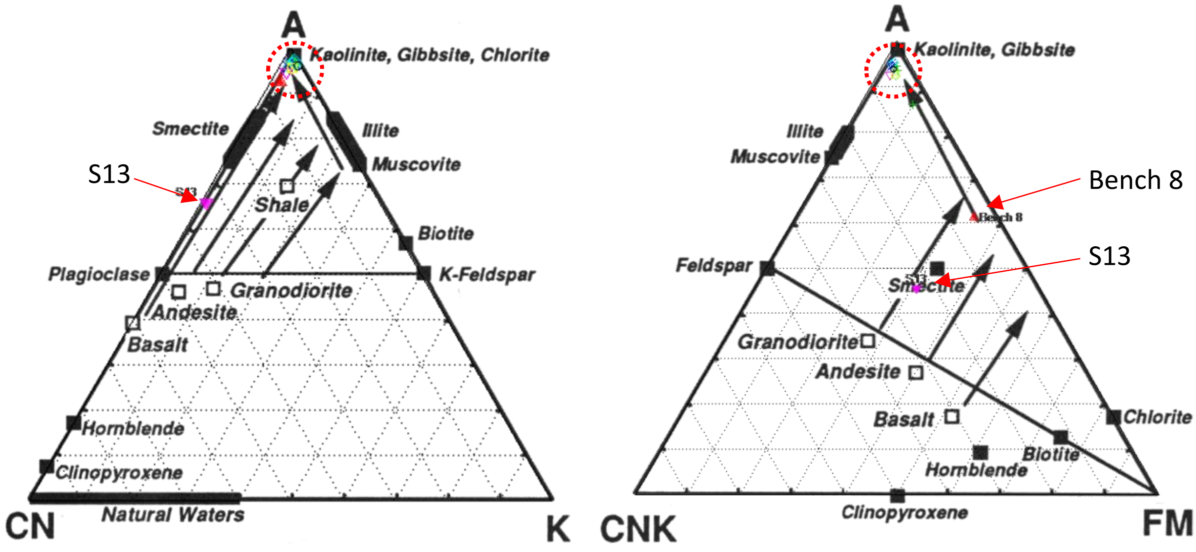

Figure 4.10 Ternary plots of A-CN-K and A-CNK-FM where, in mole fraction, A = Al_2O_3 , C = CaO (silicate fraction only), N = Na_2O, K = K_2O, F = total Fe as FeO, and M = MgO (after Nesbitt and Young (1984, 1989) and McLennan et al. (1993, Figure 1)*). Plotted are simplified compositions of major minerals, typical rock types, natural waters and the samples from this study. Arrows indicate the general trends of weathering exhibited by various rock types. The dashed circles indicate where the majority of the samples are located.*

4.3.2.4. Sedimentary Sorting

There are numerous petrographic methods that can be used to study sorting processes in sedimentary rocks. The most unambiguous is to evaluate the textural maturity of the sediments, using grain sizes and shapes, in conjunction with mineralogy. Sorting is typically attributed to an increase of more resistant minerals (e.g. quartz, zircon, tourmaline, and rutile) at the expense of clay minerals. This results in an elevated SiO_2/Al_2O_3 ratio versus a depletion in the total abundance of most trace elements.

For the course-grained proportion, Zr abundance can be used as a geochemical indicator as Zr is commonly associated with sandstones and shows higher values, when compared to average shale (Dypvik and Harris, 2001). While Zr does show a mild negative correlation against Al, it does not show a correlation towards SiO_2.

Within sandstones that contain a high degree of sorting, there is an expectation that there would be a reduction in elements with small ionic radius (e.g. Al and Rb) in favour of larger more resistant elements (e.g. Zr and Si). Based on these assumptions, Figure 4.11 indicates that the values from the Zonderwater samples (S13-S15) indicate a higher amount of sorting compared to the Grootegeluk samples.

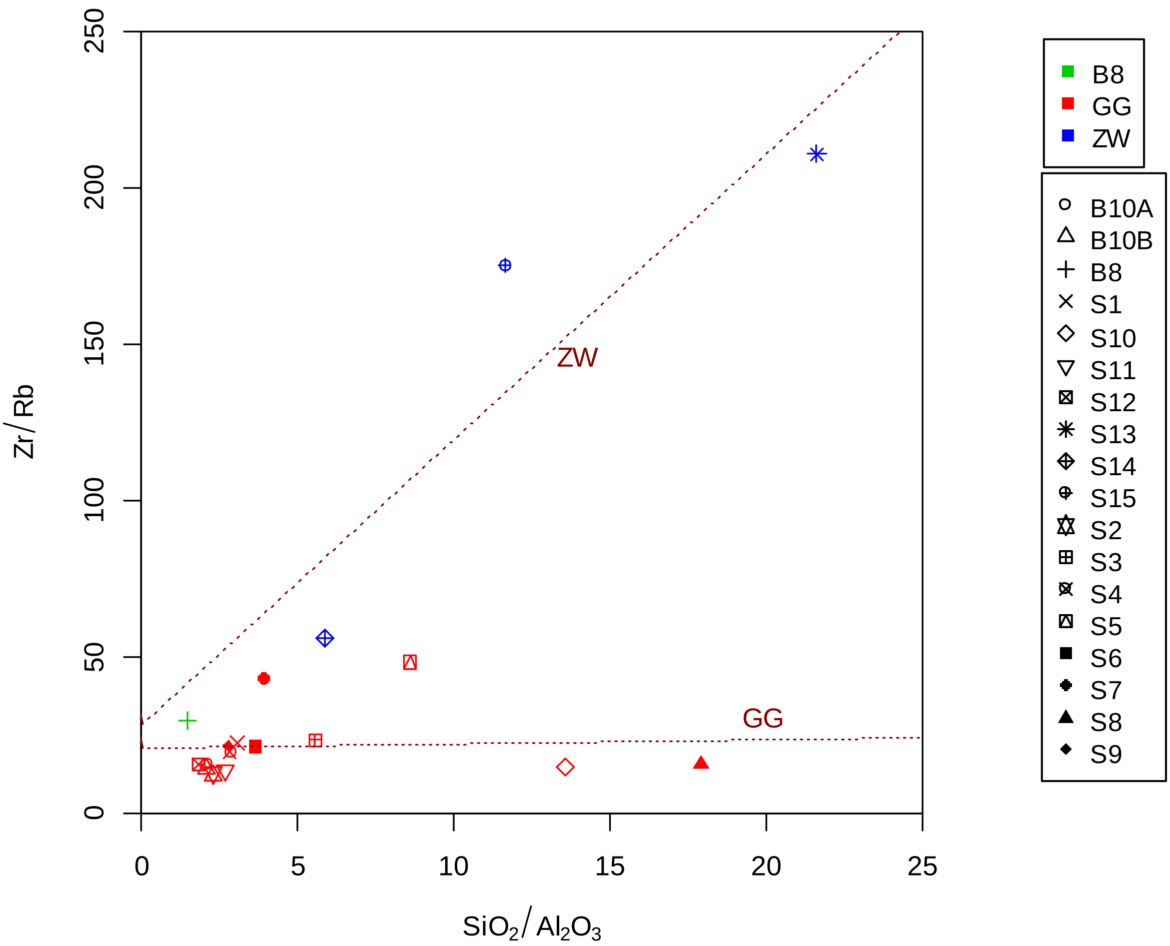

Figure 4.11 Plot of SiO_2/Al_2O_3 against Zr/Rb with the samples grouped by locality and bench. The dotted lines indicate the linear fits for the Grootegeluk (GG) and Zonderwater (ZW) sample groups.

4.3.2.5. Th and U in relation to the other elements

The primary hypothesis of this study was that elevated values of Th and/or U within the Waterberg Coalfield, are likely to be greater than the global average (0.5 - 10 ppm U; 0.5 - 10 ppm Th). While the majority of the samples taken conform to the global average there were two samples, S15 and S13, that contained elevated values.

As shown in Figure 4.13 and Figure 4.14, there is a depletion of Na in both S13 and S15 in comparison to the other samples. While S13 and S15 follow similar trends with regards to Ag, Y and Zr where both show considerable elevated values with S13 being higher, there are several plots where the S15 values is only slightly above that of the other samples i.e. Ti and Ge. The only time when this relationship is inverted is in the Th plot where the S13 sample plots among the other samples.

An analysis of Figure 4.14 shows that, in comparison to the other samples, sample S13, from borehole ZR442LQ34GT located on the Zonderwater study area, is enriched in Y, Ca, Mn, Ti, U, Nb, P, Zr, Ag, V, and Ni and is depleted in Na, Al, Bi and K. Th is the only element that sample S15 (borehole ZR442LQ39GT located in the Zonderwater study area), is enriched in. Both the sample from Bench 8 and sample S8 are highlighted in the Figure 4.14 as they are of interest – Bench 8 due to the gamma analysis which had identified the bench as a prospective zone for further study, and S8 due to the depletion in nearly all elements. The depletion in S8 is likely to be due to the high SiO_2 percentage (91.71%) which indicates the sample was most likely a mudstone, quartz-arenite or quartz-wacke due to the Al_2O_3 (5.12%) content.

4.3.3. Major element analysis for Bench 8 at Grootegeluk

An interrogation of the major element analyses in Exxaro's database for the Grootegeluk Mine geological ash composition from Bench 8 yields Table 4.4 and Figure 4.12. The results classify all the samples from Bench 8 as "Shale" or "Fe-Shale".

While the database did not contain values for the full suite of trace elements, what follows is an attempt to utilise what data was available to derive as much information as possible. Th/U ratios can be used to determine redox conditions in the depositional environment and tend to be more reliable than Cr/V and Ni/Co ratios. As previously discussed Cr/V ratios can be used in the absence of Th/U ratios to determine redox conditions in the depositional environment but are not as reliable as Th/U (Dypvik and Harris, 2001). A study of the Cr/V ratios for Bench 8 reveals an average of 0.98 which indicates a slight general dysoxic setting and therefore anoxic depositional environment.

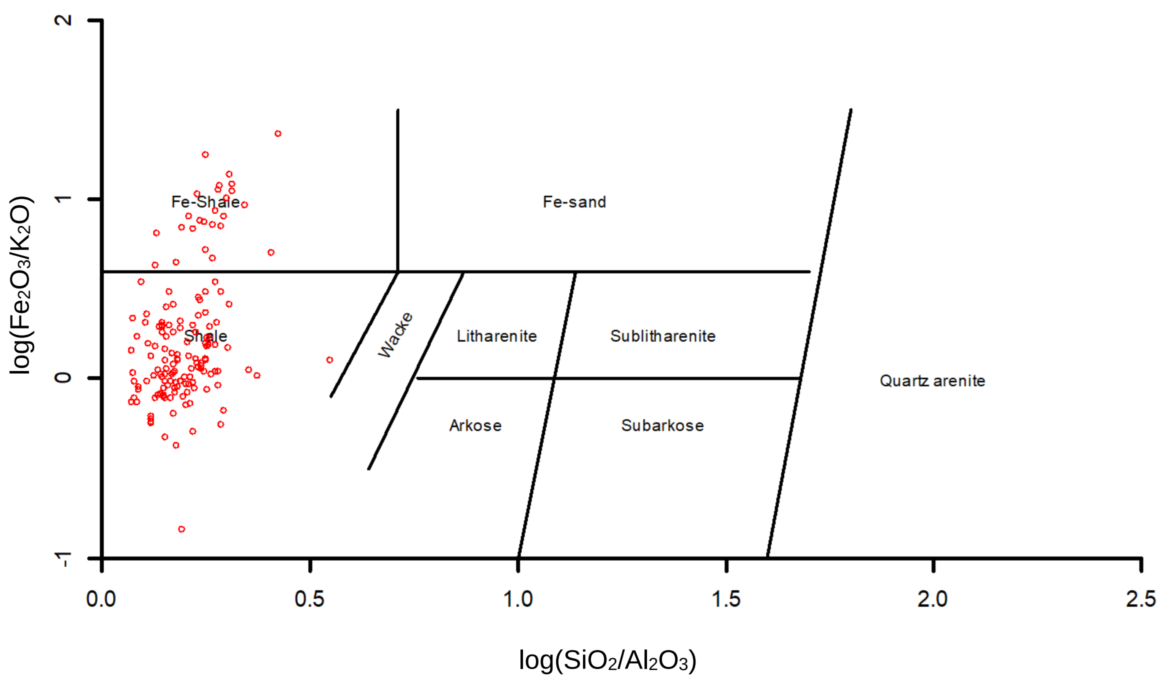

Figure 4.12 Scattergram showing log (SiO_2/Al_2O_3) vs log (Fe_2O_3/K_2O) with Bench 8 plotted, the majority of the samples plot as "shale". Classification systems from Herron (1988).

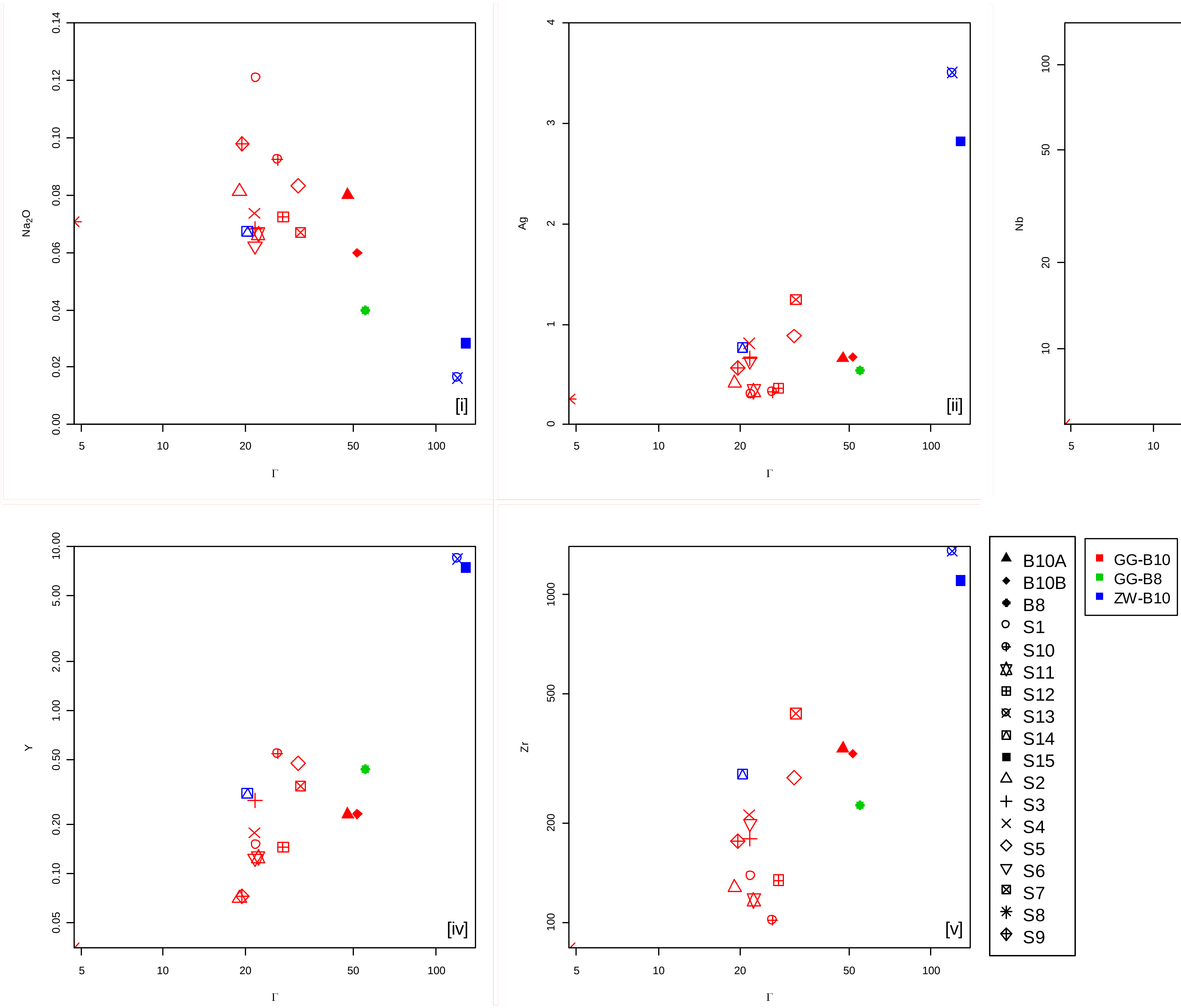

Figure 4.13 A Multiple plot of API Gamma (Γ), calculated as (8 x U (ppm)) + (4 x Th (ppm)) + (12 x K_2O (%)), versus Na_2O (%), Zr (ppm), Nb (ppm), As (ppm), Ag (ppm), and Y (ppm). With samples S13 and S15 depicted as blue circle with a horizontal cross and solid square respectively. The plots show occurrences where there is a coefficient of determination (R^2) value greater than 0.5.

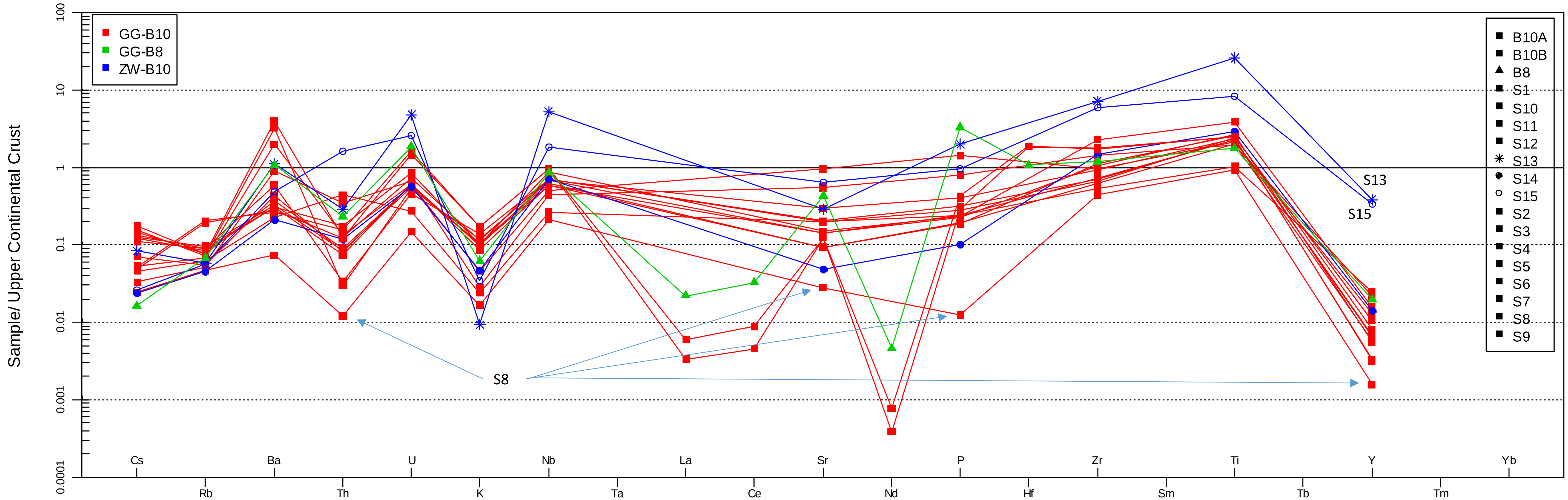

Figure 4.14 Spider plot of the analysis normalised against the Upper Continental Crust ((Taylor and McLennan, 1995)*. Of interest within the figures are the two samples that displayed elevated Th and U values, samples S13 and S15 indicated as blue stars and circles respectively. The elemental signatures of these samples show elevated Nb, P_2O_5, Pb and Zr; and depletion in K_2O, Na_2O, and Al_2O_3.*

Table 4.4 Descriptive statistics for the major elements for Bench 8 from Grootegeluk geological database.

	Mean	Standard Error	Median	Mode	Standard Deviation	Sample Variance	Kurtosis	Skewness	Minimum	Maximum	n
Depth	88.97	0.61	87.62	70.64	22.19	492.22	1.59	0.27	28.30	152.90	1312
SiO_2	56.15	0.16	56.80	58.50	5.83	33.97	6.95	-0.90	14.04	98.68	1312
Al_2O_3	33.97	0.13	34.12	34.90	4.83	23.28	2.20	-0.57	0.71	44.77	1312
Fe_2O_3	1.66	0.05	1.06	1.10	1.98	3.92	155.71	8.60	0.04	43.56	1311
TiO_2	2.73	0.04	2.23	2.19	1.59	2.53	17.77	3.57	0.44	17.50	1311
P_2O_5	0.42	0.01	0.26	0.13	0.47	0.22	19.71	3.53	0.01	5.16	1312
CaO	1.91	0.10	0.73	0.21	3.51	12.30	44.00	5.35	0.00	45.45	1311
MgO	0.57	0.02	0.37	0.23	0.69	0.48	43.68	5.33	0.00	8.59	1312
Na_2O	0.12	0.01	0.08	0.20	0.19	0.04	196.93	12.29	0.00	3.60	1129
K_2O	0.57	0.01	0.55	0.51	0.21	0.05	3.80	1.31	0.13	1.81	1312
SO_3	0.83	0.03	0.48	0.20	1.02	1.04	11.37	2.80	0.01	8.57	1155
MnO	0.05	0.00	0.02	0.01	0.09	0.01	68.89	7.05	0.00	1.14	1112
Ba	0.14	0.00	0.11	0.06	0.13	0.02	10.35	2.60	0.01	1.19	1311
Sr	0.05	0.00	0.03	0.02	0.05	0.00	17.63	3.44	0.00	0.48	1291
Cr_2O_3	0.08	0.00	0.06	0.06	0.07	0.01	9.22	2.54	0.00	0.57	1054
V_2O_5	0.13	0.01	0.07	0.03	0.26	0.07	74.95	7.68	0.00	3.51	1055
ZrO_2	0.14	0.00	0.10	0.07	0.13	0.02	20.64	4.03	0.02	1.20	1069
CIA	0.93	0.00	0.96	0.97	0.09	0.01	17.02	-3.50	0.17	0.99	1128
Cr/V	0.98	0.02	0.88	1.00	0.71	0.50	82.63	6.55	0.05	12.57	1047

4.4. Discussion

This section attempts to consolidate and interpret the information and analysis mentioned previously.

4.4.1. Geophysics (Phase 2)

The downhole geophysics, which was used as a precursor for the geochemical sampling, yielded the most noteworthy evidence of either elevated U or Th within these three localities at the Waterberg Coalfield. This was demonstrated by targeting gamma API values that exceeded 300 API. The rationale behind selecting 300 API as the threshold was due to the fact that typical shale API values range between 100 to 300, and assuming that the majority of the shale API consists of K, thus any value above 300 would be of interest and, in all likelihood, be associated with either Th or U.

The analysis of the geophysics yielded several observations, namely: 1) there were no gamma anomalies, where the API value was recorded as greater than 300 API units, identified within the Clarens, Greenwich (Molteno), and Grootegeluk (Volksrust) Formations; 2) an anomaly was identified in a single borehole within the Lisbon (Elliot) Formation; 3) the anomalies were concentrated within the Eendragtpan (Beaufort) and Swartrant (Vryheid) Formations.

The anomaly within the Lisbon (Elliot) Formation is located directly above the Molteno Formation (see Figure 4.15), and the geological logs recorded the bedding in the location of the anomaly as a brown mudstone. Considering location, lack of other Elliot Formation anomalies, gamma API values

(37cm thick with an average API of 532.53 and peak of 755.59), in conjunction with the host lithology marks this anomaly as an outlier. There is scope for error during logging, in particular as this section of the borehole was drilled using percussion methods, taking this into account there is a high possibility that this anomaly in actuality occurred within the upper sandstones of the Molteno Formation that is in contact with the Elliot Formation. Should the anomaly have occurred within the sandstones, and if the anomaly was associated with U, then this anomaly shows the same characteristics as a sandstone-hosted tabular U deposit.

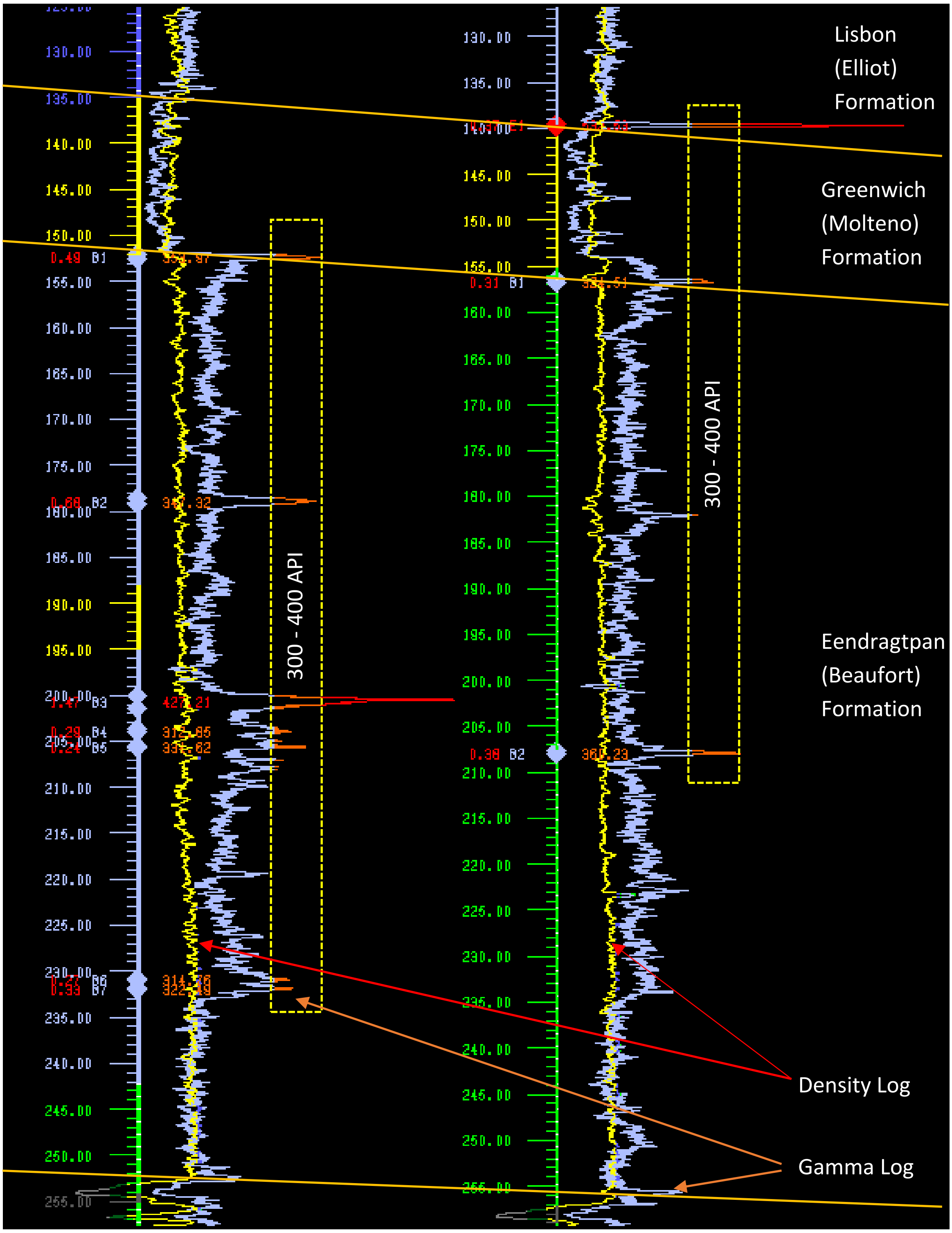

Figure 4.15 Sample of downhole geophysical logs conducted within the study, focused on the Molteno and Beaufort Formations. Log on the Left is of ZR442LQ28, and the right is of ZR442LQ38.

The anomalies within the Eendragtpan (Beaufort) Formation occurred throughout the strata, with a few of the anomalies being correlated across neighbouring boreholes. However no single anomaly persisted throughout the study area. One of the anomalies that occurred frequently, as evident in Figure 4.15, is located near or adjacent to the contact to the Molteno Formation. Considering the close proximity to the Molteno Formation, and the errors discussed with the Elliot Formation anomaly, again adds credence to the argument that the anomalies associated near to the Molteno Formation are characteristic of a sandstone-hosted tabular U deposit. While this argument is only supported by the geophysics, it does provide a model to explain the occurrence of high gamma values closely related to the Molteno Formation.

The lack of anomalies within the Grootegeluk Formation was unexpected. As the predominant thought in the literature is that the formation developed within a paleoclimate of delta abandonment with a fluctuating water table and assuming the U would have been transported into the environment in solution. Once in the environment, there should have been enrichment of U through bioaccumulation and (or) biosorption uptake into the organic material. An argument that can be made against the lack of anomalies within the Grootegeluk Formation from the locality of the boreholes themselves – is that if the boreholes had been located closer to the margins of the basin or nearer to the distributary channels there might have an anomaly detected. The lack of anomalies brings into question the provenance as suggested by Faure et al. (1996a), who postulate that the Grootegeluk and Beaufort Formations have the same provenance (granitoids and metasediments from the Damaran belt).

The distribution of anomalies within the Swartrant Formation yields the most likely results for U or Th within the Waterberg Coalfield, as identified in Figure 4.5 and Appendix G. The grouping of anomalies are spatially related to the interburden between the coal seams 1 through 4. The most notable anomaly is associated with the bottom of Bench 8. This anomaly is marked by a gradual increase in gamma API values with depth, displaying a “bell” shape with the peak value occurring near to or adjacent to the contact with the coal seam (Figure 4.16). The anomaly was found in all boreholes studied and can be used as a geophysical marker for the purposes of correlation. The cause of the anomaly is not understood. The occurrence, high gamma values, shale density, and distribution of the anomaly offers several theories as to its existence, namely: 1) an association with a marine shale, or 2) the tonstein, as identified by Spears et al. (1988).

The anomalies associated with Bench 10, typically a sandstone to siltstone interburden layer between coal seams 2 and 3, yielded the highest gamma values for all anomalies with borehole ZR442LQ34GT yielding a 1.46m thick anomaly with an average gamma API of 810.5.

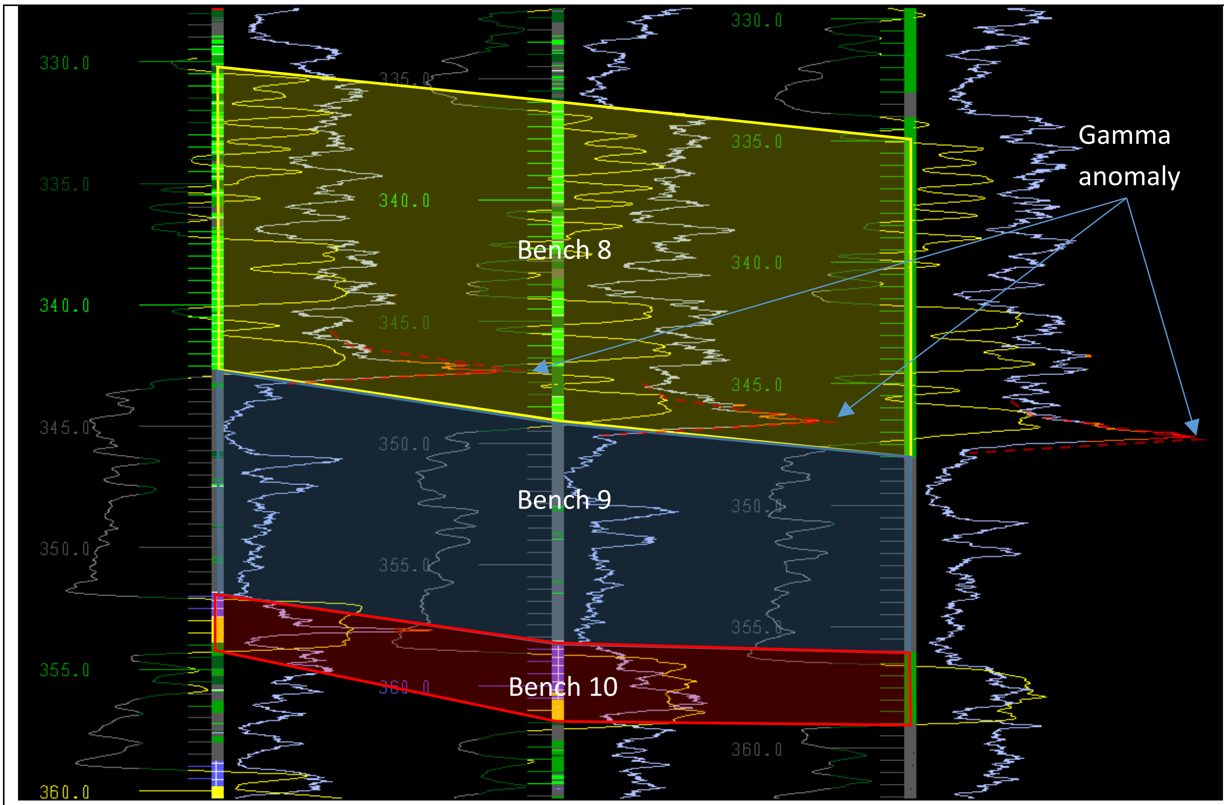

Figure 4.16 Sample of downhole geophysical logs conducted within the study, focused on Bench 8, Bench 9, and Bench 10 within the Swartrant Formation. Logs from left to right: ZR442LQ22, ZR442LQ20, and ZR442LQ31.

4.4.2. Geochemistry (Phase 3)

In contrast to the geophysics dataset, which contained 1,692,063 gamma values, the geochemical dataset was limited to 18 samples. The borehole samples, S1 to S15, were selected at random from core that was available to the author, while the bulk samples analysis, B8, B10A and B10B was supplied by the Grootegeluk Mine.

A comparison of the gamma values against calculated gamma values (Figure 4.17) reveals that there is a correlation and that the gamma values obtained from the geophysics can be used to extrapolate an approximate U and Th value using the trend equation of $y = 0.2213x$, where $y = (8 \text{ x U (ppm)}) + (4 \text{ x Th (ppm)}) + (12 \text{ x } K_2O \text{ (\%)})$. However, it should be noted that the results of analysis of gamma values versus radiogenic elements i.e. K, Th, and U; (Figure 4.6) indicated that the gamma API values were more influenced by changes in U than by Th or K_2O, suggesting that the ratios (8.U; 4.Th; 12.K_2O) used should instead be biased in favour of U and (or) Th. It should also be noted that the equation should only apply to Bench 10 due to the limitation of chemical analysis.

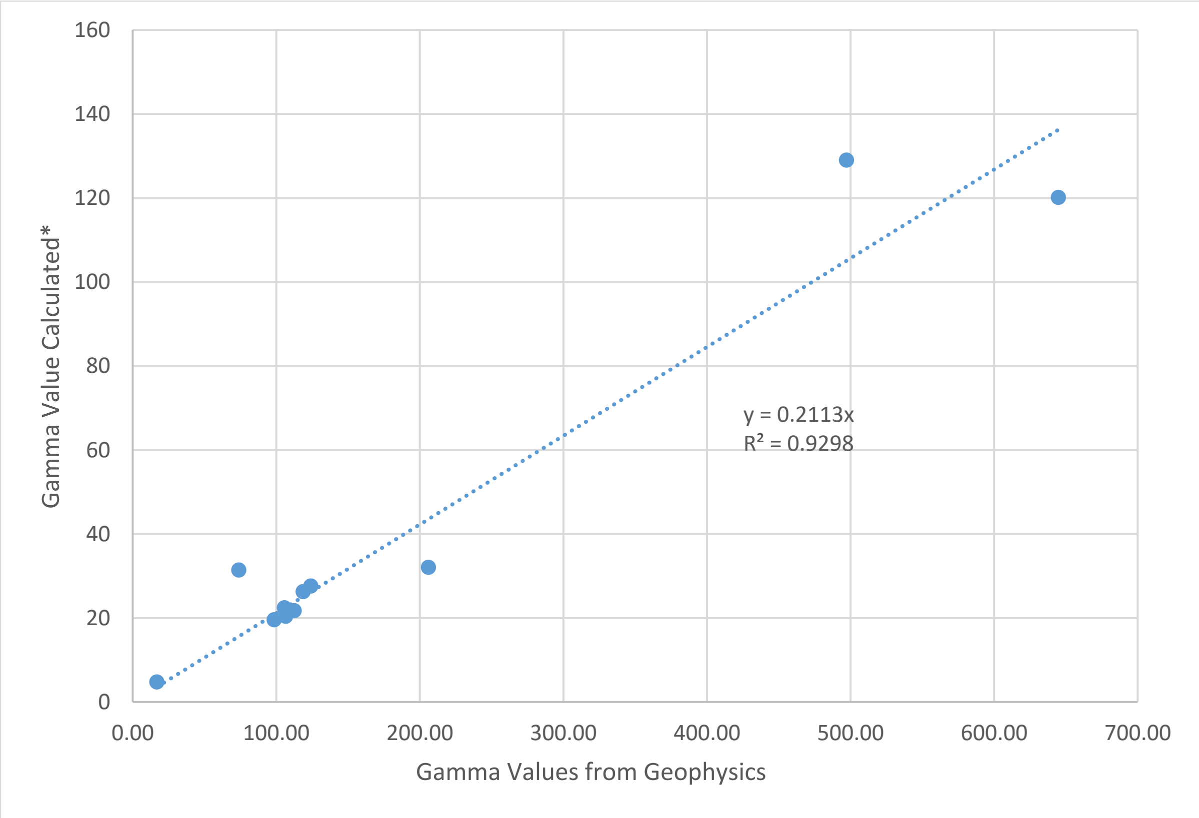

*Figure 4.17 Plot indicating the geophysics gamma values against calculated Gamma API values, *calculated using Equation 1.*

The concentration and ratios of relatively immobile elements, based on a study of Figure 4.7, indicates that the Grootegeluk Bench 10 samples and Bench 8 sample have predominantly the same provenance. The average composition of the provenance area is dominantly "granitic", possibly close to a granodioritic composition. While the Zonderwater Bench 10 samples are more mafic and indicate a provenance area that is dominantly “basaltic”

The classification based on elemental ratios indicates the majority of samples are “shale”, with several classified as “wacke”, “litharenite” and “sublitharenite”. Due to the random nature of the sampling in conjunction with Bench 10 typically being classified, by hand sample, as a “shaly banded sandstone” this accounts for the variation in the classification.

Correlation analysis of the geochemical samples, indicated that both the K_2O and Al_2O_3 are strongly negatively correlated to SiO_2 and therefore associated with the clay proportion. Contradictory to this are the Rb/Sr ratios which yielded a median ratio of 0.125. While Rb displayed a strong correlation with both K_2O and Al_2O_3, which indicates that Rb is likely associated with the clay component, the low ratio either suggests that 1) the Rb is associated with illite and is related to preferential retention of Rb compared to Sr, with the additional Sr associated with other minerals; or 2) there has been little to no weathering or there is external enrichment occurring. The abundance of Zr as a clay proportion indicator, in the absence of significant proportions of ferromagnesian minerals and sulphides, yields a median value of 128.615, in comparison to the Upper Continental Crust (Taylor and McLennan, 1995) value of 190, indicates that the clay proportion is diminished.

The concentration and ratios of mobile elements, as suggested by the Index of Alteration (CIA), reveals that the samples are highly depleted in the mobile elements. High CIA values (Table 4.3) can be interpreted in several ways. The values could indicate that: 1) these sediments have undergone a high degree of chemical weathering perhaps as a result of severely wet and humid palaeo-climatic conditions; 2) that alteration during deposition and (or) burial may have taken place because of the highly acidic pore-waters in the organic-rich sediments and (or); 3) that the source of these sediments may have been high Al, and low alkaline and alkaline earth sediments or meta-sediments. It is difficult to distinguish between the possible factors causing the residual nature of the sediments, and inferring palaeo-climatic conditions based on the chemistry of the sediments is not prudent.

The elemental ratios Th/U and Cr/V (Table 4.3), which are used to determine redox conditions in the depositional environment, indicate both Bench 10 and Bench 8 were deposited under reducing conditions. For Bench 8 this is expected as the horizon is characterised by alternating dark-grey carboniferous mudstones and mudstones, while Bench 10 is characterised as a sandstone with shale bands (Figure 2.5). The inclusion of the black shale bands is further evidence indicative of the anoxic environment and supports the Th/U and Cr/V findings.

In an attempt to find common factors that would provide insight into the U and Th enrichment, several elements were identified namely: Na_2O, Ag, Nb, Y, and Zr. Each of the elements indicated a strong correlation with both U and Th. While the association with Zr is understandable, as U is associated with zircon, the association with Nb and Y are not clearly understood but could be associated with certain heavy minerals such as pyrochlore. Comparing the trace analysis against other standards, namely the Upper Continental Crust (Taylor and McLennan, 1995), reveals that the samples are predominantly depleted in most trace elements with the exception of Ti. The samples with elevated U and Th also displayed increased values for Ti, Nb, P_2O_5, Pb, and Zr.

Chapter 5

Conclusions

The purpose of this study was to determine the distribution and quantities of radioactive trace elements, in particular U and Th, within the Waterberg Coalfield. While the literature and the geophysics provided indications that there are indeed elevated radioactive trace elements within the Waterberg Coalfield, sampling limitations have restricted a comprehensive analysis. However, there are several observations and (or) claims that can be made:

5.1.1. Observations based on the downhole geophysics (Phase 2):

Downhole geophysical profiles show that: 1) There are no gamma anomalies within the Clarens, Greenwich (Molteno), and Grootegeluk (Volksrust) Formations; 2) There are gamma anomalies within the Eendragtpan (Beaufort) Formation. These are commonly associated with khaki-yellow mudstones cited by Siepker (1986) and Brandl (1996). These anomalies are randomly distributed throughout the Formation; and 3) within the Swartrant (Vryheid) Formation there are two main trends, with the second trend showing sub-trends. The first anomaly is associated with the interburden or Bench 8 layer. This trend is marked by a gradual increase of the gamma response with depth, typically peaking around 16±2m as measured from the top of the Formation (see Figure 4.16). The gamma API values range between 301.47 to 357.05 at Grootegeluk, and 310.03 to 394.32 at Zonderwater. The trend may be indicative of a black shale with regression over time resulting in the gradual increase in gamma with depth, an alternative hypothesis is that the gamma anomalies is that of a tonstein as identified by Spears et al. (1988). Regardless of cause, the first trend was observed across the study area and would be useful as a geophysical marker as part of future exploration within the Waterberg Coalfield. The second anomaly is associated with high gamma values in the interburden between seams 1, 2, and 3. The second trend is defined by very high gamma API values. The anomalies associated with the second trend did not occur in all boreholes studied and in occurrences where they were encountered the anomaly didn't persist to neighbouring boreholes. Considering the lithologies where the anomalies were observed, it is likely that the anomalies coincide with changes in the depositional environment as opposed to U and Th being introduced diagenetically (this is supported by the CIA values for the samples)

5.1.2. Observations based on the sample analysis (Phase 3):

Based on the chemical analysis of Bench 10, it can be concluded that: 1) The mean values for U and Th abundances are 2.89 ppm and 2.47 ppm respectively, while the median values were 1.69 ppm and 1.3 ppm. These values are well within the global average (0.5 - 10 ppm U; 0.5 - 10 ppm Th) as defined by Swaine (1990). According to the classification of Herron (1988) as shown in Figure 4.8, the majority plot as shale (7), followed by wacke (4), litharnenite (2), sublitharnenite (2), Fe-shale (1) and Fe-sand (1)

a) Correlations between Al/K and Rb/Sr, as well as Zn abundance indicate a high level of weathering as these are used as indications of clay content. To support the correlations the Index of Alteration (CIA) shows the samples have been highly to completely altered.
b) The Th/U ratios indicate that bench 10 was deposited under reducing conditions.
c) The anomalous U and Th samples, S13 and S15 respectively, in comparison to the median values for the samples, show that elevated values for Y, Zr, Nb and Ag and depleted values for Na and Al.

While a single sample was taken of Bench 8 during this study, a study of the Exxaro ash composition database reveals that the majority of the samples would classify as “shale” or “Fe-shale” using the classification of Herron (1988). Additionally, the Cr/V ratios indicate that Bench 8 was deposited within an anoxic environment.

The overall conclusion of the study was that while there was some U and Th, as would be expected in such an environment, there was not significant quantities found for exploitation purposes and it is unlikely that the radioactive elements will pose a health risk within the region. As such there is little cause for concern regarding the mining of coal within the Waterberg Coalfield, in particular pertaining to U or Th.

Chapter 6

Recommendations

The following recommendations are suggested for further studies:

1. The gamma anomaly identified in Bench 8 is a target of interest as it was identified throughout the study area. Based on the gamma values it is expected that either Th or U will be predominate cause of the increased radioactivity associated with the anomaly, of which shows a gradual increase towards the base the interburden. It is suggested that this may be the tonstein as identified by Spears et al. (1988). As part of the study it would of interest to conduct a zircon analysis for dating purposes to ascertain the age of the source.
2. Due to the sporadic nature of the gamma anomalies within Bench 10, in conjunction with sampling challenges encountered within this study, it was not possible to determine a common cause for the anomaly. In this author's option, it is likely to have been due to U enriched fluid movement within the interburden along pre-existing faults, together with deposition along carbonaceous beds due to the redox potential.
3. Additional Isotope studies would further aid in provenance studies within the basin itself, as there was little literature that focused on the Waterberg Coalfield.
4. Based on the values in this study there is very little evidence to suggest that there is enough U or Th within Bench 10 or Bench 8 for either to be considered economical. Additionally, both the Bench 8 and Bench 10 material is currently being deposited either: 1) onto the discard dumps at the Grootegeluk Mine, or 2) used as backfill material within the void. However, keeping the above in mind, the following can be considered:- The presence of the U, in combination other acid forming minerals that are known to occur (Aphane and Vermeulen, 2015), there is the possibility that if the water that is permeating through the dump is acidic, it would be enriched in U and other dissolved metals, which, in itself may be economically recovered.
5. As part of the literature review, an attempt was made to ascertain possible sources of U. Several possible sources were suggested namely the Bushveld Complex, or elevated values associated with marine shales. However, one source was identified to the southeast of the Waterberg Coalfield that may warrant further study: the Glenover Phosphate Complex, which is a known U host within the region (85 to 425 ppm eU Values - Cole (1998)). Cole (1998) states that the U host is unknown at the Glenover Phosphate Complex but may include the apatite or monazite. To add further credence to the argument, Verwoerd (1986) states that carbonatites are geochemically enriched in large-ion lithophile elements like U, Th, Nb, Zr, and the rare elements. Based on the elevated values of Nb, Y and Zr associated with the Th and U anomalies found in this study this points towards the Glenover alkaline Complex, as a possible source for the elevated U within the Waterberg Coalfield.

References

Alberts, B.C. 1982. The planning and establishment of the Grootegeluk Coal Mine. Journal of The South African Institute of Mining and Metallurgy, 82, 341–352.

Anhaeusser, C.R. and Maske, S. (eds.) 1986. Mineral Deposits of Southern Africa. The Geological Society of South Africa, 2335pp.

Aphane, V. and Vermeulen, P.D. 2015. Acid mine drainage and its potential impact on the water resources in the Waterberg coalfield, South Africa. South African Journal of Geology, 118, 55–70.

Banzi Geotechnics 2014. Barker's Coalfields Map of South Africa.

Barbolini, N. 2010. Palynology of a coal seam in Karoo deposits of Botswana and correlation with southern African coal-bearing strata. Master of Science Thesis. University of the Witwatersrand, 204pp.

Barker, O.B. 1999. A techno-economic and historical review of the South African Coal Industry in the 19th and 20th centuries. In: H.J. Pinheiro (Editor) A Techno-economic and Historical Review of the South African Coal Industry in the 19th and 20th Centuries and Analyses of Coal Product Samples of South African Collieries 1998–1999. South African Bureau of Standards, 1–63.

Bester, M. and Vermeulen, P.D. 2010. Investigation of potential water quality and quantity impacts associated with mining of the shallow Waterberg coal reserves, west of the Daarby Fault, Limpopo Province, South Africa. Water SA, 36, 531–542.

Beukes, N.J. 1985. Sedimentologie van die Ellisrassteenkoolveld. Finale verslag, WNNR, KWP, NGP: Steenkoolgeologieprojek. (Report to the CSIR Coal Geology Project). Pretoria, CSIR, 15pp.

Beukes, N.J., Siepker, E.H. and Naudé, F. 1991. Genetic stratigraphy of the Waterberg Coalfield. Unpaginated Abstract, Conference on South Africa's Coal Resources, Witbank November 1991.

Bordy, E.M. and Catuneanu, O. 2002. Sedimentology and paleontology of upper Karoo aeolian strata (Early Jurassic) in the Tuli Basin, South Africa. Journal of African Earth Sciences, 35, 301–314.

Bordy, E.M., Hancox, P.J. and Rubidge, B.S. 2005. Responce to Turner, B.R. and Thomson, K., Discussion on 'Basin development during deposition of the Elliot Formation (Late Triassic - Early Jurassic), Karoo Supergroup, South Africa' (South African Journal of Geology, 107, 397-412) - A reply. South African Journal of Geology, 108, 454–461.

Bordy, E.M.M., Knoll, F. and Bumby, A. 2010. New data on the palaeontology and sedimentology of the Lower Jurassic Lisbon Formation (Karoo Supergroup), Ellisras Basin, South Africa. Neues Jahrbuch für Geologie und Paläontologie - Abhandlungen, 258, 145–155.

Brandl, G. 1993. [Geological Map Of] Sheet 2326 Ellisras.

Brandl, G. 1996. The Geology of the Ellisras area. Explanation Sheet 2326. Pretoria, Geological Survey of South Africa, 49pp.

Buermann, E.F.W. 1982. The establishment of infrastructure for the Grootegeluk Coal Mine *. Journal of The South African Institute of Mining and Metallurgy, 82, 353–355.

Cadle, A.B., Cairncross, B., Christie, A.D.M.D.M. and Roberts, D.L.L. 1993. The Karoo Basin of South Africa: type basin for the coal-bearing deposits of southern Africa. International Journal of Coal Geology, 23, 117–157.

Cairncross, B. 2001. An overview of the Permian (Karoo) coal deposits of southern Africa. Journal of African Earth Sciences, 33, 529–562.

Catuneanu, O., Hancox, P.J. and Rubidge, B.S. 1998. Reciprocal flexural behaviour and contrasting stratigraphies: A new basin development model for the Karoo retroarc foreland system, South Africa. Basin Research, 10, 417–439.

Catuneanu, O., Wopfner, H., Eriksson, P.G., Cairncross, B., Rubidge, B.S., Smith, R.M.H. and Hancox, P.J. 2005. The Karoo basins of south-central Africa. Journal of African Earth Sciences, 43, 211–253.

Cillié, J.F. 1951. Waterberg coalfield, records of boreholes 41-100. Bulletin of the Geological Survey of South Africa, 21, 381.

Cillié, J.F. 1957. Waterberg coalfield, records of boreholes 101-143. Bulletin of the Geological Survey of South Africa, 23, 276.

Cillié, J.F. and Visser, H.N. 1945. Waterberg coalfield, records of boreholes 21-40. Bulletin of the Geological Survey of South Africa, 16, 132.

Cole, D.I. 1998. Uranium. In: M.G.. Wilson and C.R. Anhaeusser (Editors) The Mineral Resources of South Africa: Handbook. Pretoria, Council for Geoscience, 642–658.

Cole, D.I. 2008. A Review of Uranium Deposits in the Karoo Supergroup of South Africa. In: Adapted from poster presentation at AAPG International Conference and Exhibition. Cape Town, South Africa, 1–9.

Cox, K., Bell, J. and Pankhurst, R. 1979. The Interpretation of Igneous Rocks. London, Great Britain, George Allen & Unwin, 450pp.

De Jager, F.S.J. 1986. Coal occurrences of the central, north-western, northern and eastern Transvaal. In: C.R. Anhaeusser and S. Maske (Editors) Mineral Deposits of Southern Africa 2. Johannesburg, Geological Society of South Africa, 2047–2055.

Demetriades, A. 2014. Basic Considerations: Sampling, the Key for a Successful Applied Geochemical Survey for Mineral Exploration and Environmental Purposes. In: H. Holland and K. Turekian (Editors) Treatise on Geochemistry. Elsevier, 1–31.

Dreyer, J.C. 1994. Total utilization of the coal resource: The Grootegeluk experience. Proceedings of the XVth CMMI Congress, Symposium Series S14, 153–164.

Dreyer, C. 2006. An overview of the geology of the Waterberg Coalfield: implications for future exploitation. In: Presented at the Fossil Fuel Foundation of South Africa Conference: The Waterberg Coalfield 2006 and beyond – quo vadis? Lephalale (previously Ellisras),.

Dypvik, H. and Harris, N.B. 2001. Geochemical facies analysis of fine-grained siliciclastics using Th/ U, Zr/ Rb and (Zr+Rb)/ Sr ratios. Chemical Geology, 181, 131–146.

Ellis, D. V. and Singer, J.M. 2007. Well Logging for Earth Scientists. Dordrecht, Springer Netherlands, 692pp.

Exxaro (Pty) Ltd 2015. Exxaro - 2014-2015 Consolidated mineral resources and ore reserves report (CMRR). Pretoria, 100pp.

Falcon, R.M.S. 1986. A brief review of the origin, formation and distribution of coal in Southern Africa. In: C.R. Anhaeusser and S. Maske (Editors) Mineral Deposits of Southern Africa 2. Johannesburg, Geological Society of South Africa, 1879–1898.

Faure, K. 1993. Mineralogy and geochemistry of the carbonaceous mudstones, and coal petrogenesis of the Grootegeluk Formation in the Waterberg Coalfield, South Africa. PhD Thesis Thesis. University of Cape Town, 208pp.

Faure, K., Armstrong, R.A.A., Harris, C. and Willis, J.P. 1996a. Provenance of mudstones in the Karoo Supergroup of the Ellisras basin, South Africa: Geochemical evidence. Journal of African Earth Sciences, 23, 189–204.

Faure, K., Harris, C. and Willis, J.P. 1995. A Profound Meteoric Water Influence on Genesis in the Permian Waterberg Coalfield, South Africa: Evidence From Stable Isotopes. SEPM Journal of Sedimentary Research, Vol. 65A, 605–613.

Faure, K., Willis, J.P. and Dreyer, J.C.C. 1996b. The Grootegeluk Formation in the Waterberg Coalfield, South Africa: facies, palaeoenvironment and thermal history — evidence from organic and clastic matter. International Journal of Coal Geology, 29, 147–186.

Ferreira, G. and Coreejes, A.G.R. 1982. Capital and cost control systems used in the establishment of the Grootegeluk Coal Mine. Journal of The South African Institute of Mining and Metallurgy, 370–375.

Fossil Fuel Foundation (FFF) 2013. The South African Coal Roadmap. Pretoria, South Africa, 37pp.

Fourie, C.J.S. 2009. Final Report on the Waterberg Geophysics Project. Report no. CSIR/NRE/MIN/ER/2009/0026/B, DMS Document number: 174407. Johannesburg, 170pp.

Fourie, C.J.S., Du Plessis, S.J. and Henry, G. 2008. New airborne geophysical data from the Waterberg coalfield. South Africa's major future energy source. In: Proceedings, Science Real and Relevant Science, 2nd Annual Council for Scientific and Industrial Research Biennial Conference. 8.

Fourie, C.J.S., Henry, G. and Maré, L.P. 2009. The structure of the Karoo-age Ellisras Basin in Limpopo Province, South Africa in the light of new airborne geophysical data: a preliminary report. 11th SAGA Biennial Technical Meeting and Exhibition, Swaziland, 27–32.

Fourie, C.J.S., Henry, G. and Maré, L.P. 2014. The Structure of the Karoo-Age Ellisras Basin in Limpopo Province, South Africa, in the Light of New Airborne Geophysical Data. South African Journal of Geology, 117, 193–210.

Fourie, C.J.S. and Stettler, R.H. 2011. New gravity data for the Waterberg Coalfield. In: Coaltech Research Association Annual Colloquium.

Fourie, C.J.., Stettler, R.H. and Henry, G. 2011. New Geophysical data for the Waterberg Coalfield. In: Geosynthesis Conference. Cape Town, SA,.

Gilliland, J. 1982. The planning and establishment of the coal-beneficiation plant at Grootegeluk*. Journal of The South African Institute of Mining and Metallurgy, 356–364.

Groenewald, P.B., Grantham, G.H. and Watkeys, M.K. 1991. Geological evidence for a Proterozoic to Mesozoic link between southeastern Africa and Dronning Maud Land, Antarctica. Journal of the Geological Society, 148, 1115–1123.

Hälbich, I.W. 1983. A tectonogenesis of the Cape Fold Belt (CFB). In: A.P.G. Söhnge and I.W. Hälbich (Editors) Geodynamics of the Cape Fold Belt. Spec. Publ. Geol. Soc. South Afr., 165–175.

Hambleton-Jones, B.B. 1980. The geochemistry of uranium in coal deposits and the favourability of the South African coal deposits for the precipitation of uranium. Pretoria, South Africa, Atomic Energy Board, Republic of South Africa, 35pp.

Hancox, P.J. 2016. The Coalfields of South-Central Africa: A Current Perspective. Episodes, 39, 407.

Hancox, P.J. and Götz, A.E. 2014. South Africa's coalfields — A 2014 perspective. International Journal of Coal Geology, 132, 170–254.

Herron, M.H. 1988. Geochemical Classification of Terrigenous Sands and Shales from Core or Log Data. SEPM Journal of Sedimentary Research, 58, 820–829.

Hu, Z. and Qi, L. 2014. Sample Digestion Methods. In: H. Holland and K. Turekian (Editors) Treatise on Geochemistry. Elsevier, 87–109.

IAEA 2009. World distribution of uranium deposits (UDEPO) with uranium deposit classification, IAEA-TECDOC-1629. Austria, International Atomic Energy Agency, 117pp.

Jeffrey, L.S. 2005a. Characterization of the coal resources of South Africa. Journal of The South African Institute of Mining and Metallurgy, 105, 95–102.

Jeffrey, L.S. 2005b. Challenges associated with further development of the Waterberg Coalfield. Journal of The South African Institute of Mining and Metallurgy, 105, 453–458.

Johnson, M.R. 1991. Sandstone petrography, provenance and plate tectonic setting in Gondwana context of the southeastern Cape-Karoo Basin. South African Journal of Geology, 94, 137–154.

Johnson, M.R., Van Vuuren, C.J., Hegenberger, W.. F., Key, R., Show, U. and Shoko, U. 1996. Stratigraphy of the Karoo Supergroup in southern Africa: An overview. Journal of African Earth Sciences, 23, 3–15.

Johnson, M.R., Van Vuuren, C.J., Visser, J.N.J., Cole, D.I., Wickens, H.D., Christie, A.D.M., Roberts, D.L., Brandl, G., Wickens, H.D.D. V., Christie, A.D.M., Roberts, D.L. and Brandl, G. 2006. Sedimentary rocks of the Karoo Supergroup. In: M.R. Johnson, C.R. Anhaeusser and R.J. Thomas (Editors) The Geology of South Africa. Geological Society of South Africa, Johannesburg, and Council for Geoscience, Pretoria, 461–499.

Joubert, R., Botha, B., Bruwer, B. and Steyn, B. 2016. Competent Persons' Report on Boikarabelo Coal Mine Coal Resources. Pretoria, 143pp.

Ketris, M.P. and Yudovich, Y.E. 2009. Estimations of Clarkes for Carbonaceous biolithes: World averages for trace element contents in black shales and coals. International Journal of Coal Geology, 78, 135–148.

Kolker, A. and Finkelman, R. 1998. Potentially Hazardous Elements in Coal: Modes of Occurrence and Summary of Concentration Data for Coal Components. Coal Preparation, 19, 133–157.

Kotze, A.P.L. 1982. Project planning and progress control for the Grootegeluk Coal Project*. Journal of The South African Institute of Mining and Metallurgy, 365–369.

Kruger, N. 2013. Groothoek Coal Mining Company: Groothoek Coal Mine on the farms Groothoek 504 LQ and Eendracht 505 LQ, Lephalale, Waterberg District Municipality, Limpopo Province. Archaeological Impact Assessment Report. Pretoria, 52pp.

Kumba Coal (Pty) Ltd 2005. Grootegeluk Mine: Mining Works Programme (Confidential Report). Pretoria, 411pp.

Lock, B.E. 1978. The Cape Fold Belt of South Africa; tectonic control of sedimentation. Proceedings of the Geologists' Association, 89, 263–281.

MacRae, C.S. 1987. Palynostratigraphic correlation between the lower Karoo sequence of the Waterberg and pafuri coal-bearing basins and the Hammanskraal plant macrofossil locality, republic of South Africa. South Africa, Government Printer, 217pp.

MacRae, C.S. 1991. Carboniferous sediments in the Waterberg Basin. South Africa, and identification of the Carboniferous/Permian boundary. S. Afr, J. Sci., 87, 381–387.

Mc Kenna, N. and Myburg, J.A. 2013. Independent Specialist Valuation Report on the Coal Assets of the Sekoko Coal (Pty) Limited (Sekoko Coal) – Firestone Energy Limited (Firestone) Joint Venture (Sekoko Coal – Firestone JV) at their Waterberg Coal Project, South Africa., 58pp.

McLennan, S.M., Hemming, S., McDaniel, D.K. and Hanson, G.N. 1993. Geochemical approaches to sedimentation, provenance, and tectonics. GSA Special Paper, 284, 21–40.

Mtimkulu, M.N. 2009. A Provisional Basinal Study of the Waterberg-Karoo, South Africa. Master of Science Thesis. University of Pretoria, 134pp.

Nakayama, K. and Nakamura, T. 2014. x-Ray Fluorescence Spectroscopy for Geochemistry. In: H. Holland and K. Turekian (Editors) Treatise on Geochemistry. Elsevier, 181–194.

National Planning Commission 2011. National Development Plan 2030 Our future - make it work. South Africa, 489pp.

Ndhlalose, M. 2015. Extraction of uranium associated with Springbok Flats coal samples. Master of Science Thesis. University of the Witwatersrand, 139pp.

Ndhlalose, M., Malumbazo, N. and Wagner, N.J. 2015. Coal quality and uranium distribution in Springbok Flats Coalfield samples. Journal of The South African Institute of Mining and Metallurgy, 115, 1167–1174.

Nesbitt, H.W., Markovics, G. and Price, R.C. 1980. Chemical processes affecting alkalis and alkaline earths during continental weathering. Geochimica et Cosmochimica Acta, 44, 1659–1666.

Nesbitt, H.W. and Young, G.M. 1982. Early Proterozoic climates and plate motions inferred from major element chemistry of lutites. Nature, 299, 715–717.

Nesbitt, H.W. and Young, G.M. 1984. Prediction of some weathering trends of plutonic and volcanic rocks based on thermodynamic and kinetic considerations. Geochimica et Cosmochimica Acta, 48, 1523–1534.

Nesbitt, H.W. and Young, G.M. 1989. Formation and Diagenesis of Weathering Profiles. The Journal of Geology, 97, 129–147.

Oboirien, B.O., Thulari, V. and North, B.C. 2016. Enrichment of trace elements in bottom ash from coal oxy-combustion: Effect of coal types. Applied Energy, 177, 81–86.

Olesik, J.W. 2014. Inductively Coupled Plasma Mass Spectrometers. In: H. Holland and K. Turekian (Editors) Treatise on Geochemistry. Elsevier, 309–336.

Pysklywec, R.N. and Mitrovica, J.X. 1999. The Role of Subduction-Induced Subsidence in the Evolution of the Karoo Basin. The Journal of Geology, 107, 155–164.

Roux, L. 2011. Optimal yield and cut density - Prediction of semi soft coking coal and powerstation coal in the Waterberg Coalfield, Limpopo Province. Master of Science in Engineering (Mining) Thesis. University of the Witwatersrand, 228pp.

Ryan, P.J. 1966. A Basin Analysis of the Waterberg Coalfield - 1966-0169., 59pp.

Ryan, P. 1967. Stratigraphie and palaeocurrent analysis of the Ecca Series and lowermost Beaufort Beds in the Karoo Basin of South Africa. PhD Thesis Thesis. University of the Witwatersrand, 210pp.

Siepker, E.H. 1986. Genetiese Stratigrafie en Sedimentologie van die Opeenvolging Karoo in die Westelike en Noordelike deel van die Waterbergsteenkoolveld. Master of Science Thesis. Rand Afrikaans Univerity, 200pp.

Smith, D.A.M. and Whittaker, R.R.L.G. 1986. The coalfields of southern Africa: An introduction. In: C.R. Anhaeusser and S. Maske (Editors) Mineral Deposits of Southern Africa 2. Johannesburg, Geological Society of South Africa, 1875–1878.

Snyman, C.P. 1998. Coal. In: M.G.. Wilson and C.R. Anhaeusser (Editors) The Mineral Resources of South Africa: Handbook. Pretoria, Council for Geoscience, 136–205.

Snyman, C.P. and Botha, W.J. 1993. Coal in South Africa. Journal of African Earth Sciences (and the Middle East), 16, 171–180.

South African Committee for Stratigraphy 1980. Lithostratigraphy of the Republic of South Africa, South West Africa/Namibia and the Republics of Bophuthatswana, Transkei and Venda. Geological Society of South Africa, 1-690pp.

Spears, D.A., Duff, P.M.D. and Caine, P.M. 1988. The West Waterberg tonstein, South Africa. International Journal of Coal Geology, 9, 221–233.

SRK Consulting 2006. Independent competent person's report of Exxaro. Pretoria, 463pp.

Standards South Africa 2004. SANS 10320:2004 - South African guide to the systematic evaluation of coal resources and coal reserves. Pretoria, 142pp.

Steyn, M. 2009. Coal marketing in South Africa: the intricasies of product, distribution, price and promotion in domestic and export markets. Master of Science in Engineering Thesis. University of the Witwatersrand, 153pp.

Sullivan, J.H., Camisani-Calzolari, F.A. and Eriksson, P.G. 2013. The practical application of vectar processed densities in proving the lateral continuity of coal zones and samples in the Ellisras Basin, South Africa. South African Journal of Geology, 116, 323–345.

Svendsen, J.B. and Hartley, N.R. 2002. Synthetic heavy mineral stratigraphy: applications and limitations. Marine and Petroleum Geology, 19, 389–405.

Swaine, D.J. 1990. Trace Elements in Coal. North Ryde, Australia, Butterworth & Co., 278pp.

Swaine, D.J. 1994. Trace elements in coal and their dispersal during combustion. Fuel Processing Technology, 39, 121–137.

Swaine, D.J. 1998. Trace Elements During the Mining and Beneficiation of Coal Trace Elements During the Mining and Beneficiation of Coal. Coal Preparation, 19, 177–193.

Swaine, D.J. 2000. Why trace elements are important. Fuel Processing Technology, 65, 21–33.

Tankard, A., Welsink, H., Aukes, P., Newton, R. and Stettler, E. 2009. Tectonic evolution of the Cape and Karoo basins of South Africa. Marine and Petroleum Geology, 26, 1379–1412.

Taylor, S.R. and McLennan, S.M. 1985. The Continental Crust; Its Composition and Evolution. Blackwell Science Ltd, 312pp.

Taylor, S.R. and McLennan, S.M. 1995. The geochemical evolution of the continental crust. Reviews of Geophysics, 33, 241.

Thomas, L. 2012. Coal Geology. Chichester, UK, John Wiley & Sons, Ltd, 444pp.

Trevor, T.G. and Du Toit, A.L. 1922. Coal in the northern Waterberg. S. Afr. J. Ind. Eng., 4, 164–170.

Turner, B.R. 1999. Tectonostratigraphical development of the Upper Karooforeland basin: Orogenic unloading versus thermally-induced Gondwana rifting. Journal of African Earth Sciences, 28, 215–238.

Turner, B.R. and Thomson, K. 1998. Tectonostratigraphical development of the Upper Karoo foreland basin: Orogenic unloading versus Gondwana rifting. Implications for the Mesozoic evolution of the Falkland Plateau and West Gondwana. Journal of African Earth Sciences (and the Middle East), 27, 201–201.

Van Heerden, C. 2016. Optimization of the coal reserve utilization at Grootegeluk Mine, Waterberg coalfield, with regards to the phosphorus content in coal. Master of Science in Engineering (Mining) Thesis. University of the Witwatersrand, 140pp.

Venter, F.. 1944. Waterberg coalfield, records of boreholes 1–20. Bulletin of the Geological Survey of South Africa, 15, 1–106.

Verwoerd, W.J. 1986. Mineral deposits associated with carbonatites and alkaline rocks. In: C.R. Anhaeusser and S. Maske (Editors) Mineral Deposits of Southern Africa 2. Geological Society of South Africa, 2173–2191.

Wagner, N.J. and Tlotleng, M.T. 2012. Distribution of selected trace elements in density fractionated Waterberg coals from South Africa. International Journal of Coal Geology, 94, 225–237.

Winter, H.D.L.R. 1984. Tectonostratigraphy, as applied to analysis of South African Phanerozoic basins. Transactions - Geological Society of South Africa, 87, 169–179.

Wit, M.J. De, Jeffery, M., Nicolaysen, L.O.N. and Bergh, H. 1988. Explanatory Notes on the Geologic Map of Gondwana. Tulsa, American Association Petroleum Geol.

Zhang, J., Ren, D., Zhu, Y., Chou, C.-L., Zeng, R. and Zheng, B. 2004. Mineral matter and potentially hazardous trace elements in coals from Qianxi Fault Depression Area in southwestern Guizhou, China. International Journal of Coal Geology, 57, 49–61.

Appendices

Appendix A Summary of the work done within the Waterberg Coalfield by year

Year	Worker(s)	Results
1922	Trevor and Du Toit	The discovery of coal within the northern section what is then called the Waterberg.
1944	Venter	Results of exploratory holes across the Waterberg coalfield by the Geological Survey of South Africa, Boreholes 1-20
1945	Cillie and Visser	Results of exploratory holes across the Waterberg coalfield by the Geological Survey of South Africa, Boreholes 21-40
1951	Cillie	Results of exploratory holes across the Waterberg coalfield by the Geological Survey of South Africa, Boreholes 41-100
1957	Cillie	Results of exploratory holes across the Waterberg coalfield by the Geological Survey of South Africa, Boreholes 101-143
1966	Ryan	Sedimentological study on outcropping Karoo rocks, unpublished report.
1982	Alberts	Provides a background on the history of the Grootegeluk Mine, as well as the quality & reserves in 1974 at 500Mt of metallurgical coal and 1700 Mt of power-station coal.
1985	Beukes	Sedimentological study of the Waterberg coalfield, unpublished report.
1986	Siepker	MSc thesis provides a depositional history of the Ellisras basin, the total thickness and surficial occurrence of the Grootegeluk, Goedegedacht and Vryheid formations.
1986	Smith and Whittaker	Book chapter on the coalfields of southern Africa, the Waterberg Coalfield is discussed.
1986	Falcon	Book chapter on the origin, formation and distribution of coal in Southern Africa, Waterberg coal basin discussed
1986	De Jager	Book chapter on the coal occurrences of the central, north-western, northern and eastern Transvaal, the Waterberg Coalfield is discussed
1987	MacRae	Book chapter where Palynostratigraphic correlation between the lower Karoo sequence of the Waterberg & pafuri coal-bearing basins and the Hammanskraal plant macrofossils.
1991	MacRae	Carboniferous sediments in the Waterberg Basin, and identification of the Carboniferous/Permian boundary.
1995	Faure et al.	The effect of meteoric water on the genesis of the Waterberg coalfield based off stable isotope analysis
1996	Brandl	The explanation of Sheet 2326, 1:250 000. The general geology of the Ellisras basin is covered in detail with the geographical location and geological outline provided with the sheet itself
1996	Johnson et al.	A review of the Karoo Supergroup in southern Africa. The Ellisras Basin is included.
1996	Faure et al.	Identifies the history (facies, palaeoenvironment and thermal) of the Grootegeluk Fm based off organic and clastic matter studies.
1996	Faure et al.	Provides a provenance of the mudstones within the Ellisras basin based off geochemical evidence.
1998	Snyman	Book chapter on coal within South Africa, the Waterberg coalfield is discussed
2001	Cairncross	A review of the Karoo basins of southern Africa. The Waterberg coalfield is discussed.
2003	Wakerman	PhD thesis where the author reviews all the Eyesizwe prospecting projects and considers the viability of each. Two of the projects fall within the Waterberg Coalfield: Waterberg North and Waterberg South.
2003	Kruszewska	Three samples taken from the Waterberg Coalfield are used in a review of the fluorescing macerals within the South African coals.
2004	SANS	SANS Code defines coal deposits into two types: multiple seam and thick interbedded seam deposit types. Under the thick interbedded seam definition there is the following note: "The coal deposits of the Grootegeluk formation in the Waterberg coalfield in South Africa are typical of this type"
2005	Catuneanu	A review of the Karoo basins of south-central Africa. The Ellisras Basin is discussed.

	et al.	
2005	Jeffrey	Characterization of the coal resources of South Africa, Waterberg Coalfield included
2005	Jeffrey	Challenges associated with further development of the Waterberg Coalfield
2006	Johnson et al.	Book chapter on the sedimentary rocks of the Karoo Supergroup within South Africa, the Ellisras basin is discussed.
2009	Mtimkulu	MSc thesis: A Provisional Basinal Study of the Waterberg-Karoo, South Africa
2009	Steyn	MSc thesis where an examination of all the individual activities during the marketing process of bulk commodity coal within South Africa is considered. The Waterberg is discussed with the need of infrastructure highlighted for continued development
2010	Barbolini	MSc thesis through the use of palaeopalynology correlates coal-bearing lithological units in Botswana to South Africa.
2010	Bester and Vermeulen	A scoping level study was performed to consolidate the existing information on the geohydrology and pre-mining water quantity and quality of water resources associated with the Waterberg coal reserves.
2010	Bordy et al.	A paleontological and sedimentological analyses of the Lisbon Formation to which the authors suggest that the formation (especially its upper part) was deposited in a dryland setting with well-drained soils that at least episodically supported some flora and a fauna probably dominated by basal sauropodomorphs.
2011	Dzimba	MSc thesis: Consideration of the Criteria Required for the Selection of Potential Underground Coal Gasification Sites in South Africa. Waterberg Coalfield is recommended as potential site for UCG.
2011	Roux	MSc thesis considers a review of the physical and chemical characteristics of coal to optimize the coal utilization within the Grootegeluk Mine.
2012	Mare	PhD thesis to consider the thermal history of sedimentary basins and the affects thereof on the genesis of hydrocarbon deposits within the Karoo Basin. Several samples were taken from the Ellisras Basin.
2012	Wagner and Tlotleng	Studied the coal within the Grootegeluk Mine, focusing on the trace elements in particular Hg, Cd, Se and As.
2012	Makiese	PhD thesis were sampled five coal samples collected from the Waterberg Coalfield for Hg, thesis focused on Highveld coals. Showed that Hg within Waterberg Coalfield was higher than global average.
2013	Sullivan et al.	The use of geophysics (vectar processed densities) to show variation in geology.
2014	Fourie et al.	Results & interpretation of an airborne magnetic and radiometric survey of the Ellisras Basin
2014	Hancox and Gotz	Review of South African coalfields
2015	Aphane and Vermeulen	Studied the Vryheid Formation and Volksrust Formation with regards to their acid forming potential
2016	Van Heerden	MSc thesis considered the phosphorus content in the coal to optimize the coal reserve utilization within the Grootegeluk Mine
2016	Hancox	Review of Southern-Central African coalfields

Appendix B Gamma vs Density Plots per Stata within Zonderwater.

Clarens Sandstone	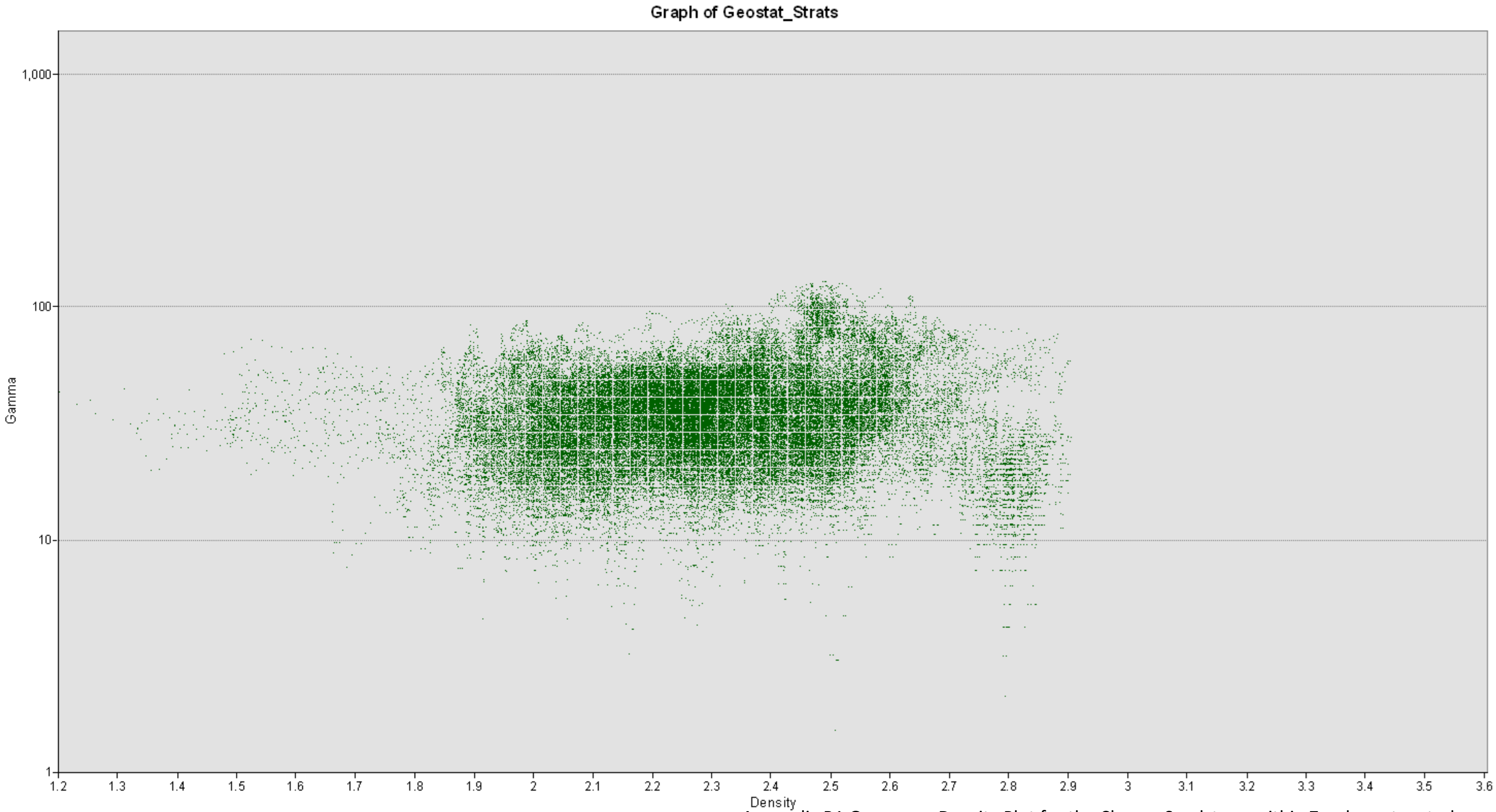 Appendix B1 Gamma vs Density Plot for the Clarens Sandstone within Zonderwater study area

Eendragtpan Formation (Beaufort)

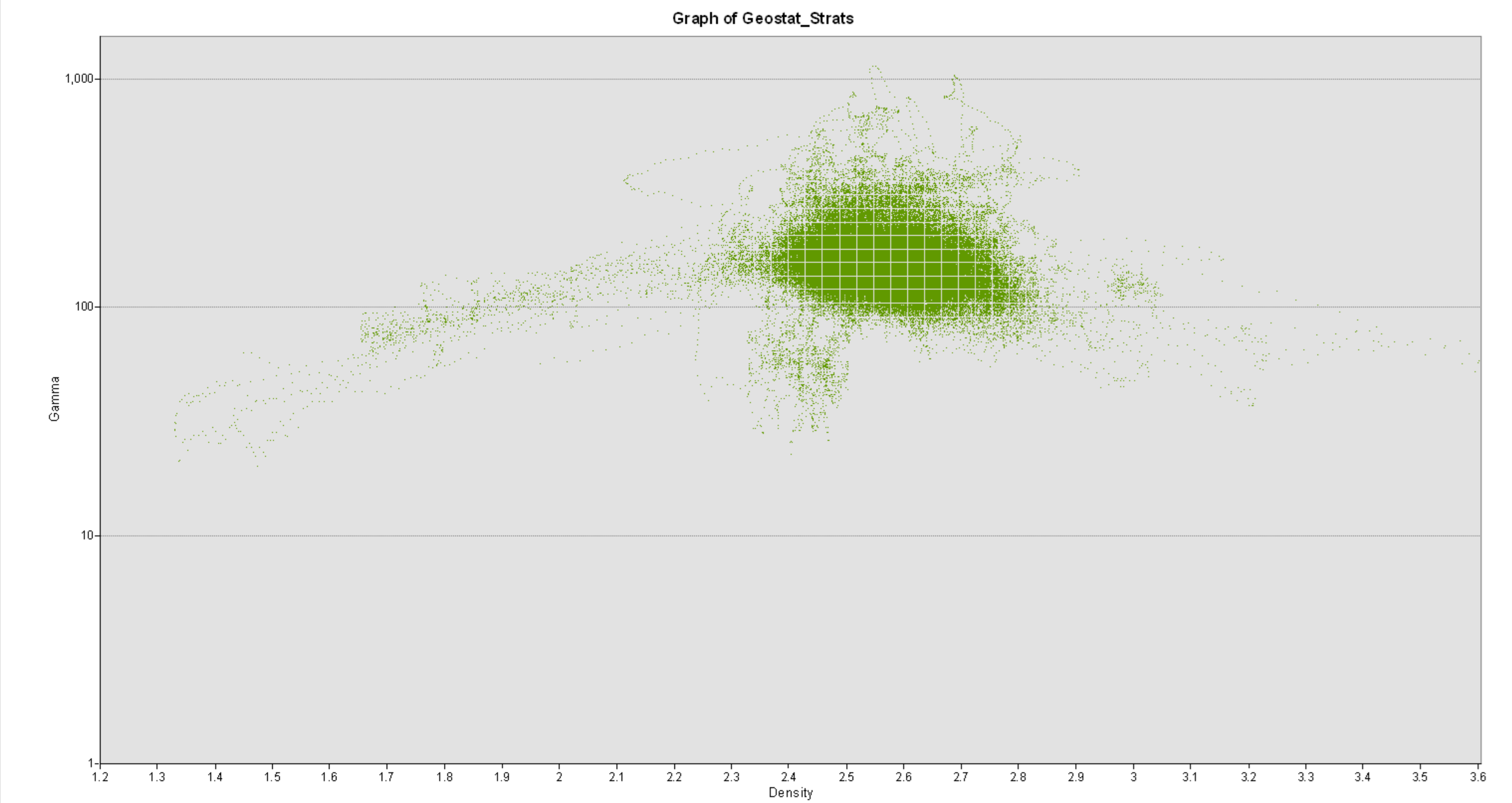

Appendix B2 Gamma vs Density Plot for the Eendragtpan Formation (Beaufort) within Zonderwater study

Lisbon Formation (Elliot)

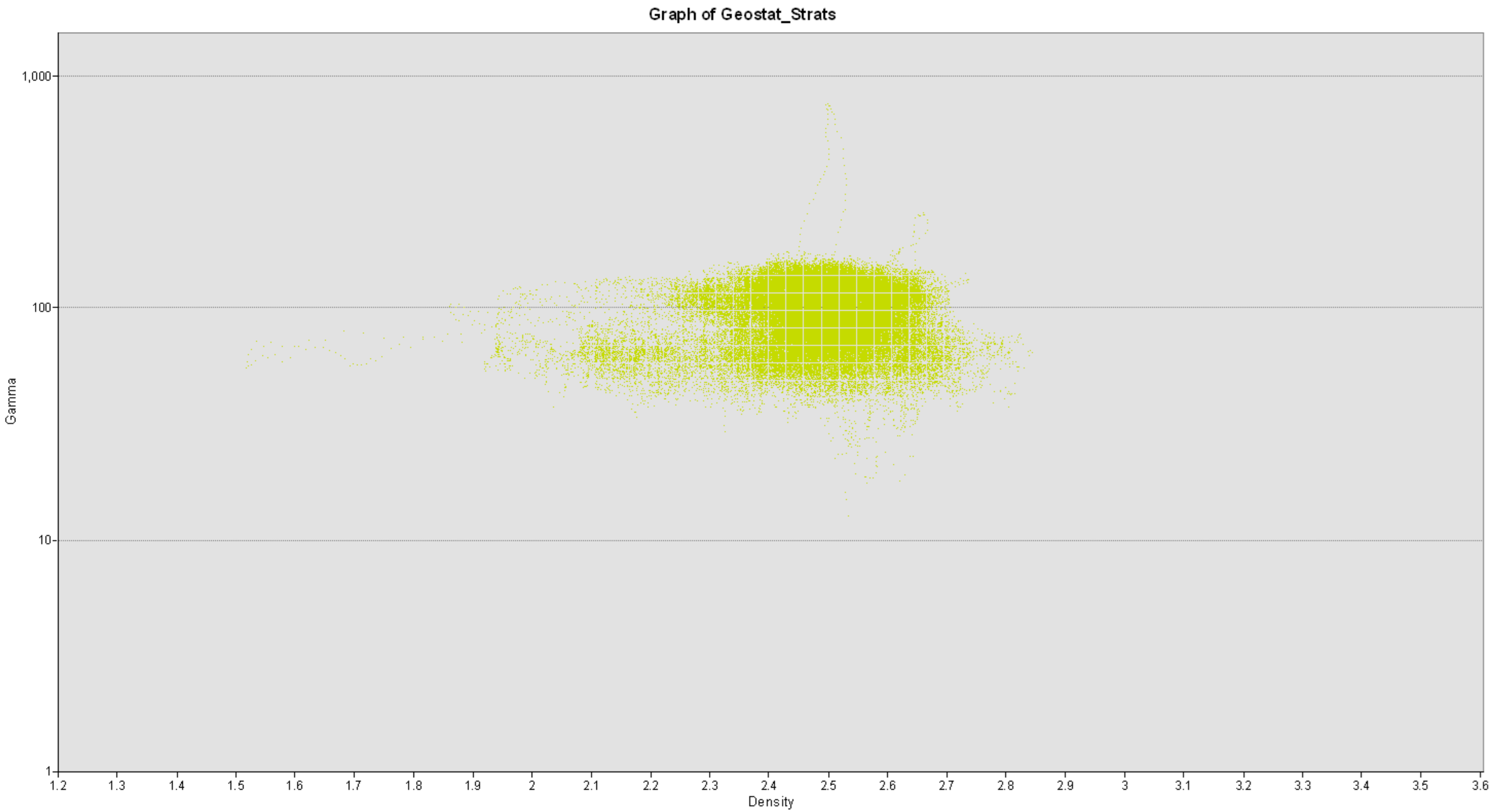

Appendix B3 Gamma vs Density Plot for the Lisbon Formation (Elliot) within Zonderwater study area

Grootegeluk Formation (Volksrust)

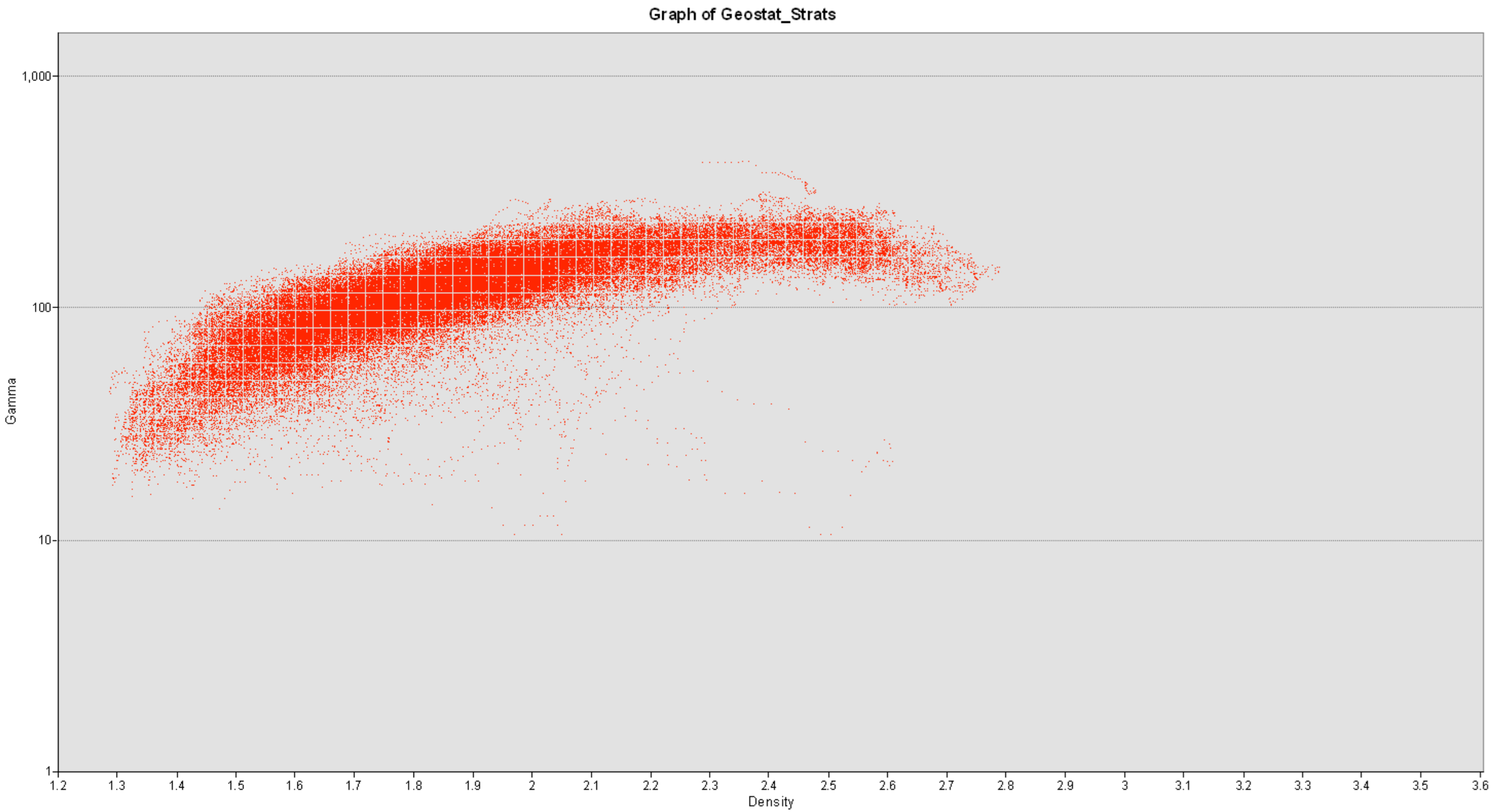

Appendix B4 Gamma vs Density Plot for the Grootegeluk Formation (Volksrust) within Zonderwater study

Greenwich Formation (Molteno)

Appendix B5 Gamma vs Density Plot for the Greenwich Formation (Molteno) within Zonderwater study

Swartrant Formation (Vryheid)

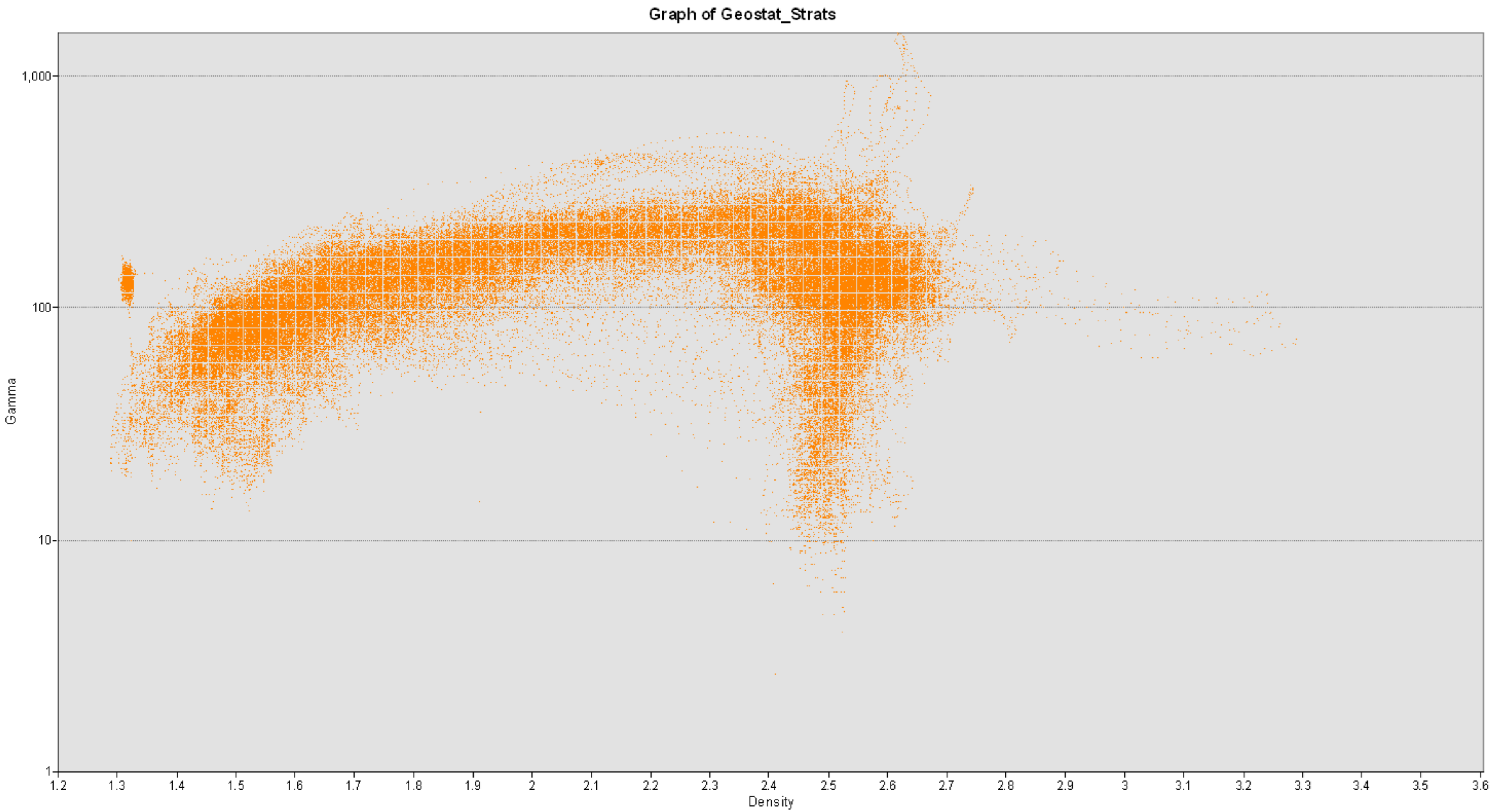

Appendix B6 Gamma vs Density Plot for the Swartrant Formation (Vryheid) within Zonderwater study area

Appendix C Statistics of the stratigraphy within the Zonderwater study area

	Gamma (API units)									Density (g/cc)									Depth (m)									
Stratigraphy	n	Min	Max	Mean	Median	Geometric Mean	Variance	Standard Deviation	Coefficient of variation	n	Min	Max	Mean	Median	Geometric Mean	Variance	Standard Deviation	Coefficient of variation	n	Min	Max	Mean	Median	Geometric Mean	Variance	Standard Deviation	Coefficient of variation	Average thickness (m)
Clarens Sandstone	67546	1.52	127.87	35.68	33.03	32.45	256.21	16.01	0.45	65650	0.38	2.90	2.29	2.29	2.28	0.05	0.22	0.10	67562	0.09	79.00	28.60	28.70	23.10	226.35	15.04	0.53	42.18
Lisbon Formation (Elliot)	142743	12.59	755.59	98.76	100.70	95.64	600.00	24.49	0.25	142743	1.52	2.84	2.49	2.50	2.49	0.01	0.09	0.04	142743	40.86	147.00	94.21	94.42	90.23	704.67	26.55	0.28	90.48
Greenwich Formation (Molteno)	24783	9.63	456.99	63.36	52.43	55.77	1374.65	37.08	0.59	24783	2.21	2.79	2.43	2.41	2.43	0.01	0.08	0.03	24783	130.01	160.00	146.16	146.76	146.03	38.59	6.21	0.04	14.71
Eendragtpan Formation (Beaufort)	179441	20.14	1131.19	159.90	152.72	154.13	2496.98	49.97	0.31	179204	1.33	3.61	2.55	2.54	2.55	0.01	0.11	0.04	179488	142.51	280.00	206.95	206.60	204.55	982.11	31.34	0.15	105.5
Grootegeluk Formation (Volksrust)	94452	10.46	427.15	121.31	117.17	110.52	2382.35	48.81	0.40	94413	1.29	2.79	1.87	1.84	1.85	0.08	0.28	0.15	94454	236.78	336.06	291.08	291.13	290.34	425.05	20.62	0.07	64.5
Swartrant Formation (Vryheid)	105789	0.00	1534.94	135.98	125.78	Not Calculated	5979.50	77.33	0.57	108884	1.29	3.29	2.07	2.10	2.03	0.18	0.43	0.21	110912	232.01	393.00	337.90	343.62	336.07	1123.07	33.51	0.10	52.63

Appendix D Correlation coefficients for major and minor elemental analyses from the study area

	Ag	*Al*	*As*	*Ba*	*Bi*	*Ca*	*Cr*	*Cs*	*Cu*	*Fe*	*Ge*	*K*	*Mg*	*Mn*	*Mo*	*Na*	*Nb*	*Ni*	*P*	*Pb*	*Rb*	*S*	*Se*	*Si*	*Sr*	*Th*	*Ti*	*U*	*V*	*Y*	*Zn*	*Zr*	*LOI*
Ag	1.00																																
Al	-0.52	1.00																															
As	0.47	0.11	1.00																														
Ba	-0.09	0.18	0.03	1.00																													
Bi	-0.45	0.72	-0.05	0.21	1.00																												
Ca	0.73	-0.41	0.37	0.01	-0.32	1.00																											
Cr	-0.22	0.09	-0.08	-0.14	0.55	0.04	1.00																										
Cs	-0.18	0.58	0.28	0.50	0.37	-0.05	-0.21	1.00																									
Cu	-0.08	-0.11	0.02	0.18	-0.16	-0.08	0.00	0.33	1.00																								
Fe	0.40	-0.06	0.30	-0.06	0.20	0.75	0.64	0.07	0.00	1.00																							
Ge	0.77	-0.13	0.42	-0.05	-0.07	0.85	0.02	-0.03	-0.35	0.72	1.00																						
K	-0.40	0.95	0.12	0.03	0.70	-0.38	-0.02	0.45	-0.30	-0.08	0.00	1.00																					
Mg	0.26	-0.05	-0.48	-0.63	0.60	0.54	0.63	-0.93	-0.60	0.67	0.82	0.29	1.00																				
Mn	0.73	-0.63	0.81	0.65	-0.18	0.87	0.34	0.81	0.49	0.93	0.69	-0.61	1.00	1.00																			
Mo	-0.18	0.53	0.15	0.23	0.59	-0.09	-0.18	0.35	-0.43	-0.03	0.17	0.63	-0.17	-0.34	1.00																		
Na	-0.81	0.40	-0.39	0.10	0.60	-0.54	0.60	0.12	0.14	-0.05	-0.58	0.29	0.33	-0.33	0.18	1.00																	
Nb	0.89	-0.37	0.51	0.01	-0.32	0.93	-0.11	-0.02	-0.18	0.64	0.93	-0.28	0.40	0.78	0.00	-0.72	1.00																
Ni	0.80	-0.40	0.59	0.14	-0.30	0.89	-0.07	0.19	0.14	0.65	0.76	-0.39	-0.62	0.90	-0.08	-0.57	0.91	1.00															
P	0.75	-0.62	0.32	0.20	-0.35	0.69	-0.16	-0.28	-0.11	0.40	0.65	-0.56	0.02	0.71	-0.16	-0.62	0.76	0.73	1.00														
Pb	0.50	-0.42	0.41	0.15	-0.18	0.51	0.30	0.26	0.50	0.52	0.25	-0.55	-0.30	0.92	-0.35	-0.19	0.46	0.72	0.37	1.00													
Rb	-0.15	0.63	-0.03	-0.20	0.43	-0.21	-0.19	0.02	-0.57	-0.08	0.25	0.81	0.47	-0.57	0.56	0.00	-0.06	-0.33	-0.22	-0.75	1.00												
S	-0.19	0.46	-0.19	-0.16	0.38	-0.26	-0.14	-0.23	-0.65	-0.18	0.16	0.65	0.51	-0.67	0.55	0.11	-0.14	-0.44	-0.18	-0.82	0.91	1.00											
Se	0.56	-0.07	0.36	0.05	-0.11	0.52	-0.01	0.03	-0.47	0.38	0.70	0.06	0.13	0.43	0.29	-0.37	0.65	0.48	0.31	0.15	0.22	0.27	1.00										
Si	0.25	-0.93	-0.29	-0.32	-0.65	0.08	-0.12	-0.64	0.18	-0.21	-0.20	-0.88	0.09	0.27	-0.54	-0.19	0.03	0.08	0.35	0.24	-0.61	-0.40	-0.18	1.00									
Sr	0.32	-0.33	0.15	0.30	-0.05	-0.01	-0.14	-0.25	0.02	-0.11	0.00	-0.37	-0.51	0.11	-0.15	-0.22	0.11	0.17	0.67	0.21	-0.24	-0.12	-0.08	0.29	1.00								
Th	0.62	-0.45	0.33	-0.15	-0.37	0.02	-0.19	-0.38	-0.06	-0.12	0.15	-0.37	0.42	0.19	-0.23	-0.48	0.26	0.19	0.31	0.31	-0.18	-0.11	0.32	0.39	0.46	1.00							
Ti	0.89	-0.45	0.49	0.00	-0.37	0.94	-0.10	-0.03	-0.11	0.64	0.90	-0.37	0.46	0.82	-0.08	-0.71	0.99	0.94	0.78	0.53	-0.15	-0.23	0.61	0.11	0.13	0.27	1.00						
U	0.92	-0.34	0.48	-0.05	-0.29	0.83	-0.12	-0.14	-0.31	0.57	0.94	-0.21	0.58	0.68	0.04	-0.76	0.96	0.80	0.76	0.33	0.09	0.03	0.70	0.01	0.18	0.42	0.94	1.00					
V	0.81	-0.49	0.48	0.16	-0.48	0.90	-0.21	-0.14	-0.16	0.52	0.85	-0.42	-0.56	0.69	-0.05	-0.72	0.94	0.87	0.88	0.35	-0.15	-0.16	0.53	0.14	0.27	0.18	0.94	0.91	1.00				
Y	-0.02	0.40	-0.10	-0.24	0.29	-0.07	-0.09	-0.27	-0.74	-0.02	0.36	0.61	0.58	-0.56	0.50	-0.08	0.06	-0.30	-0.06	-0.76	0.93	0.95	0.35	-0.42	-0.17	-0.04	-0.03	0.24	0.02	1.00			
Zn	-0.24	0.23	0.00	0.00	0.59	0.01	0.98	0.10	0.09	0.62	-0.01	0.11	0.49	0.38	-0.05	0.59	-0.13	-0.02	-0.19	0.36	-0.18	-0.20	-0.08	-0.25	-0.11	-0.17	-0.12	-0.16	-0.25	-0.18	1.00		
Zr	0.99	-0.48	0.47	-0.11	-0.41	0.73	-0.17	-0.21	-0.18	0.42	0.81	-0.35	0.56	0.72	-0.13	-0.80	0.89	0.77	0.72	0.44	-0.07	-0.11	0.63	0.20	0.27	0.62	0.89	0.94	0.81	0.08	-0.22	1.00	
LOI	-0.43	0.91	0.14	0.47	0.60	-0.27	0.08	0.63	-0.15	0.02	-0.03	0.82	-0.33	-0.55	0.47	0.31	-0.24	-0.27	-0.43	-0.31	0.51	0.36	0.08	-0.94	-0.25	-0.39	-0.31	-0.21	-0.29	0.34	0.23	-0.39	1.00

Appendix E Ash oxide and trace elementresults for selected borehole samples

ID	140/91.73/S1	140/92.79/S4	140/93.77/S2	140/94.86/S3	141/105.75/S8	141/106.64/S7	141/108.45/S6	141/109.39/S5	142/96.41/S12	142/97.27/S9	142/97.88/S10	142/98.25/S11	BH34/327.55/S13	BH34/329.16/S14	BH39/343.60/S15
SiO_2	63.39	64.12	59.04	76.71	91.71	71.17	69.10	82.44	49.17	62.69	89.21	61.58	74.39	78.24	83.09
Al_2O_3	20.52	22.51	25.53	13.75	5.12	18.17	18.88	9.58	26.58	22.31	6.56	22.67	3.44	13.28	7.14
BaO	0.03	0.02	0.04	0.12	<0.009	0.02	0.02	0.05	0.24	0.20	0.01	0.02	0.07	0.01	0.03
CaO	0.21	0.07	0.07	0.05	0.02	0.04	0.04	0.03	0.06	0.05	0.02	0.04	1.27	0.28	0.07
Cr_2O_3	0.22	0.02	0.04	0.03	<0.010	0.02	0.01	0.02	0.03	0.02	<0.010	0.02	0.02	<0.010	<0.010
Fe_2O_3	1.69	0.60	0.42	0.30	0.06	0.25	0.29	0.10	0.36	0.26	0.19	0.30	1.77	0.25	0.19
K_2O	0.29	0.35	0.47	0.15	0.06	0.34	0.33	0.10	0.38	0.40	0.08	0.34	0.03	0.16	0.12
MgO	0.14	<0.010	0.04	<0.010	<0.010	<0.010	<0.010	<0.010	0.01	0.01	<0.010	0.01	<0.010	<0.010	<0.010
Mn_3O_4	0.04	<0.010	<0.010	<0.010	<0.010	<0.010	<0.010	0.01	<0.010	<0.010	<0.010	<0.010	0.07	0.01	<0.010
Na_2O	0.12	0.07	0.08	0.07	0.07	0.07	0.06	0.08	0.07	0.10	0.09	0.07	0.02	0.07	0.03
P_2O_5	0.04	0.03	0.05	0.23	<0.004	0.04	0.04	0.13	0.05	0.06	0.04	0.03	0.32	0.02	0.15
SO_3	0.09	0.09	0.09	0.10	0.09	0.09	0.10	0.10	0.09	0.10	0.10	0.09	0.08	0.09	0.09
TiO_2	1.13	1.27	1.21	1.06	0.46	1.93	1.34	0.99	1.13	1.17	0.51	1.01	12.96	1.46	4.18
V_2O_5	0.01	0.01	0.02	0.02	<0.004	0.01	0.01	0.02	0.02	0.02	0.01	0.02	0.07	<0.004	0.03
LOI	11.18	9.95	12.71	7.13	2.60	7.61	8.94	6.17	21.64	11.95	3.30	12.95	3.92	5.89	3.56
Ag	0.30	0.81	0.41	0.66	0.26	1.24	0.63	0.88	0.36	0.56	0.32	0.33	3.51	0.77	2.82
As	4.12	5.68	13.36	3.95	0.72	2.90	4.36	3.00	5.66	5.66	3.80	7.83	10.38	2.92	10.10
Bi	0.44	0.17	0.25	0.26	0.05	0.20	0.30	0.10	0.21	0.39	0.10	0.15	0.03	0.06	0.08
Cs	0.26	0.46	0.41	0.20	0.09	0.49	0.46	0.12	0.65	0.57	0.17	0.55	0.31	0.09	0.10
Cu	77.01	154.18	74.61	78.53	82.52	71.58	77.17	73.81	82.68	88.19	72.62	67.98	61.67	74.85	72.30
Ge	0.91	0.73	0.68	0.61	0.46	0.79	0.71	0.54	0.74	0.70	0.50	0.61	2.24	0.61	0.99
Mo	1.51	0.69	2.21	1.37	0.33	0.93	2.85	0.50	1.53	6.65	2.03	3.73	1.90	0.47	0.95
Na	896.51	546.22	604.01	506.08	525.37	496.51	461.35	619.36	537.39	726.78	685.01	493.32	120.47	500.45	210.01
Nb	14.54	15.71	17.47	12.73	5.37	21.88	17.28	11.12	17.81	17.15	6.66	14.77	131.39	17.82	45.53
Ni	67.35	76.46	80.31	64.36	43.61	73.08	64.99	58.62	67.66	81.34	59.17	64.99	207.39	50.22	91.08
Pb	212.68	154.20	139.71	132.47	95.15	159.02	160.60	128.11	157.07	151.23	157.63	145.10	245.73	126.07	202.47
Rb	6.15	10.75	10.12	7.64	5.26	10.06	9.30	5.70	8.61	8.16	6.84	8.55	6.44	5.08	6.32
Se	0.05	0.02	0.03	0.02	0.02	0.06	0.01	0.01	0.07	0.06	0.07	0.06	0.13	0.04	0.09
Sr	49.20	32.57	70.21	335.53	9.79	52.41	49.54	193.08	70.89	103.29	69.45	32.57	102.19	17.05	222.11
Th	0.87	0.90	0.36	1.43	0.13	1.87	0.79	3.72	1.33	0.32	4.71	0.96	3.04	1.25	17.49
U	1.72	1.55	1.27	1.69	0.41	2.39	1.67	1.87	2.01	1.49	0.76	1.64	13.43	1.60	7.15
Y	0.15	0.18	0.07	0.28	0.03	0.34	0.12	0.47	0.14	0.07	0.54	0.13	8.46	0.31	7.51
Zn	1674.65	141.71	337.81	156.01	39.93	125.96	219.39	128.62	302.46	225.10	95.44	189.83	87.81	72.78	75.59
Zr	138.51	212.92	127.58	179.79	83.30	434.63	199.64	275.52	134.46	176.50	101.25	116.81	1357.30	283.99	1107.01

Appendix F: Major, trace element and sulphur speciation data for bulk samples

ID	Bench 8A	Bench 10A	Bench 10B	
Major Elements				
SiO2	27.04	55.33	55.48	%
Al2O3	17.94	26.54	26.45	%
Fe(total)	5.13	0.28	0.27	%
Fe2O3	7.34	0.4	0.39	%
TiO2	0.88	1.23	1.23	%
CaO	0.75	0.04	0.04	%
MgO	0.28	0.11	0.11	%
Na2O	0.04	0.08	0.06	%
K2O	0.21	0.58	0.57	%
MnO	0.01	0	0	%
P	0.1	0.02	0.03	%
Ba	0.06	0.02	0.01	%
Sr	0.02	0	0	%
V	0.01	0.01	0.01	%
Cr	0.01	0.02	0.02	%
Cu	0	0	0	%
Zn	0.01	0.01	0.01	%
Zr	0.02	0.04	0.04	%
C	27.5	3.75	3.75	%
S	6.42	0.07	0.06	%
L.O.I	43.75	14.29	14.2	%
% ASH	56.25	85.71	85.8	%
CIA	94.72	97.43	97.53	
Total Trace Elements				
Ag	0.54	0.66	0.67	mg/kg
As	14.07	4.38	4.07	mg/kg
Au	0.01	0.01	0.01	mg/kg
B	15.9	17.67	16.38	mg/kg
Ba	588.81	152.1	143.18	mg/kg
Be	5.79	2.13	2.04	mg/kg
Bi	1.36	0.3	0.31	mg/kg
Cd	0.12	0.28	0.26	mg/kg
Ce	2.1	0.29	0.56	mg/kg
Co	6.09	13.12	12.97	mg/kg
Cr	68.59	131.07	126.61	mg/kg
Cs	0.06	0.18	0.19	mg/kg
Cu	19.64	18.22	17.08	mg/kg
Ga	24.79	16.92	16.97	mg/kg
Ge	2.29	1.17	1.16	mg/kg
Hf	6.27	10.77	10.89	mg/kg
Hg	2.46	0.13	0.09	mg/kg
Ho	0.01	0	0	mg/kg
Ir	0.03	0.02	0.03	mg/kg

La	0.66	0.1	0.18	mg/kg
Li	59.34	64.22	63.19	mg/kg
Mn	107.54	22.25	21.98	mg/kg
Mo	3.95	4.6	4.47	mg/kg
Nb	21.42	24.03	24.08	mg/kg
Nd	0.12	0.01	0.02	mg/kg
Ni	54.91	36.09	35.72	mg/kg
Pb	36.43	19.7	20.88	mg/kg
Pt	0.03	0.03	0.03	mg/kg
Rb	7.66	21.47	22.73	mg/kg
Sb	1.79	0.21	0.2	mg/kg
Sc	9.25	12.15	10.59	mg/kg
Se	0.62	0.12	0.04	mg/kg
Sn	5.16	3.55	3.57	mg/kg
Sr	151.27	42.82	42.86	mg/kg
Ta	1.2	1.32	1.37	mg/kg
Te	0.31	0.31	0.32	mg/kg
Th	2.5	1.3	1.65	mg/kg
Tl	0.38	0.17	0.17	mg/kg
U	5.2	4.14	4.49	mg/kg
V	82.08	98.77	97.01	mg/kg
W	3.21	3.34	3.4	mg/kg
Y	0.43	0.23	0.23	mg/kg
Zn	40.34	69.43	69.25	mg/kg
Zr	227.57	338.93	327.26	mg/kg
Sulphur Speciation				
Total Sulphur	6.42	0.07	0.06	%
S (sulphide)	5.23	0.02	0.02	%
S (sulphate)	0.02	0.01	0.01	%
S (other)	1.18	0.04	0.03	%

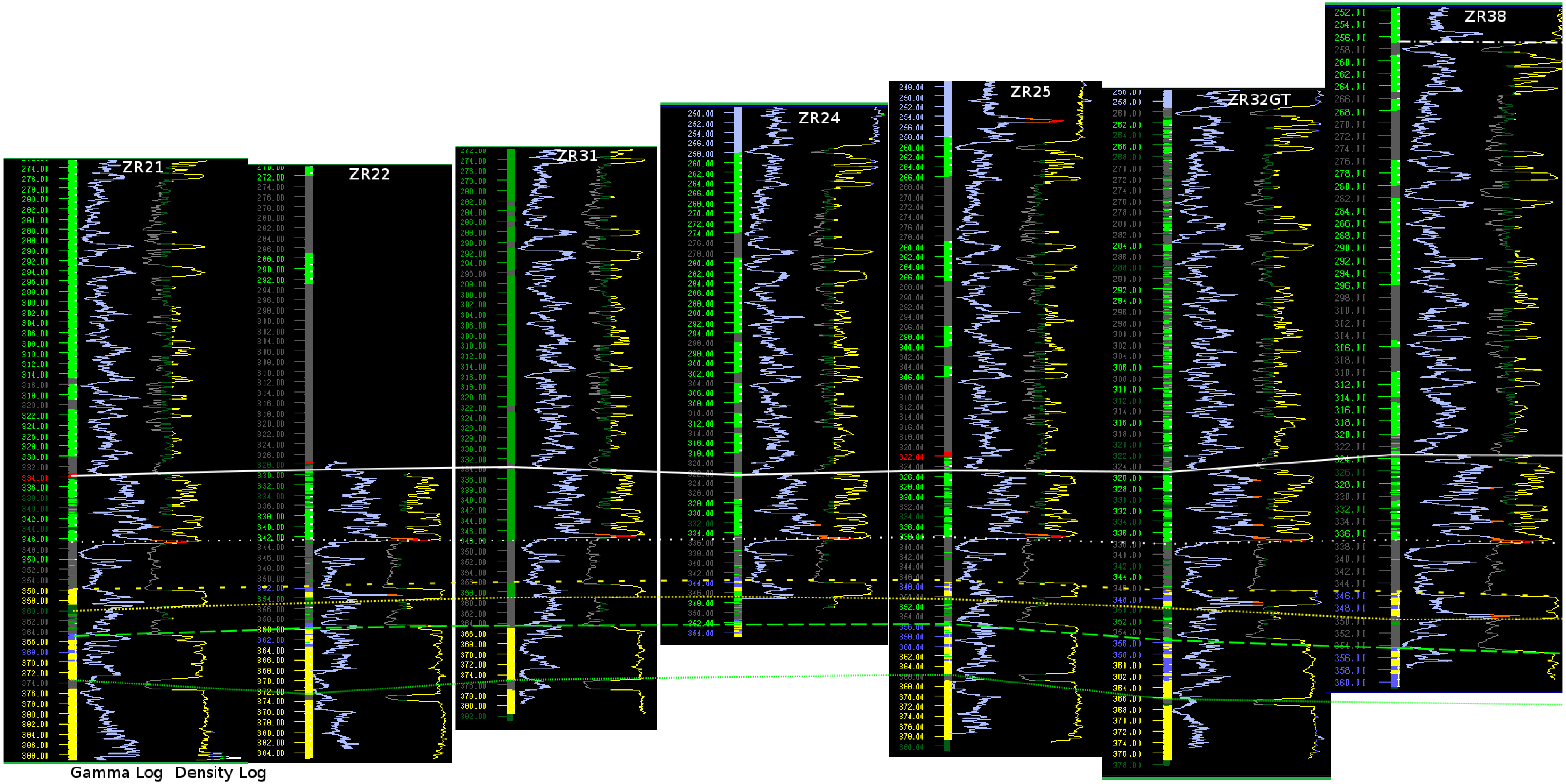
ZR21
ZR22
ZR31
ZR24
ZR25
ZR32GT
ZR38
Gamma Log
Density Log

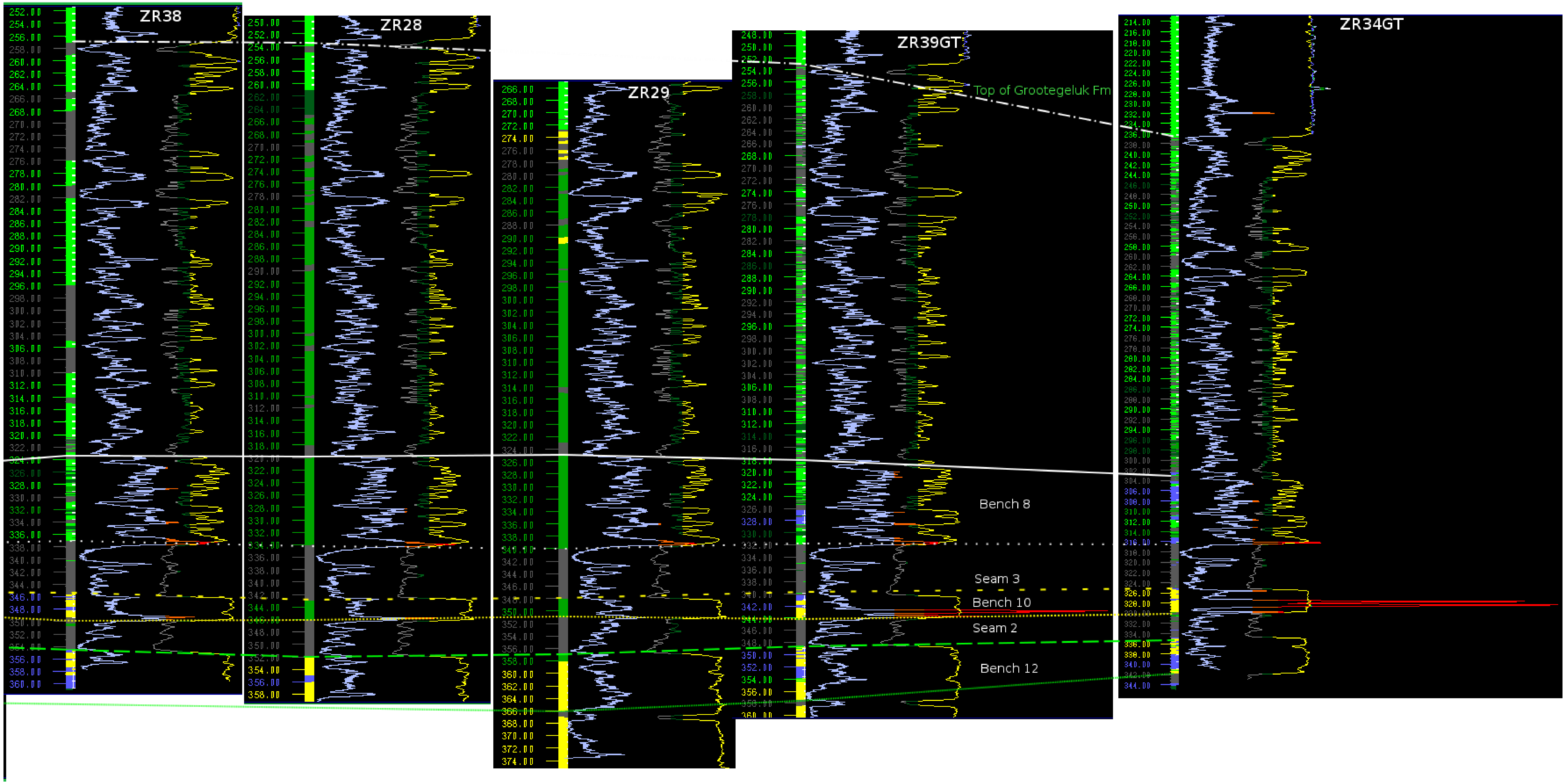
ZR38
ZR28
ZR29
ZR39GT
ZR34GT
Top of Grootegeluk Fm
Bench 8
Seam 3
Bench 10
Seam 2
Bench 12